Feedback regulation and coordination of the main metabolism for bacterial growth and metabolic engineering for amino acid fermentation

Feedback regulation and coordination of the main metabolism for bacterial growth and metabolic engineering for amino acid fermentation

Kazuyuki Shimizu[1,2] and Yu Matsuoka[3]

[1]Kyushu institute of Technology, Iizuka, Fukuoka 820-8502, Japan

[2]Institute of Advanced Biosciences, Keio university, Tsuruoka, Yamagata 997-0017, Japan

[3]Department of Fisheries Distribution and Management, National Fisheries University, Shimonoseki, Yamaguchi, 759-6595, Japan

Abstract

Living organisms such as bacteria are often exposed to continuous changes in the nutrient availability in nature. Therefore, bacteria must constantly monitor the environmental condition, and adjust the metabolism quickly adapting to the change in the growth condition. For this, bacteria must orchestrate (coordinate and integrate) the complex and dynamically changing information on the environmental condition. In particular, the central carbon metabolism (CCM), monomer synthesis, and macromolecular synthesis must be coordinately regulated for the efficient growth. It is a grand challenge in bioscience, biotechnology, and synthetic biology to understand how living organisms coordinate the metabolic regulation systems.

Here, we consider the integrated sensing of carbon sources by the phosphotransferase system (PTS), and the feed-forward/feedback regulation systems incorporated in the CCM in relation to the pool sizes of flux-sensing metabolites and α ketoacids. We also consider the metabolic regulation of amino acid biosynthesis (as well as purine and pyrimidine biosyntheses) paying attention to the feedback control systems consisting of (fast) enzyme level regulation with (slow) transcriptional regulation. The metabolic engineering for the efficient amino acid production by bacteria such as *Escherichia coli* and *Corynebacterium glutamicum* is also discussed (in relation to the regulation mechanisms). The amino acid synthesis is important for determining the rate of ribosome biosynthesis. Thus, the growth rate control (growth law) is further discussed on the relationship between (p)ppGpp level and the ribosomal protein synthesis.

Key words: Metabolic regulation, flux sensing, feed-forward regulation, amino acid synthesis, purine and pyrimidine syntheses, αketoacid, metabolic engineering, feedback

regulation, robustness, growth rate control.

1. Introduction

Living organisms such as bacteria are often exposed to continuous changes in the growth environment, which would endanger their survival without proper adjustment against such environmental fluctuations. Therefore, bacteria have evolved complex but efficient (global) regulatory systems that enable them to monitor the growth environment, and modulate the metabolism in order to rapidly adapt to the environmental changes for survival. To accomplish this, bacteria must integrate the complex and dynamically changing information on the environmental condition, and must make decision on how efficiently uptake nutrients and effectively modulate the metabolism for the cell growth and survival. It is a grand challenge in bioscience (in particular for systems biology), biotechnology (for the design of microbial cell factories), and synthetic biology (for the design of gene networks and for the minimum genome engineering) to understand how living organisms perceive a variety of growth environment, and orchestrate (coordinate and integrate) the metabolic regulation systems for the cell growth and survival.

The primary concern of the cell is the nutrient availability around the cell (as well as physicochemical conditions). Various sensing systems that can mediate the diverse and temporally distinct responses have evolved in bacteria. In particular, canonical two-component systems which comprise several sensors and the cognate response regulators are typically used for sensing and signaling by phosphorylation upon sensor activation (Alvarado et al 2020, Francis and Porter 2019). Integration of the inputs (sensor information) of various nutrient sources (obtained by such sensors) forms a bow-tie structure, in which various inputs are fed into a central core such as glycolysis (fan-in) to produce energy and precursor metabolites, and 'fan-out' for the synthesis of building blocks of macromolecules (Whitacre 2012). This architecture has evolved (Friedlander et al 2015), enabling the robustness of the metabolic networks (Csete and Doyle 2004).

Among nutrients, carbon sources are of primal importance for energy generation (catabolism) and for the production of the precursor metabolites for the cell synthesis (anabolism). The phosphoenolpyruvate (PEP): carbohydrate phosphotransferase system (PTS) plays important roles for this in bacteria. PTS is shared by eubacterial species (Deutscher et al 2014), and it can handle more than 20 different sugars (hexoses and hexitols) (Barabote and Saier, Jr. 2005). PTS is made up of two components: (sugar

independent) enzyme I (EI) and histidine phosphorylatable protein (HPr), and (sugar specific) enzyme II consisting of EIIA and EIIBC (Gorke and Stulke 2008). The phosphate is transferred from PEP via EI, HPr, EIIA, and EIIBC to the incoming sugar. Thus, PEP is crucial (as the phosphate donor) for the phosphorylation of PTS. The information obtained by the individual sugar-specific PTS components is integrated through phosphotransfer reactions via (sugar-independent) EI and HPr. Thus, the core part (EI) senses the overall influx of PTS sugars, and serves as a global sensor of carbon source availability (Somavanshi et al 2016). Namely, the phosphorylation states of PTS components serve as the sensors of carbon source availability (and its 'quality').

Among PTS components, EIIA plays an important role for carbon catabolite repression (CCR) as a central processing unit, where its phosphorylation state modulates the activity of adenylate cyclase (Cya), and in turn regulates the level of the signaling molecule, cyclic adenosine monophosphate (cAMP). Then, the cAMP combined with cAMP receptor protein (Crp), cAMP-Crp controls the carbohydrate uptake (selective carbon source uptake) in *Escherichia coli* (Golke and Stulke 2008). In addition to EIIA, the phosphorylation state of HPr can be also a sensor of exogenous sugar availability (Rodinova et al 2017, Choe et al 2017). Moreover, the phosphorylation state of EI monitors the overall influx of carbon sources, and affects the chemotaxis signaling (Somavanshi et al 2016, Lux et al 1995, Neumann et al 2012).

Once the nutrient availability was monitored, the next step is to modulate the metabolism. In order to control the metabolism in response to the environmental changes, hundreds of transcription factors (TFs) regulate thousands of gene expression (for the transcriptional regulation) (Liu, R. et al 2020, Santos-Zavaleta et al 2019), and thus, the regulation system seems to be quite complex with entangle of many regulation loops. This must be disentangled by the coordination of different regulation loops, in which some specific metabolites integrate different sources of information, thus significantly reducing the complexity of the regulation systems (Kotte et al 2010, Kochanowski et al 2013, 2017, Chubukov et al 2014, Huergo and Dixon 2015, Monteiro et al 2019). Namely, the information obtained by many sensors is rather integrated into the limited number of flux sensors in the elegant with economic way (Kotte et al 2010, Litsios et al 2018).

Catabolism provides energy and building blocks for the cell synthesis, in which the intracellular α-ketoacids also play important roles as the signaling metabolites for the coordination between protein (cell) synthesis (anabolism) and carbon source uptake (via PTS) (catabolism) in *E. coli* (You et al 2013).

The metabolic intermediates of the central carbon metabolism (CCM) must be

converted to monomers such as nucleotides, amino acids, and lipids for biomass synthesis. Therefore, CCM, monomer synthesis, and macromolecular synthesis must be coordinately regulated for the cell growth. In particular, amino acid synthesis is important for determining the rate of ribosome biogenesis. Amino acids (AAs) are synthesized in the species-dependent manner, and also depending on the growth condition (Liu, Y.-K. et al 2020). Aminoacyl-tRNA synthetases implement the correct assignment of AAs to their codons, and link tRNA molecules with their AA cargo for protein synthesis (Kaiser et al 2020). Thus, each amino acid must be produced properly (timely) when it is needed for ribosome synthesis (by need-based regulation). This can be typically attained by the end-product inhibition (feedback regulation), which can act on enzyme abundance (through transcriptional regulatory cues) and enzyme activities (through allosteric feedback inhibition). Understanding of the regulation systems also contributes to the metabolic engineering for the efficient AA fermentation. In particular, deregulation of the feedback control system allows the overproduction of the specific amino acid, while reducing the other amino acid production, thus affecting the cell growth rate (and productivity). In relation to AA synthesis, purine and pyrimidine biosyntheses are also important due to their close link with AA synthetic pathways. A long-standing hypothesis postulates that the bacterial growth rates are determined by the numbers of highly efficient ribosomes (factories that produce proteins) per cell in response to the availability of nutrients (Potrykus and Cashel 2018). The availability of nutrients (via amino acid synthesis) affects the translational responses involving dynamic folding of ribo-switches during translation initiation or the synthesis of alarmones, thus modulating the cellular physiology and metabolism.

The feed-forward and feedback control systems play important roles for the metabolic (glycolytic) regulation (Locasale 2018). In particular, the negative-feedback control system is robust against disturbances (disturbance rejection) and uncertainties, and plays an important role to keep the process at the desired state, and thus underlies homeostasis (Agrawal et al 2019). Moreover, the feedback control system is effective in speeding up the responses. The concept of 'robustness' is closely related to 'homeostasis' (Kitano 2004, 2007, Stelling et al 2004). The notion of *robustness* (in contrast to *fragility*) is important for the engineering system in general, and in a broad sense, robustness of a system refers to its ability to withstand adverse (perturbed) conditions (Khammash 2016).

Here, we consider the integrated sensing of carbon sources by PTS, and the feed-forward/feedback regulation systems incorporated in the central carbon

metabolism (CCM) in relation to the pool sizes of flux-sensing metabolites and αketo acids. We also consider the metabolic regulation of amino acid biosynthesis (as well as purine and pyrimidine biosyntheses) paying attention to the feedback regulation by enzyme abundance (transcriptional regulation) and its activity (allosteric regulation). Metabolic engineering practices for the efficient amino acid fermentation are also reviewed in relation to the metabolic regulation systems. Moreover, we also consider how the availability of nutrients (via AA availability) affects the translational responses (activities) by the synthesis of alarmones. Although attention is somewhat focused on the metabolic regulation/engineering of Gram-negative bacteria such as *E. coli*, the similarities to and differences from Gram-positive bacteria such as *Bacillus* sp. and *Corynebacterium* sp. will be also discussed.

2. Regulation of the central carbon metabolism

2.1 Feed-forward/feedback regulation of the glycolytic flux by the phosphorylation state of PTS

The regulation of the glycolytic flux is important for the cell growth and overflow metabolism (Shimizu and Matsuoka 2019a). The glycolytic flux has been shown to be inferred by the flux-signaling metabolite, fructose 1,6-bisphosphate (FBP) via feed-forward (allosteric) activation of pyruvate kinase (Pyk), giving linear relationship between FBP concentration and the glycolytic flux (thus *flux-sensing* ability is incorporated) in *E. coli* (Kotte et al 2010, Kochanowski et al 2013), allowing quick adjustment of the glycolytic flux (van Heerden et al 2014). Such flux-sensing ability allows the cell to recognize the on-going (time-varying) metabolism quantitatively (Litsios et al 2018) by integrating the information on the available nutrients (Somavanshi et al 2016). However, the feed-forward regulation system is noise-sensitive, which must be compensated by the feedback control to retain the robustness.

In accordance with the increase in the glycolytic flux, the PEP/PYR (pyruvate) ratio decreases due to the feed-forward activation of Pyk and PEP carboxylase (Ppc) by the increased pool size of FBP, and thus EIIA becomes more dephosphorylated in *E. coli* (Hogema et al 1998, Bettenbrock et al 2007, Kremling et al 2008). This means that the feed-forward regulation system is closed by the feedback regulation by the decreased phosphorylation of PTS (and in turn by decreasing the carbon source uptake). Moreover,

the feed-forward activation of Pyk and Ppc by FBP causes the pool sizes of αketoacids such as pyruvate (PYR) and oxaloacetate (OAA) to increase, in which pyruvate is then converted to acetyl coenzyme A (AcCoA), and in turn OAA and AcCoA are condensed to yield αketoglutaric acid (αKG) (**Fig. 1**). The accumulated αKG inhibits EI of PTS (Doucette et al 2011) by binding to the C-terminal region of EI, in which two ligands, PEP and αKG, compete for the 'same' binding site of EI, thus affecting (interrupting) the phosphorylation of PTS by PEP (Venditti et al 2013, 2015). This forms another nested feedback regulation (**Fig. 1**). Namely, there exist two routes for the modulation of Cya by αketoacids, one by inhibiting the phosphorylation of PTS (in particular EIIA) through EI, and the other by directly inhibiting Cya (**Fig. 1**). Both cause the reduction of the cAMP level, resulting in the enhanced CCR.

Figure 2a shows how the fraction of the phosphorylated EIIA changes with respect to the cell growth rate, where the phosphorylation state is higher for the non-PTS carbohydrates than the PTS sugars (Bettenbrock et al 2007, Kremling et al 2008). This is the enzyme level regulation, and it indicates that EIIA becomes less phosphorylated (which enhances CCR) as the cell growth rate increases. The cAMP level or the LacZ expression level (as a reporter of cAMP-Crp activity) also exhibits a negative linear correlation with the specific growth rate (**Fig. 2b**) (designated as C-line) (You et al 2013, Towbin et al 2017). This indicates that cAMP-Crp activity decreases (which enhances CCR) as the cell growth rate increases. The C-line is a common response pattern represented by carbon-catabolic genes, mediated by cAMP-Crp regulation, where both PTS-sugars and non-PTS carbohydrates are located on the same line, unlike the case of EIIA phosphorylation (**Fig. 2a**). Namely, the C-line reflects the coordination of the cell's proteome depending on the demands for ribosomes and metabolic enzymes for the cell synthesis (Scott et al 2010, You et al 2013). This C-line is determined by different carbon sources, including the case of using multiple carbon sources (Hermsen et al 2015) (rectangular symbol in **Fig. 2b**), where the availability of multiple carbon sources allows the cell to grow faster than the case of using glucose (Wang, X. et al 2019). Thus, the 'quality' of carbon source(s) can be measured by the cAMP level.

From the time-scale point of view, the regulation system represented by C-line is effective for the steady state with slow transcriptional regulation, while the fast regulation is realized by the phosphorylation state of PTS components. Thus, the

inhibition of EI by αKG (and also the lower PEP/PYR ratio by the increased FBP concentration) is effective for detecting the rapid change in the nutrient availability. This is the enzyme level closed-loop (negative feedback) regulation. Namely, even though α ketoacids can directly inhibit Cya (You et al 2013), the inhibition of EI by αKG (signaling route) is useful for the rapid response, independent of the direct inhibition of Cya. This implies that the knockout of PTS components affects the response speed (as well as C-line), resulting in less sugar uptake rate and less growth rate (Liang et al 2015, Jung et al 2019). Therefore, if *pts* genes were knocked out, the activation of Cya by EIIA-P (signaling route) is not expected, and thus the C-line becomes lower as compared to the wild-type strain (as shown by the grey triangle in **Fig. 2b**) (You et al 2013).

2.2 Activation of Cra by FBP via F1P and the coordination between Cra and cAMP-Crp

The feed-forward regulation of the glycolysis by FBP is reinforced by the transcriptional regulation via the catabolite repressor/activator (Cra) in *E. coli*. It has long been believed that FBP regulates Cra (FruR) in *E. coli* (Ramseier et al 1993, Saier and Ramseier 1996, Kotte et al 2010), and thus, the glycolytic flux-dependent biosensor has been developed by utilizing Cra-regulated promoter such as *ppsA* promoter (Lehning et al 2017). However, FBP may not directly bind to Cra at the millimolar concentration, while fructose 1-phosphate (F1P) does bind to Cra *in vitro* (Folly et al 2018), where *in vivo* FBP concentrations are less than about 10 mM (Kochanowski et al 2013, 2017), one or two orders of magnitude lower than that can induce Cra (Ramseier et al 1993, Folly et al 2018).

The problem of low affinity of FBP to Cra can be overcome by the indirect signaling via F1P through the reaction by fructose kinase (FruK), where FruK can catalyze the reaction from FBP to F1P, and thus FBP information (pool size) may be converted to F1P by FruK in *E. coli* (Singh et al 2017). Note that the expression of *fruBKA* operon is activated by cAMP-Crp (Shimada et al 2011a), and thus this signaling becomes active at lower glycolytic flux or under gluconeogenesis. This can be verified by the *fruK* gene knockout (Molchanova et al 1992, Singh et al 2017). This implies the existence of the signal transduction via enzymatic conversion of FBP to F1P by FruK, followed by F1P

binding to Cra (**Fig. 3**) (Singh et al 2017). In fact, the pool sizes of both FBP and F1P are certainly (negatively) correlated with the activity of Cra (in response to the cell growth rate) (Kochanowski et al 2017, Gerosa et al 2015). Note that FBP inhibits Cra activity (via F1P), in which Cra represses the expression of the rate-controlling glycolytic genes, and thus this system forms the 'positive' feedback regulation (**Fig. 3**). This must be closed by the negative feedback regulation to retain the stability and robustness. Namely, Cra is involved in the inner feed-forward regulation with positive feedback regulation, while PTS (and cAMP-Crp) is involved in the outer negative-feedback regulation in *E. coli*.

On the other hand, Folly et al. (2018) also showed that FBP does bind to the central glycolytic genes repressor (CggR) within the millimolar physiological concentrations in *Bacillus subtilis*. In Gram-positive bacteria like *B. subtilis*, CggR controls the transcription of the *gapA* operon composed of five glycolytic genes, where FBP acts as an inhibitor of CggR (Zorrilla et al 2007, Chaix et al 2010), and thus FBP activates the lower glycolysis via CggR (by the positive feedback regulation). Many Gram-positive bacteria (including *B. subtilis*) do not possess cAMP for CCR (Fujita et al 2009). Instead, FBP is involved in CCR by the pleiotropic catabolite control protein A (CcpA) (Ludwig et al 2002). CcpA uses phosphoprotein from HPr, where FBP and glucose 6-phosphate (G6P) stimulate the binding to CcpA, and function as co-repressors to fine-tuning of CcpA. Thus, HPr (instead of EIIA) plays the central role for CCR in Gram-positive bacteria such as *Bacillus* species (Deutscher et al 2014, Fujita et al 2009). CCR occurs by the binding of the complex of CcpA and P-Ser-HPr (seryl-phosphorylated form of HPr) to the catabolite responsive elements (*cre*) of the target operons (Fujita 2009). Thus, CggR is involved in the inner positive feedback regulation of the glycolysis via FBP, while CcpA is involved in CCR (with negative feedback regulation).

2.3 Coordinated regulation of the glycolytic flux by Csr and cAMP-Crp

The Csr (carbon storage regulator) (or Rsm: repressor of secondary metabolites), also plays an important role in the adaptation to the change in the nutrient availability, where CsrA is the transcription factor for switching the direction of the glycolytic and gluconeogenic fluxes. Namely, CsrA activates the expression of the glycolytic pathway genes (such as *pfkA* and *pykF*), while represses the expression of the genes (*fbp*, *ppsA*, and *pckA*) encoding gluconeogenic enzymes (Sabnis et al 1995, Timmermans and Merderen 2010, Revelles et al 2013, Morin et al 2016, Potts et al 2017) in the reverse

fashion as regulated by Cra in *E. coli*.

The cAMP-Crp and CsrA are closely linked via PTS (Leng et al 2016, Pannuri et al 2016, Potts et al 2017), where unphosphorylated EIIA of PTS dominates during the uptake of preferred carbon source such as glucose, and binds to the GGDEF-EAL domain of CsrD, where the turnover of non-coding small RNAs (sRNAs) CsrB/C is regulated by CsrD for cleavage by RNase E (Suzuki et al 2006, Vaklskas et al 2016, Leng et al 2016). The CsrA activity is antagonized (repressed) by CsrB/C, which contain multiple CsrA binding sites. Namely, at higher glycolytic flux, unphosphorylated EIIA becomes dominant, which activates CsrD, and in turn activates CsrA by decreasing the activity of CsrB/C, thus activating the glycolysis, forming the 'positive' feedback regulation (**Fig. 4**). Moreover, the CsrD is activated by the direct binding of the uphosphorylated EIIA, and it is repressed by CsrA, forming the feedback loop (**Fig. 4**) to speed-up the response to the steady state (Adamson and Lim 2013, Leng et al 2016). Therefore, there exist multiple regulation loops, in which PTS is involved in the positive feedback regulation via CsrA, and it is also involved in the outer negative feedback regulation by cAMP-Crp.

CsrA is widely observed among eubacteria (White et al 1996, Mercante et al 2006), and regulates the expression of the genes related to virulence factors (Bhat et al 2009), quorum sensing, motility (by modulating *flh* gene expression) (Wei et al 2001, Yakhnin et al 2013), stringent response (Edwards et al 2011), ion storage regulation (Potts et al 2017, Pourciau et al 2019), (σ^E dependent) cell envelope stress response (Yakhnin et al 2017), biofilm formation, cyclic di-GMP synthesis, and peptide uptake etc. (Edwards et al 2011). CsrA is also involved in the carbon storage regulation (glycogen synthesis) (Romeo et al 1993, Yang et al 1996) in maintenance of the energy charge during metabolic adaptation during glycolysis/gluconeogenesis as well as nutrient starvation for survival (Morin et al 2017), where CsrA represses the expression of *glgCAP* genes encoding the enzymes for glycogen synthesis (Sabnis et al 1995, Timmermans and Merderen 2010, Revelles et al 2013). As the cell growth rate increases (with higher glycolytic flux), the metabolism changes from energetically efficient respiration to inefficient respiro-fermentative metabolism (Shimizu and Matsuoka 2019a, 2019b), in which the activity of cytochrome, Cyo of the respiratory chain is repressed, while the activity of Cyd is enhanced by CsrA at higher growth rate (Potts et al 2019). Note that the reverse regulation is made by cAMP-Crp at lower growth rate (Shimada et al 2011a, Kim, D. et al 2018). In the absence of glucose, the BarA-UvrY two-component signal transduction system is also involved in CsrA system, and activated by the

phosphorylation of membrane-bound BarA in response to the short-chain-carboxylic acid-containing (R-COOH) metabolites such as formate and acetate (**Fig. 4**) (Suzuki et al 2002, Chavez et al 2010, Zere et al 2015, Pannuri et al 2016) and by ppGpp (Edwards et al 2011, Zere et al 2015). The phosphorylated BarA then trans-phosphorylates UvrY. The phosphorylated UvrY in turn interacts with *csrB/C* transcription, affecting CsrA system, when short-chain fatty acids are present, and the gluconeogenesis is activated (Suzuki et al 2002, Chavez et al 2010) (**Fig. 4**).

3. Metabolic regulation and engineering of amino acid biosynthetic pathways

In addition to the metabolic regulation of CCM, the regulation of amino acid synthesis is also important for the cell growth in view of ribosome synthesis. Moreover, understanding on the metabolic regulation of the amino acid biosynthesis is useful for the metabolic engineering for the efficient amino acid fermentation. Among amino acid producers, *E. coli* and *C. glutamicum* have attracted much attention for their use in industrial (amino acid) fermentation (Ginesy et al 2015, D'Este et al 2018, Dong et al 2016a).

Allosteric feedback inhibition (in biosynthetic pathways) allows to retain the homeostasis of end-products. Although the primary target of metabolic engineering for the specific amino acid production is to remove such allosteric feedback inhibition, it must be careful by considering how the deregulation affects the metabolism. Namely, even if the allosteric inhibition was removed, additional regulatory mechanisms accomplish the homeostasis, keeping the similar levels of fluxes through the corresponding pathways (Sander et al 2019), in which the abundance of the pathway enzymes is regulated by the transcriptional regulation either by the transcriptional attenuation (Yanofsky 1981) or via transcription factors (Cho et al 2013).

In principle, metabolic engineering practice may be initiated by considering the followings: (1) overexpression of the target amino acid biosynthetic pathway genes (including the feedback-inhibition-resistant genes), (2) disruption of the degradation/branched pathway genes, (3) modification of the (membrane) transport system, (4) reduction of cytotoxicity caused by the products (and solvent tolerance for the pretreated ligno-cellulosic biomass), and (5) modulation of CCM for the over-production of precursor metabolites and cofactors (such as NADPH). In particular, metabolic regulation analysis is useful for the development of the cell factories for the useful metabolite production (Shimizu 2017). The disruption/repression of the by-product pathway affects the cell growth, causing the decrease in the productivity,

while contributing to the increase in the yield and titer of the target amino acid.

3.1 One carbon amino acid and cysteine biosyntheses

The one carbon network generates the carbon units to be used for the nucleotide precursors for anabolic metabolism, redox maintenance, and the substrates for methylation (Yang et al 2016). L-serine is the central for this, and it is currently used for the cosmetic and pharmaceutical industries, as well as a platform for the production of ethanolamine and ethylene glycol (Pereira et al 2016). Current attention is focused on the microbial production of L-serine from renewable feedstocks (Zhang, X. et al 2018).

In bacteria, L-serine is synthesized from 3-phosphoglycerate (3PG) in the glycolysis, where 3PG is oxidized to yield 3-phosphohydroxypyruvate (3PHP) by the reaction catalyzed by 3-phosphoglycerate dehydrogenase (PHGDH) (encoded by *serA*), in which PHGDH is allosterically inhibited by L-serine (**Fig. 5**).

The basic strategy for the efficient L-serine production is the overexpression of $serA^{fbr}$ (feedback-inhibition resistant to L-serine), *serC*, *serB*, and exporter genes, and the deletion of the degradation pathway genes such as *glyA* (encoding serine hydroxymethyltransferase, SHMT) and the deaminase genes *sdaAB* and *tdcG* (encoding deaminases I, II, and III, respectively) as well as the genes encoding L-serine uptake transporters in *E. coli* (**Fig. 5**). Although the suppression of the cleavage of serine to pyruvate and NH_4^+ (by deaminase) is effective for the accumulation of L-serine, loss of the ability to deaminate L-serine severely impairs the cell growth (and cell division), due to the interference with peptidoglycan synthesis, thus weakening the cell wall (Zhang et al 2010). L-serine is also metabolized by SHMT to yield glycine, as well as 5,10-methylenetetrahydrofolate (the source of single-carbon (C_1) compounds, important for the biosynthesis of purines, thymidine, methionine, choline, and lipids). Therefore, the complete inactivation of *glyA* gene negatively affects the biomass synthesis, causing starvation of C_1 units, which are usually formed from serine via SHMT or via glycine cleavage (GCV). Thus, it is better to modulate the *glyA* gene expression by the modification of its regulatory region. Note that glycine can be also produced from threonine via threonine dehydrogenase (Simic et al 2002). Recent metabolic engineering practices for L-serine production and the performances are summarized in **Tables 1** and **2** (Mundhada et al 2015, 2016, Zhu et al 2015, Gu et al 2014, Wang, C. et al 2020, Zhang, X. et al 2020, Xu et al 2015).

Cysteine biosynthesis is the primary pathway for incorporating sulfur into cellular components. Cysteine is a precursor of methionine, thiamine, and coenzyme A, and it plays an important role in the biogenesis of [Fe-S] clusters. Moreover, cysteine-derived

proteins such as thioredoxin and glutathione play important roles in protecting the cells against oxidative stress (Guedon and Martin-Verstraete 2006). As a result of crucial role in cellular physiology and the reactivity of SH group, cysteine metabolism is tightly controlled. The 1st step in the cysteine biosynthesis (from serine) involves the serine acetyltransferase (SAT), encoded by *cysE*, where SAT is strictly inhibited by L-cysteine (**Fig. 5**), and thus the appropriate mutation of *cysE* can desensitize the feedback inhibition by L-cysteine. The intracellular cysteine level is sensed via O-acetylserine (OAS) by the master regulator CysB, which activates the expression of most of the genes encoding the proteins involved in the sulfur transport system and cysteine biosynthetic pathway (**Fig. 5**) (Takumi and Nonaka 2016, Jovanovic et al 2003). Thus, the (allosteric) feedback inhibition of SAT by L-cysteine is coupled with the 'positive' transcriptional regulation by CysB.

In *E. coli*, cysteine is decomposed by cysteine desulfidase (encoded by *yhaM*) into hydrogen sulfide, pyruvate, and ammonium (Nonaka and Takumi 2017). The cysteine desulfhydrase (CD) is responsible for L-cysteine degradation, and CD activity is caused by tryptophanase (TNase) (encoded by *tnaA*) and cystathionine β-lyase (CBL) (encoded by *metC*), where CBL catalyzes the conversion of cystathionine to homoserine, pyruvate, and ammonia, while TNase contributes primarily to L-cysteine degradation (Awano et al 2003, 2005). Therefore, the basic strategy for L-cysteine production is the overexpression of $serA^{fbr}$, *serB*, *serC*, $cysE^{fbr}$, *cysB*, *cysM* etc. and the deletion (or the repression of the expression) of *tnaA*, *sdaA*, *yhaM* etc. (Takumi et al 2017, Kondo and Hirasawa et al 2019, Liu, H. et al 2018, 2020) (**Tables 1** and **2**).

3.2 Histidine biosynthetic pathway

In bacteria, histidine biosynthesis is associated with ten biochemical reactions with the enzymes that catalyze the conversion of two precursors, phosphoribosyl pyrophosphate (PRPP) and ATP into histidine (**Fig. 6**) (Winkler and Ramos-Montanez 2009, Alifano et al 1996). The 1st step, the condensation of PRPP and ATP to form phosphoribosyl-ATP, catalyzed by the ATP-PR transferase (HisG) is the limiting pathway for histidine biosynthesis. Allosteric feedback inhibition of HisG by histidine is made by the competitive inhibition by AMP and ADP, and the competitive product inhibition by PR-ATP. Thus, the histidine-mediated feedback inhibition of HisG plays a critical role in the regulation of histidine biosynthesis. Histidine biosynthesis is also regulated at the transcriptional level by the *hisLGDCBHAFI* operon (Winkle and Ramos-Montanez 2009). Therefore, the feedback-inhibition resistant *hisG* ($hisG^{fbr}$)

together with the enhancement of this operon is the main determinant for the efficient L-histidine production. Moreover, 5-aminoimidazole-4-carboxyamide ribonucleotide (AICAR), which is formed not only during histidine biosynthesis but also during the purine biosynthesis, acts as a natural analogue of AMP, and HisG is also inhibited by AICAR (**Fig. 6**) (Malykh et al 2018). Note that the expression of the histidine biosynthetic pathway genes is also repressed by ArgR (Cho et al 2013, Santos-Zavaleta et al 2019). Moreover, PurR is a global regulator for the control of purine and pyrimidine biosynthesis, which interferes with histidine biosynthesis via the common precursors, in which PurR represses the PRPP synthesis, catalyzed by Prs (PRPP synthetase). Therefore, deletion of *purR* contributes to the histidine production in *E. coli* (Doroshenko et al 2013), but careful analysis must be made as mentioned later in the section of purine and pyrimidine syntheses. Metabolic engineering practices for histidine fermentation are given in **Tables 1** and **2**.

3.3 Glutamate family amino acid synthetic pathways

The glutamate family amino acids (GFAAs) such as ornithine, proline, citrulline, and arginine are of industrial interest due to their uses as feed and food additives, in cosmetics, and for the synthesis of pharmaceuticals (Jensen et al 2015). There are typically two types of metabolic control mechanisms. In *E. coli* (and *B. subtilis*), arginine biosynthesis follows a linear pathway, where N-acetylglutamate (NAG) is first synthesized from glutamate and AcCoA by N-acetylglutamate synthase (NAGS) (encoded by *argA*), which is strongly inhibited by L-arginine (and also by L-citrulline) (**Fig. 7a**). The ornithine acetyltransferase (OAT) is also feedback-inhibited by L-ornithine and L-citrulline (Hao et al 2015, Udaka 1966). On the other hand, in *C. glutamicum* (and *Brevibacterium* sp.), arginine biosynthesis follows a cyclic pathway, where N-acetylglutamate synthase (NAGS) (encoded by *argJ*) catalyzes the 1st step by the transacetylation reaction between glutamate and N-acetylornithine (NAO) to form NAG and ornithine, and not inhibited by L-arginine. Instead, the enzyme of the next step, N-acetylglutamate kinase (NAGK) (encoded by *argB*) is (allosterically) inhibited by L-arginine (and also by L-citrulline) (Utagawa 2004) (**Fig. 7b**).

ArgR (in a complex with L-arginine) represses the transcription of the genes involved in the biosynthesis and transport of arginine (and histidine) (Caldala et al 2006, Maas 1994), and activates the transcription of the genes responsible for arginine metabolism. Therefore, in order to enhance the arginine production, it has been considered to overexpress the feedback resistant *argA* together with the knockout of *argR* in *E. coli* (Ginesy et al 2015).

In *C. glutamicum*, the arginine biosynthetic pathway genes are arranged in two operons, *argCJBDFR* and *argGH*. These operons are repressed by ArgR (Ikeda et al 2009). The enzyme activity of NAGK is feedback inhibited by L-arginine and L-citrulline (Xu, M. et al 2012). Therefore, the metabolic engineering strategy for L-arginine production (Man et al 2016) and L-ornithine production (Wu, X.-Y. et al 2020, Zhang, B. et al 2018a,b, Zhang, B. et al 2017) is to relax such feedback inhibition, and modulate the CCM to increase the supply of NADPH and precursor metabolites (Wu, X.-Y. et al 2020). ArgR is also involved in the regulation of *gltB* and *gdh*. The expression of *argCJBDF* and *argGH* operons is repressed not only by ArgR but also by FarR, where acyl-responsive transcription factor, FarR also represses the expression of *gdh* gene (Zhan et al 2019). Several metabolic engineering strategies have been attempted by deregulating the feedback control systems for L-arginine fermentation (Ikeda et al 2009, Xu et al 2012, Shin et al 2014, Park et al 2014, Zhan et al 2019, Xu, M. et al 2020) (**Tables 1** and **2**).

In *C. glutamicum*, ArgB is inhibited by both arginine and citrulline, and therefore, the combined mutation (*argB26* and *argB31*) together with Δ*argR* gave efficient arginine/citrulline fermentation. In the citrulline fermentation, *argG* may be deleted to prevent the conversion from citrulline to L-arginine, but the complete knockout significantly affects the cell growth (Hao et al 2015, Eberhardt et al 2014) (**Tables 1** and **2**).

Proline is also synthesized from glutamate via essentially three steps of enzymatic reactions by consuming two moles of NADPH, in which the 1st enzyme, γ-glutamyl kinase (GK) (encoded by *proB*) is (allosterically) inhibited by L-proline (**Fig. 7**). Several metabolic engineering strategies with $proB^{fbr}$ (feedback-inhibition resistant *proB*) allow efficient L-proline fermentation (Noh et al 2017, Long et al 2020) (**Tables 1** and **2**).

In the L-ornithine production, *argF* gene may be disrupted to block the pathway from L-ornithine to L-citrulline (**Fig. 7**), thus relieving the feedback inhibition of NAGK by L-citrulline and L-arginine at the same time (Zhang, B. et al 2017). Moreover, the *proB* gene may be also deleted (Kim, S. Y. et al 2015, Shu et al 2018) (**Tables 1** and **2**). However, the deletion/inactivation of *argF* and *proB* negatively affect the cell growth, and the strain becomes arginine (and proline) auxotrophy (Wu, X.-Y. et al 2020). This problem may be overcome to some extent by attenuating *argF* and *proB* by changing the ribosome binding site and translational initiation codon (Zhang, B. et al 2018a, Wu, X.-Y. et al 2020).

3.4 Branched chain amino acid biosynthesis

The biosynthetic pathways of the branched chain amino acids (BCAAs) such as L-valine, L-leusine, and L-isoleusine can be used for the components of cosmetics, pharmaceuticals, animal feed additives, and precursors for the chemical synthesis of herbicides (Park and Lee 2010). In *E. coli*, three acetohydroxy acid synthase (AHAS) isoenzymes (encoded by *ilvBN*, *ilvGM*, and *ilvIH*) have distinct biochemical properties and regulatory mechanisms (Park et al 2012). On the other hand, *C. glutamicum* possesses only one AHAS (encoded by *ilvBN*) (Dong et al 2016b), and *B. subtilis* possesses AHAS (encoded by *ilvHB*) or ALS (encoded by *alsS*) (Gao et al 2021). The AHAS catalyzes the condensation of two molecules of pyruvate to form 2-acetolactate (for L-valine and L-leusine biosyntheses), while it also catalyzes the condensation of one molecule of pyruvate and 2-ketobutyrate (produced from L-threonine) to form 2-aceto-2-hydroxybutyrate (for L-isoleusine biosynthesis) (**Fig. 8**).

The 2-acetolactate is converted (with NADPH) to 2,3-dehydroxyisovalerate by acetohydroxy acid isomeroreductase (AHAIR) encoded by *ilvC*, of which expression is induced by 2-acetolactate, mediated by the positive transcription factor IlvY. Namely, 2-acetolactate and 2-aceto-2-hydroxybutyrate are the substrates for IlvC, and co-inducers of (LysR-type regulator) IlvY, which enhances *ilvC* gene expression via positive regulation (**Fig. 8**). Thus, the modification of this regulation system enabled L-valine production by *E. coli* (Geraskina et al 2019) (**Tables 1** and **2**).

The global regulator, leusine responsive protein (Lrp) is involved in the regulation of BCAA biosynthesis in *E. coli*. It activates the expression of the *ilvIH* genes and represses the expression of the *ilvGMEDA* operon. Lrp also represses the expression of the *livJ* and *livK* genes (encoding the BCAA transporter) and *leuE* (*yeaS*) gene (encoding the L-leusine exporter). In fact, Lrp is a global regulator, that controls many genes (Shimada et al 2015, Kroner et al 2019), and the deletion of *lrp* gene causes the decrease in the cell growth rate (Shimada et al 2015), while its overexpression contributes to the L-isoleusine production (Park et al 2012).

Several metabolic engineering approaches have been attempted for L-valine fermentation using *C. glutamicum* (Chen et al 2015, Wang, X. et al 2018, Schwentner et al 2018) (**Tables 1** and **2**).

In *C. glutamicum*, the *leuA*-encoded 2-isopropylmalate synthase (IPMS) is inhibited by L-leusine (**Appendix 1**), and thus the primary target for the L-leusine production is to construct the feedback-inhibition-resistant variant ($leuA^{fbr}$). Moreover, deletion of *ltbR* (encoding LtbR, which represses the expression of the leusine biosynthetic

pathway genes *leuBCD*) and the feedback-inhibition-resistant AHAS have been considered for the efficient L-leusine production (Vogt et al 2014). Along this line, several approaches have been attempted for L-leusine production (Huang et al 2017, Wang, Y.-Y. et al 2019, Feng et al 2018) (**Tables 1** and **2**).

The threonine dehydratase (encoded by *ilvA*) is under the feedback inhibition by L-isoleusine (**Fig. 8**), and thus the primary target for isoleusine production is to deregulate such inhibitory effect (as well as other mutation as explained in the next section).

3.5 Aspartate family amino acid biosynthesis

The aspartate family amino acids (AFAAs) such as threonine, isoleusine, methionine, and lysine (as well as homoserine) have wide industrial applications for the feed additives (animal feeds) and as precursors for the synthesis of high value-added drug intermediates (Dong et al 2011).

Three aspartate kinase (Ask) isoenzymes, Ask I, II, and III, each encoded by *thrA*, *metL*, and *lysC*, respectively, differ in their regulation mechanisms in *E. coli* (**Fig. 9**) (Chassagnole et al 2001), while Ask is encoded only by *lysC*, and its activity is synergistically inhibited by L-threonine and L-lysine in *C. glutamicum* (and *Brevibacteium flavum*) (Shiio and Miyajima 1969) (**Appendix 2**). The regulation of the *thr* operon is attenuated by the leader sequence (*thrL*), and this must be mutated for L-threonine fermentation (Zhao et al 2018). Thus, the primal target for L-threonine production is the removal of the allosteric feedback inhibition of Ask, and the transcriptional attenuation by *thrL* in *E. coli*. The strategy of overexpression of *thrABC* cluster is often used to increase the L-threonine production (Zhao et al 2018). Although L-threonine binds to the allosteric sites of Ask and homoserine dehydrogenase (HSDH), serving as a non-competitive inhibitor, it acts as a competitive inhibitor on homoserine kinase (Hsk). Thus, the reduction of the feedback inhibition of Hsk enhances the L-threonine biosynthesis (Petit et al 2018). Several metabolic engineering strategies have been considered for L-theronine production (Zhao et al 2018, Dong et al 2016b, Yang et al 2019, Lee et al 2018) (**Tables 1** and **2**).

L-isoleusine is produced from threonine, and its production can be enhanced by the overexpression of $thrABC^{fbr}$, $ilvA^{fbr}$, $ilvIH^{fbr}$, *ilvCED*, as well as *lrp* in *E. coli* (Park et al 2012), and in *C. glutamicum* (Wang et al 2019, Yin et al 2013, 2014, Dong et al 2016b) (**Tables 1** and **2**).

L-methionine is the sulfur-containing amino acid, essential in mammals, and it is also involved in methyl group transfer via its derivative, S-adenosylmethionine (SAM),

intermediate in the polyamine biosynthetic pathway. Homoserine succinyltransferase (HST) (encoded by *metA*) is allosterically inhibited by both methionine and SAM (Ferla and Patrick 2014) (**Fig. 9**). Moreover, the expression of the methionine biosynthetic pathway genes, *metA*, *metB*, *metC*, *metE*, as well as *metL* (encoding Ask), and *metK* (encoding SAM synthetase, SAMS) is repressed by methionine repressor, MetJ (Usuda and Kurahashi 2005) (**Fig. 9**). Thus, the deletion of *metJ* and *thrBC*, together with the mutation of *metK*, followed by the *metA* mutation allowed the efficient methionine production in *E. coli* (Usuda and Kurahashi 2005). Along this line, several strategies have been attempted for the efficient L-methionine production (Huang et al 2017, 2018, Park et al 2017) (**Tables 1** and **2**).

Homoserine (hydroxybutyric acid) is the intermediate for the production of L-threonine and L-methionine from aspartate (**Fig. 9**). Therefore, L-homoserine concentration can be increased by inactivating the expression of *thrBC* genes (to prevent L-threonine production) and *metA* gene (to prevent L-methionine production) as well as *lysA* gene (to prevent L-lysine production) (Li, Y. et al 2016). Moreover, the overexpression of *thrA*, *metL*, and *lysC* can contribute to the enhanced L-homoserine production in *E. coli* (Li, H.B. et al 2016, Liu, P. et al 2020) (**Tables 1 and 2**).

Lysine is used in the animal feedstock, pharmaceuticals, and cosmetics, comprising a multibillion-dollar market (Yokota and Ikeda 2017). The L-lysine biosynthetic pathway starts from L-aspartate with pyruvate by dihydrodipicolinate synthase (DDPS) (encoded by *dapA* gene), and enters into the diaminopimelate (DAP) pathway. Whereas the *E. coli* DDPS activity is inhibited by L-lysine (**Fig. 9**), no such control is observed in *C. glutamicum* (Li et al 2017) (**Appendix 2**).

The diaminopimelate (DAP) pathway starts from aspartyl-semialdehyde, where there exist four variant pathways in bacteria: succinylase, acetylase, dehydrogenase, and aminotransferase pathways (Xu, J.-Z. et al 2019a). *E. coli* uses only the succinylase pathway for *meso*-DAP synthesis, while *Corynebacterium* sp. uses both succinylase and dehydrogenase pathways, *Bacillus* sp. posesses the acetylase and dehydrogenase pathways, and *Clostridium* sp. utilizes dehydrogenase and aminotransferase pathways (Xu, J.-Z. et al 2019b). Among them, the dehydrogenase pathway converts tetrahydrodipicolinate (THDP) to *meso*-DAP in a single step, catalyzed by diaminopimelate dehydrogenase (encoded by *ddh*), which is useful for the L-lysine production (Liu et al 2015). Various strategies have been attempted for L-lysine production by *E. coli* and *C. glutamicum* (Xu, J.-Z. et al 2019b, Wu, W. et al 2019, Xu et al 2018, Lindner et al 2013) (**Tables 1** and **2**).

3.6 Aromatic amino acid biosynthesis

The aromatic amino acids (phenylalanine, tyrosine, and tryptophan) are the final products of the aromatic biosynthetic pathway, which contains the shikimic acid (SA) pathway, followed by the chorismic acid (CHA) synthetic pathway (**Fig. 10**). Aromatic amino acids can be used as the precursors of various aromatic compounds (Huccetogullari et al 2019, Li et al 2020). In *E. coli*, DAHP (3-deoxy-D-arabino-heptulosonate-7-phosphate) synthase (DAHPS) isoenzymes, AroG, AroF, and AroH are subject to allosteric inhibition by L-phenylalanine, L-tyrosine, and L-tryptophan, respectively. AroG contributes about 80 %, AroF about 15 %, and AroH about 5 % of the overall DAHPS activity (Tribe et al 1976, Sprenger 2007), and thus the mutation of *aroG* becomes important for the aromatic amino acid fermentation.

The bi-functional enzyme, chorismate mutase/prephenate dehydrogenase (TyrA/PheA), catalyzes the shared 1st step (conversion of CHA to prephenate, PPA) in the L- phenylalanine and L-tyrosine biosynthetic pathways, as well as the 2nd step in the L-tyrosine synthetic pathway (the subsequent NAD^+-dependent oxidative decarboxylation of prephenate to 4-hydroxyphenylpyruvate, HPP), and the 2nd step in the L-phenylalanine biosynthetic pathway (prephenate to phenylpyruvate, PPY) (**Fig. 10**). TyrA subunit (encoded by *tyrA*) and PheA subunit (encoded by *pheA*) of the chorismate mutase are allosterically inhibited by L-tyrosine and L-phenylalanine, respectively. Tyrosine aminotransferase (encoded by *tyrB*) is allosterically inhibited by L-tyrosine (Keseler et al 2013, Sprenger 2007). Feedback-inhibition-resistant mutants of TyrA and PheA enzymes have been used for the efficient production of L-tyrosine and L-phenylalanine (Rodriguez et al 2014).

Noting that AroL and AroA are the limiting pathway enzymes for the phenylalanine production, the overexpression of $pheA^{fbr}$, *aroL*, and *aroA*, together with inactivation of TyrR gave the efficient L-phenylalanine production (Ding et al 2016, Liu, Y. et al 2018, Wu, J. et al 2019) (**Tables 1** and **2**). Note that two shikimate kinases are encoded by *aroL* and *aroK*, where the expression of *aroL* is regulated by TyrR (with tyrosine or tryptophan as a co-repressor) (Polen et al 2005), while the activity of AroK is free from such regulation (Ding et al 2016).

The L-tyrosine biosynthesis is affected by the TyrR-mediated repression, affecting the expression of *aroF*, *aroL*, *tyrP*, *aroP* (encoding aromatic amino acid permease), and *aroG* genes (Rodriguez et al 2014). The basic strategy for L-tyrosine production is thus the deletion of *tyrR* as well as the overexpression of the feedback-inhibition-resistant derivatives of *aroG* and *tyrA*. These mutations enabled the efficient L-tyrosine production (Lutke-Verloh and Stephanopoulos 2007, Santos et al 2012, Chavez-Bejar et

al 2008, Kim, S.C. et al 2015, Kim, B. 2018) (**Tables 1** and **2**).

L-tryptophan is a hydrophobic aromatic amino acid with an indole side chain. Feedback inhibition by L-tryptophan is exerted on DAHP synthase (encoded by *aroH*) and anthranillate synthase, AS (encoded by *trpED*) in *E. coli* (**Fig. 10**). Furthermore, the genes of *trpLEDCBA* operon are repressed by TrpR. Another regulation is made by the attenuation through *trpL* (Trondle et al 2020). Several metabolic engineering approaches have been attempted so far (Panichkin et al 2016, Niu et al 2019, Liu et al 2019, Trondle et al 2020) (**Tables 1** and **2**). In the L-tryptophan biosynthesis, the overexpression of $aroG^{fbr}$, $aroF^{fbr}$, and $trpE^{fbr}$, as well as the tryptophan synthetic pathway genes, *trpEDCBA* must be considered. Moreover, the deletion of *trpR* and *trpL* genes is effective (Azuma et al 1993, Chen et al 2018b, Gu et al 2012, Jing et al 2018).

In the L-tryptophan biosynthetic pathway, the indole glycerol phosphate synthase (IGPS) is feed-forward inhibited by anthranilate (ANT) non-competitively in *E. coli* (**Fig. 10**), while it is feed-forward activated in *S. cerevisiae* and *Aspergillus niger* (Chen et al 2018a). Since the feed-forward inhibition prevents the flux toward L-tryptophan biosynthesis, the replacement of the feed-forward inhibition by the feed-forward activation system with the heterologous expression of *trpC* (encoding IGPS) is effective for L-tryptophan synthesis in *E. coli* (Chen et al. 2018a) (**Tables 1** and **2**).

In the case of L-tryptophan biosynthesis, additional precursors such as L-serine, PRPP, and glutamine are required (**Fig. 10**), and thus the metabolic engineering approach to increase such precursors is also useful (Panickkin et al 2016, Trondle et al 2020, Li, M. et al 2020). PRPP can be increased by the overexpression of *prs* gene. The 2nd reaction catalyzed by PSAT (encoded by *serC*) in the L-serine synthetic pathway requires glutamate, while glutamine is required at the reaction of anthranillate synthase (AS) (encoded by *trpE*), and thus these reactions are coupled.

4. Metabolic regulation of purine and pyrimidine syntheses and the interaction with amino acid synthesis

In relation to the amino acid synthesis, the synthesis of purine and pyrimidine is also important for biomass synthesis, where purine and pyrimidine nucleotids are subunits of nucleic acids and precursors for the synthesis of nucleotide cofactors (such as NAD etc.) (Moffatt and Ashihara 2002). The biosynthetic pathways of purine and pyrimidine are closely linked with amino acid synthetic pathways, and thus the proper understanding of the metabolic regulation mechanisms of purine and pyrimidine biosyntheses is also important for amino acid fermentation. In particular, histidine and arginine synthetic

pathways are closely connected with purine and pyrimidine synthetic pathways.

The biosynthetic pathway of histidine is closely entwined with purine biosynthesis (and C_1 metabolism). Namely, PRPP is the common precursor for both histidine and purine synthetic pathways. The 1st intermediate (in the histidine synthetic pathway), PR-ATP is formed by the condensation of PRPP and ATP, catalyzed by HisG, in which ATP is synthesized in the purine synthetic pathway. Moreover, AICAR (formed in the 5th step of the histidine synthetic pathway) is rerouted to the purine biosynthesis, enabling to regenerate ATP (**Fig. 11a**).

The *de novo* purine synthetic pathway begins with the transfer of an amino group from glutamine to PRPP, giving phosphoribosylamine, PRA. Then, the subsequent reactions yield AICAR. One molecule of AICAR is also produced in the synthesis of each histidine molecule, and thus AICAR tends to accumulate unless it is appropriately consumed in the latter part of purine synthesis. In the histidine production, HisG is inhibited by purine nucleotides, in particular ADP and AMP via competitive inhibition with PR-ATP (Malykh et al 2018). Moreover, HisG is sensitive to the inhibition by AICAR, a structural analog of AMP, and thus the inhibitory effect of AICAR on HisG must be reduced for the efficient histidine fermentation by activating the conversion of AICAR to purine synthesis, where this can be attained by the overexpression of *purH* and *purA* encoding the latter part of the purine synthetic pathway in *E. coli* (**Fig.11a**) (Malykh et al 2018). As mentioned above, AICAR is synthesized by the parallel pathway from PRPP, and thus the former purine synthetic pathway may be removed by the knockout of the 1st purine synthetic pathway gene, *purF*, thus reducing the AICAR production (Wu, H. et al 2020). Note that *de nove* biosynthesis of purines is linked with C_1 metabolism, in which the conversion of AICAR by PurH is 10-formyltetrahydrofolate (fTHF) dependent, and thus the C_1 metabolism must also be activated to enhance the reaction catalyzed by PurH (**Fig. 11a**). The major source for THF is the reaction of SHMT (encoded by *glyA*) that converts serine to glycine, and simultaneously generates 5,10-methylene-tetrahydrofolate (mTHF) (**Fig. 11a**). The GCV (glycine cleavage) system may be activated to enhance the fTHF production via mTHF production (Kikuchi et al 2008, Zhang et al 2018b, Schwentner et al 2019). Note that *C. glutamicum* does not possess GCV system, and thus this must be heterologously expressed (Schwentner et al 2019).

The arginine and pyrimidine biosynthetic pathways are connected through a common metabolite, carbamoylphosphate (CP), in which CP is a precursor common to the synthesis of arginine and pyrimidine (**Fig. 11b**) (Charlier et al 2018). In most Gram-negative bacteria (including *E. coli*), CP is produced by a single enzyme,

carbamoylphosphate synthase (CPSase), encoded by the *carAB* operon. Namely, CPSase must distribute the high-energy CP for the needs of both pathways (Caldara et al 2008, Charlier et al 2018). All CPSases use one molecule of bicarbonate, two molecules of Mg^{2+}ATP, and one molecule of glutamine (or ammonia) to synthesize CP. *E. coli* CPSase consists of two subunits, a small glutaminase subunit (encoded by *carA*) and a large subunit (encoded by *carB*), that catalyzes the synthesis of CP (from ammonia), and also carries the effector binding sites (Charlier et al 2018). The large subunit of CPSase is composed of four domains, in which the C-terminus constitutes the allosteric domain. Namely, CPSase is activated by ornithine and inosine 5'-monophosphate (IMP), and inhibited by uridine monophosphate (UMP) (**Fig. 11b**) (Caldara et al 2008; Charlier et al 2018). The activation of CPSase by ornithine is crucial in accelerating the ornithine transcarbamylase (OTCase) reaction via the accumulation of CP for the arginine synthesis. The antagonistic effects of UMP and IMP on CPSase allow the correct balance between purine and pyrimidine syntheses for biomass synthesis. Moreover, the expression of *carAB* is transcriptionally repressed by ArgR, and thus *argR* gene knockout contributes to the formation of CP for arginine fermentation. The antagonistic effects of ornithine (activator) and UMP (inhibitor) on CPSase activity and the consumption of CP as a substrate by two carbamoylating enzymes (OTCase and aspartate transcarbamylase, ATCase, a paralog of OTCase) involved in the synthesis of arginine and UMP further ensure this delicate balance between CP production and its consumption for the requirements in both pathways (**Fig. 11b**) (Charlier et al 2018).

In the arginine fermentation, the (allosteric) feedback-inhibition resistant mutant *argA** together with the transcriptional mutant Δ*argR* has been employed (**Tables 1** and **2**). However, ArgR is the global regulator, and has a regulatory function beyond arginine metabolism (Cho et al 2011), and the cell growth rate of *argA**Δ*argR* mutant becomes low, thus deceasing the productivity, while increasing the titer (and yield). The arginine titer can be further increased by the overexpression of the arginine exporter gene *argO*, but the specific growth rate becomes significantly low (by about 70 %) as compared to the wild-type strain (Sander et al 2019). The decrease in the cell growth rate is mainly due to the limitation of the pyrimidine synthesis. Namely, the pyrimidine nucleotide biosynthesis competes with arginine biosynthesis at the branch point of OCTase (encoded by *argFI*) and ACTase (encoded by *pyrBI*) (**Fig. 11b**) (Caldara et al 2008), in

which pyrimidine nucleotide synthesis becomes limited by Δ*argR* mutation for the enhanced arginine production, and in turn affects the cell growth. Therefore, the appropriate knockdown (instead of complete knockout) of *argR* (by CRISPR-Cas9) may be considered for the trade-off between arginine synthesis and the cell growth (Sander et al 2019).

The purine repressor (PurR) plays the essential role for the homeostasis of purine and pyrimidine concentrations in the cell. Upon availability of purine and pyrimidine nucleotides, PurR tightly regulates (represses) the expression of the genes encoding the enzymes involved in the biosynthesis of IMP and the conversion of IMP to AMP and GMP (**Fig. 11a**) (Cho et al 2011). Moreover, PurR also regulates the expression of *prs* (He et al 1993) and serine transport and metabolic pathways to produce fTHF (Cho et al 2011). Therefore, *purR* gene knockout in $hisG^{fbr}\Delta hisL$ strain can improve the histidine producion by increasing the cell growth rate to some extent as compared to $hisG^{fbr}\Delta hisL$ strain, but not to the level of the wild-type strain (*E. coli*) (Doroshenk et al 2013). Note that PRPP is not only a precursor of histidine and purine syntheses, but also a precursor of other synthesis of pyrimidine, tryptophan, and NAD (Jensen et al 2008). Moreover, PurR also represses the expression of the enzymes of the early steps of pyrimidine biosynthesis (and transport), in which PurR directly regulates *pyrB* and *pyrI* genes (which encode the catalytic and regulatory subunits of ATCase, respectively), and also the initial step enzymes encoded by *pyrC* and *pyrD*, as well as *carAB* (encoding CPSase) (**Fig. 11b**) (Cho et al 2011). Therefore, the effect of *purR* gene knockout on the metabolism is complex, and the effect of modulating the expression of *purR* gene must be carefully analyzed for the efficient amino acid fermentation.

5. Growth rate control

In order to optimize the growth rate under various environmental conditions, the cell must adjust the metabolism for the optimal resource allocation through balancing the cellular investment on the metabolic and ribosomal proteins (Scott et al 2010, You et al 2013), where protein synthesis lies at the core of the cell growth (Dai et al 2016, 2018, Klumpp et al 2013). Ribosome drives protein translation, and thus the cell growth rate is enhanced by increasing the amount of ribosomes. As shown in **Fig. 12a**, the fraction of ribosomal protein is linearly correlated with the growth rate, in which the slope of the

line quantitatively matches the rate of ribosome translation in *E. coli* (Scott et al 2010, Dai et al 2016). The mass fraction of ribosomal protein, φ_r can be expressed as the linear equation with respect to the cell growth rate, μ (Scott et al 2010, Dai et al 2016) such that

$$\varphi_r = \varphi_0 + \mu/\gamma \qquad (1)$$

where φ_0 is the intercept, and γ is the constant (that determines the translational efficiency) (Scott et al 2010).

Many bacteria (and also Archaea) induce a stringent response under nutrient starvation and other stressful conditions. The alarmone signal, guanosine (penta) tetra phosphate, (p)ppGpp is a key secondary messenger, and reshapes the metabolism and physiology by coordinately modulating the cell growth, transcription, translation, and ribosome assembly, thus enabling the survival under stressful condition (Steinchen and Bange 2016). The alarmone, (p)ppGpp accumulates in response to the starvation of nutrients (via AA limitation), and inhibits rRNA transcription. The cell growth rate and the ribosome content are linearly correlated by the so-called *growth rate control* (GRC) (Scott et al 2010). The relationship between (p)ppGpp and the ribosomal protein synthesis during the exponential growth remains to be long standing puzzle (Zhu et al 2019).

The intracellular concentration of (p)ppGpp is determined by RelA-SpoT Homologues (RSHs), which are used to integrate and transform environmental cues into (p)ppGpp levels in Beta-proteobacteria and Gamma-proteobacteria (Ronneau and Hallez 2019), where (p)ppGpp is synthesized by the mono-functional alarmone synthetase, RelA, while it is degraded by the bi-functional SpoT (Hauyliuk et al 2015). On the other hand, in genera outside of such bacteria, there is typically a single RelA/SpoT homologue protein (termed as Rel or RSH) with linked functional hydrolase and synthetase domains (Hauryliuk et al 2015, Atkinson et al 2011, Hogg et al 2004).

The source of ribosomal protein is amino acids (AAs), where AA availability is sensed by RelA, which then generates (p)ppGpp upon AA limitation in *E. coli*, where (p)ppGpp is known as magic spot, as it affects diverse set of biochemical and biophysical events such as antibiotic tolerance (persistence), biofilm formation, competence, virulence/pathogenesis, motility, sporulation (Steinchen and Barge 2016, Hauryliuk et al 2015), as well as the cell size control (Westfall and Levin 2018, Vadia et

al 2017). Its synthesis is activated by the presence of uncharged transfer RNA (tRNA) (without AA) by the allosteric regulation by RelA. During the exponential growth phase with enough nutrients, AAs are delivered in the form of aminoacylated tRNA to the ribosomal acceptor site (A-site), resulting in the lower level of (p)ppGpp (Hauryliuk et al 2015). Upon AA starvation, deacylated tRNAs (not conjugated to AAs) accumulate, and enter the A-site, which then activates RelA (Traxler et al 2008). The regulatory mechanism for the linear relationship between the ribosomal protein synthesis (and the cell growth rate) is thus enforced by ppGpp, as it (together with DksA) inhibits rRNA transcription, thereby limiting the formation of ribosomes (Bosdriesz et al 2015, Klumpp et al 2013, Ross et al 2016, Shin et al 2021).

The ppGpp (or pppGpp) is synthesized by the transfer of pyrophosphate moiety from GDP (or GTP) and ATP (Atkinson et al 2011, Hauryliuk et al 2015). The (p)ppGpp level is modulated by the synthetase activities of RelA and SpoT, and by the hydrolase activities of SpoT and guanosine pentaphosphate phosphohydrolase (Gpp) to keep the basal (p)ppGpp at the optimal level. Rapid conversion of pppGpp to ppGpp by Gpp implies that ppGpp plays the main regulatory role (as compared to pppGpp) (Mechold et al 2013). The increased (p)ppGpp promotes the amplification of RelA-mediated positive feedback regulation (Beljantseva et al 2017, Sanyal and Harinarayanan 2020), which is effective for the rapid increase in (p)ppGpp for the stringent response. This is compensated by the hydrolysis activity of SpoT and Gpp (**Fig. 13**). This system makes the allosteric regulation to be inherently faster without *de novo* production of mRNA and protein (Shyp et al 2012), enabling the rapid amplification of a small input response, but may become noise sensitive inherent to the positive feedback regulation, while SpoT can dampen the (p)ppGpp synthesis, and play the *noise-filtering* role (Traxler et al 2008).

As shown in **Fig. 12b**, ppGpp concentration decreases with respect to the cell growth rate. Since the transcription of ribosomal RNAs is inhibited by ppGpp (Dennis et al 2004), the ribosome synthesis rate decreases as ppGpp level increases (Bosdriesz et al 2015, Giordano et al 2016), and φ_r may be expressed as

$$\varphi_r = k_r/(1 + [\mathrm{ppGpp}]/K_{i,\mathrm{ppGpp}}) \qquad (2)$$

where k_r and $K_{i,\mathrm{ppGpp}}$ are the constants. By equating Eqs.(1) and (2), we have

$$[\mathrm{ppGpp}] = b/(\mu + a) - c \qquad (3)$$

where $a \equiv \varphi_0 \gamma$, $b \equiv K_{i,ppGpp} \gamma k_r$, and $c \equiv K_{i,ppGpp}$. Thus, the ppGpp level deceases with respect to the cell growth rate as shown in **Fig. 12b**.

It is important to understand the long-standing paradigms for the key regulatory steps of translation (Tollerson II and Ibba 2020). Translation is a complex and dynamic process that must occur rapidly to optimally decode genetic information (Morgan et al 2018, Dai et al 2016, 2018). Initiation of mRNA translation is usually the rate-limiting step of protein synthesis. The initiation phase of translation begins with the formation of the 30S initiation complex, which is then joined by the large 50S ribosomal subunit to yield 70S initiation complex with the aminoacyl-tRNA, carried to the ribosomal A-site by the elongation factor, EF-Tu. Three initiation factors such as IF1, IF2, and IF3 determine the kinetics and fidelity of the overall initiation process (Gualerzi and Pon 2015). The mRNA translation requires the action of several guanosine nucleotide-binding factors. In addition to their substrates such as GDP and GTP, IF2 and the elongation factor G (EF-G) interact with ppGpp, and inhibits the activity of GTPase, where IF2 is more responsive to ppGpp than EF-G during the stringent response *in vivo* (Mitkevich et al 2010).

The ribosome-associated GTPase (G-protein) (CgtA, ObgE, Obg, or Yhbz) interacts with SpoT to enhance the hydrolase activity under nutrient rich condition in *E. coli* (Jiang et al 2007, Raskin et al 2007, Zhang Y. et al 2018). CgtA primarily functions as a sensor of phosphorylated guanosines (Wout et al 2004, Persky et al 2009, Feng et al 2014). In the nutrient rich condition, GTP pool size becomes higher, and CgtA transiently associates with ribosome and acts as a 50S assembly factor favoring translation (Feng et al 2014). On the other hand, it becomes a 50S-anti association factor when the intracellular (p)ppGpp concentration increases (upon nutrient starvation), where GTPase strongly binds to ppGpp and stick to the 50S subunit, thereby preventing its association with 30S subunit (Feng et al 2014). In addition to ribosomes, CgtA also interacts with SpoT (but not RelA) in *E. coli* (and *Vibrio cholerae*) (Wout et al 2004, Raskin et al 2007). Namely, CgtA can be a *gate keeper* that maintains (p)ppGpp levels low under nutrient rich condition (**Fig. 14**) (Jiang et al 2007, Raskin et al 2007).

6. Concluding remarks

The cell metabolism changes upon mutation of the pathway genes in CCM, in which the pool sizes of the precursor metabolites for the amino acid synthesis also change (Ishii et al 2007). The feedback regulation systems for CCM and amino acid

biosynthesis play important roles for the robustness and homeostasis, in which the interface metabolites (αketo acids) play important roles for the coordination between the two systems. Namely, the feedback regulation system via cAMP-Crp (or the phosphorylation state of PTS) serves for the homeostasis of αketoacids, while the allosteric feedback regulation systems of amino acid biosynthesis allow the homeostasis of the terminal amino acids (to be utilized for the ribosomal protein synthesis for the cell growth) (**Fig. 15**). Thus, the perturbation of amino acid synthesis affects the pool sizes of αketo acids (and PEP and AcCoA), and in turn affects the CCM. In fact, when *E. coli* was cultivated with glucose minimum medium supplemented with casamino acids (CAA), an undefined mixture of amino acids and oligopeptides, the high growth could be attained by the catabolism of amino acids (in CAA), causing the accumulation of αketo acids such as pyruvate and OAA, which inhibit PTS, resulting in the reduced glucose uptake rate (Zampieri et al 2019). In this way, each subsystem of CCM and amino acid biosynthesis retains robustness by the feedback regulation systems, while the overall system is *resilient* to variations in the growth environment, in which the interface metabolites (such as αketo acids) play important roles for the coordination between the two systems. In fact, the overall system consists of CCM, AA synthesis, and also macromolecular (protein) synthesis, each having the negative feedback system for the robust cell growth, and the coordination is made by the interface metabolites.

The integration of fluxes by the specific metabolites (flux sensing metabolites and αketo acids) is useful in the sense that the noises of the fluxes at some points in time (Patang et al 2018, Fuentes et al 2021) can be smoothed over the past time, and thus the signal transduction to the transcription factors can be made reliably, similar to the integral feedback control for the robust adaptation in noisy bio-molecular systems (Briat et al 2016).

Allosteric feedback regulation plays an essential role in the fast adaptation to the abrupt environmental changes, while transcriptional regulation plays important roles for fine-tuning of the expression of the pathway genes toward the new steady state. Thus, a major reorganization of metabolism must be made first by the enzyme level regulation in response to the nutrient shifts, but it is not enough to cope with the change in the flux

direction, and requires the transcriptional regulation. Namely, if the preferred carbon source (such as glucose) was switched to gluconeogenic carbon source (such as acetate), the lag phases occur until the new steady state is attained, in which sole enzyme level regulation cannot cope with the requirement of the reversed flux changes (for gluconeogenesis), and must wait for the change in the abundance of the required pathway enzymes (and the expression of the new pathway enzymes) by the transcriptional regulation. Therefore, there is a tradeoff between the cell growth rate and the lag times for the adaptation to the gluconeogenic condition in *E. coli* (Basan et al 2020, Schinck et al 2021). Namely, during growth on glucose, the expression of the irreversible glycolytic enzymes such as Pfk and Pyk is activated, while the expression of the corresponding (irreversible) gluconeogenic pathway enzymes such as Fbp and Pps (and also Pck) is repressed by the lower activity of Cra (Shimada et al 2011b) in response to the increased concentration of FBP to avoid futile cycling, in which FBP is a flux sensor of the glycolysis. Thus, the faster growing cells (with preferred carbon source) require a longer time to activate the transcription factors for gluconeogenesis in response to the new (gluconeogenic) medium, while slow growing cells resume the new steady state more quickly, implying universal tradeoff between growth and adaptability. The similar trade-off exists between rapid growth (or proliferation) and survivability, in which the cell death rate becomes higher for the nutrient starvation as the pre-growth rate is higher (Biselli et al 2020). Note that the enzymes 'sandwiched' between the two irreversible enzymes are reversible, and can be lumped into 'super-enolase enzyme' (Schink et al 2021) or can be integrated for channeling (Hollinshead et al 2016).

In the growth-starvation switch (Lempp et al 2019, Xu, Y.-F. et al 2012), glucose-acetate transition (Enjarbert et al 2013, 2015, Kotte et al 2014), and glucose-nitrogen starvation switch (Brauer et al 2006, Doucette et al 2011), the pool sizes of the upper glycolysis (such as G6P/F6P, FBP, and DHAP/GAP) sharply drop, while the concentration of PEP (and also 3PG/2PG) in the lower glycolysis increases. The reason for the rapid accumulation of PEP is due to the shut-down of PTS and the shut-off of Ppc (and Pyk) via ultrasensitive allosteric regulation by FBP (and also by AcCoA) (Xu, Y.-F. et al 2012). Because of the drain of the metabolites in the upper glycolysis, the pool sizes of the pentose phosphate (PP) pathway also decrease accordingly. Therefore, the limited gluconeogenic flux soon after the switch of the carbon sources prevents the biomass synthesis, in which R5P and E4P are required for the biosynthesis of nucleotides and aromatic amino acids. This causes the lag phases, where the amino acid limitation is detected by RelA, causing ppGpp level to increase to stop the cell growth. Moreover, the shut-off of Pyk (and Ppc) causes pyruvate and

AcCoA pool sizes to be significantly decreased. The carbon starvation can then be detected by SpoT due to lower level of fatty acid via the low pool size of AcCoA, thus increasing the ppGpp level to stop the ribosome synthesis for the cell growth. Namely, the cell growth rate is tightly regulated via RelA and also SpoT by the different signaling routes in the case of carbon source starvation. The pool sizes of the TCA cycle intermediates (including αKG) decrease upon carbon starvation (Lempp et al 2019, Xu, Y.-F. et al 2012), and thus NAD(P)H and ATP (GTP) concentrations decrease, while ADP and AMP pool sizes increase. The TCA cycle and the glyoxylate pathway are eventually activated as the gluconeogenic carbon source is assimilated (Lempp et al 2019).

On the other hand, during the nutrient up-shift (from acetate medium to rich medium including glucose), the ppGpp level drops to nearly zero by the feed-forward regulation, while it eventually increases in accordance with the nutrient consumption. Production of amino acids with acylated (charged) tRNA allows the resumption of translation, which causes the reduction of RelA-mediated (p)ppGpp production, thus providing a slow negative feedback regulation (by activating the transcription of AA biosynthetic genes) (Traxler et al 2011). Therefore, a fast positive feedback regulation system is compensated by the slow negative feedback regulation (**Fig. 13**). This system gives a very sensitive *toggle* system, where such system rapidly turns on the response to the stimuli, robustly maintain its status, and turns off the regulatory action when the stimuli disappeared (Kim et al 2007).

Although living organisms must adjust the metabolisms in response to the change in the (growth) environmental condition, the cell's adaptation to the fluctuating nutrient availability may not be optimized at the single-cell level. For example, if the available carbon sources were changed from the preferred carbon source (such as glucose) to the gluconeogenic carbohydrate such as acetate (or vice versa), the enzyme level regulation cannot cope with such changes quickly, but has to wait for the (slow) transcriptional regulation for the induction of gluconeogenic (glycolytic) pathway genes (as the lag phases). It seems to be too late with such a strategy under certain competitive circumstances. This may be overcome to some extent by the non-active ribosome, preparing for the rapid response to the newly available nutrients (Kafri et al 2016, Dai et al 2016, Metzl-Ras et al 2017). In addition to this strategy, the cells may cope with the change in the nutrient condition and uncertainty by the heterogenity of the population (Kotte et al 2014, Dai et al 2016). Namely, the lag times after nutrient shifts can be explained from the two stochastically generated subpopulations depending on the

concentrations of the gluconeogenic carbon source (such as acetate) with conditional bet-hedging (Kotte et al 2014). In fact, bifurcation analysis on the positive feedback regulation via Cra indicates the emergence of multiple steady states (two stable and one unstable) depending on the acetate concentration (Kotte et al 2014). Moreover, even if the mixture of non-preferred carbon sources is consumed in a hierarchical way, the single-cell analysis revealed 'all-or-none' behavior for the induction of nutrient-specific transport gene expression, where sub-populations consume one, the other, or both sugars through cross-repression (for example, in the case of L-arabinose over D-xylose), and the population size (fraction of each sub-population) depends on the concentration of each carbon source (Koirala et al 2015, Beisel and Afroz 2016).

In relation to the feedback regulation, the (transient) dynamics becomes important, where the feedback control system with higher order system (with multiple enzyme reaction steps) inherently causes damped oscillation. Namely, the allosteric (negative) feedback regulation of the multi-step enzymatic process causes damped oscillations, while monotonic changes are observed for the system without feedback regulation but with slow responses (Chevalier et al 2019). There exists a trade-off between the quick response and the overshoot of the damped oscillation, where the strength of the feedback regulation is determined by the binding of the terminal metabolite (amino acid) to the active site of the 1st enzyme of the corresponding pathway, which may have been optimized by evolution.

The metabolic regulation systems consist of the (fast) enzyme level and the (slow) transcriptional regulation systems, where the time scales of such regulation systems are (one or two orders of magnitude) different (He et al 2019, Lempp et al 2019), and thus those can be decoupled, and may be controlled rather independently without much interaction between the two control loops. However, the allosteric inhibition of the 1st enzyme of the amino acid synthetic pathway affects the transcriptional regulation of the pathway genes. Namely, in the amino acid synthetic pathways, the closer the enzyme is to the beginning of the pathway, the shorter the response time of the activation of its promoter and the higher its promoter activity (Zaslaver et al 2004). This ensures that pathway enzymes are only made when they are needed (Schmidt et al 2016, Zaslaver et al 2004, Gerosa et al 2013). This 'just-in-time' transcription program can be attained by the relax of the allosteric feedback inhibition of the 1st enzyme of the pathway, followed by the transcriptional regulation of the subsequent genes. On the other hand, in the (continual) rapid nutrient fluctuations (second-to-minute scale), the cells must cope with only the (allosteric) enzyme level regulation, while the transcriptional regulation cannot catch up with the rapid nutrient fluctuations, resulting in the different growth response

as compared to the nutrient shift once, in which both enzyme level and transcriptional regulations determine the biosynthesis (Nguyen et al 2021).

Finally, the conventional metabolic engineering approaches must be reconsidered from the point of view of robustness against perturbations in view of metabolic regulation. In the typical metabolic engineering approach for the amino acid fermentation, the 1st attempt is to remove the allosteric feedback inhibition (and then to modulate the transcriptional repression). However, care must be taken from the point of view of robustness against genetic perturbations. For example, in the feedback-dysregulated mutants, all the concentrations of the terminal amino acids certainly increase, which then activate the transcriptional regulation via transcription factors (such as ArgR, TrpR, TyrR, and Lrp) and leader peptides (such as *hisL*, *trpL*, and *thrL*), and repress the abundances of the corresponding pathway enzymes (**Fig. 15**). Thus, the enzyme abundance becomes lower in the dysregulated pathways. Even though the mutant shows the similar growth, the feedback-dysregulated mutant with lower enzyme abundance becomes sensitive (and *fragile*) against perturbation of gene expression (Sander et al 2019), and thus it must be careful in the industrial application. Moreover, although the knockout of (global) transcription factors and the leader peptides can contribute to the increase in the terminal amino acid, it causes the increase in the abundances of the corresponding pathway enzymes (and others in the case of global regulators) (more than those required for the biosynthesis). This also negatively affects the cell growth rate due to the increased protein cost, and therefore, it must be careful in the industrial application.

Abbreviations

2-PG: 2-phosphoglycerate
3-PG: 3-phosphoglycerate
3PHP: 3-phosphohydroxypyruvate
α-KG: α-ketoglutaric acid
AA: amino acid
AcCoA: acetyl coenzyme A
ADP: adenosine diphosphate
AFAA: aspartate family amino acid
AHAIR : acetohydroxy acid isomeroreductase
AHAS: acetohydroxy acid synthase
AMP: adenosine monophosphate

ANT: anthranilate
AICAR: 5-aminoimidazole-4-carboxyamide ribonucleotide
AS: anthranillate synthase
Ask: aspartkinase
ATP: adenosine triphosphate
cAMP: cyclic adenosine phosphate
CCR: carbon catabolite repression
CHA: chorismic acid
Cra: catabolite repressor/ activator
Crp: cAMP receptor protein
Csr: carbon storage regulator
Cya: adenylate cyclase
DADH: diaminopimelate dehydrogenase
DAHP: 3-deoxy-D-arabino-heptulosonate-7-phosphate
DAHPS: 3-deoxy-D-arabino-heptulosonate-7-phosphate synthase
DAP: diaminopimelate
DAPDH: diaminopimelate dehydrogenase
DDPS: dihydrodipicolinate synthase
DHAP: dihydroxy acetonephosphate
E4P: erithrose 4-phosphate
EI: enzyme I of PTS
EII: enzyme II of PTS
F1P: fructose 1-phosphate
F6P: fructose 6-phosphate
FBP: fructose 1,6-bisphosphate
Fbp: fructose bisphosphatase
FruK: fructose kinase
G6P: glucose 6-phosphate
GAP: glyceraldehyde 3-phosphate
GK: γ-glutamyl kinase
Gpp: guanosine pentaphosphate phosphohydrolase
GRC: growth rate control
HPP: 4-hydroxyphenylpyruvate
HPr: histidine phosphorylatable protein
HSDH: homoserine dehydrogenase
HSK: homoserine kinase

HST: homoserine succinyltrasferase
IF: initiation factor
IGPS: indole glycerol phosphate synthase
IPMS: 2-isopropylmalate synthase
Lrp: leusine responsive protein
NAG: N-acetylglutamate
NAGK: N-acetylglutamate kinase
NAGS: N-acetylglutamate synthase
OAA: oxaloacetate
OAT: ornithine acetyltransferase
OCD: ornithine cyclodeaminase
Pck: pyruvate carboxykinase
PDH: pyruvate dehydrogenase
PEP: phosphoenol pyruvate
PHDH: 3-phosphoglycerate dehydrogenase
PRPP: phosphoribosyl pyrophosphate
Prs: PRPP synthetase
PSAT: 3-phosphoserine aminotransferase
PSPH: 3-phosphoserine phosphatase
Pfk: phosphofructokinase
ppGpp: tetra phosphate
pppGpp: penta phosphate
PPA: prephenate
Ppc: PEP carboxylase
PP pathway: pentose phosphate pathway
Pps: PEP synthase
PPY: phenylpyruvate
PTS: phosphotransferase system
Pyk: pyruvate kinase
PYR: pyruvate
R5P: ribulose 5-phosphate
rRNA: ribosomal RNA
SA: shikimic acid
SAM: S-adenosylmethionine
SEDH: serine dehydratase
SHMT: serine hydroxymethyltransferase

TCA cycle: tri-carboxylic acid cycle
TF: transcription factor
THDPA: tetrahydrodipicolinate
tRNA: transfer RNA

Conflict of interest

Both authors KS and YM declare that they have not conflict of interest.

Authors' contributions

Both authors KS and YM contributed equally in preparing the manuscript.

Funding

This work was supported in part (Y. Matsuoka) by Grant-in-Aid for Scientific Research (C) (21K12118) from Japan Society for the Promotion of Science.

Appendix

Appendix 1

Branched chain amino acid synthetic pathway in *C. glutamicum* (blue line shows enzyme level regulation, while red line shows transcriptional regulation)**:**

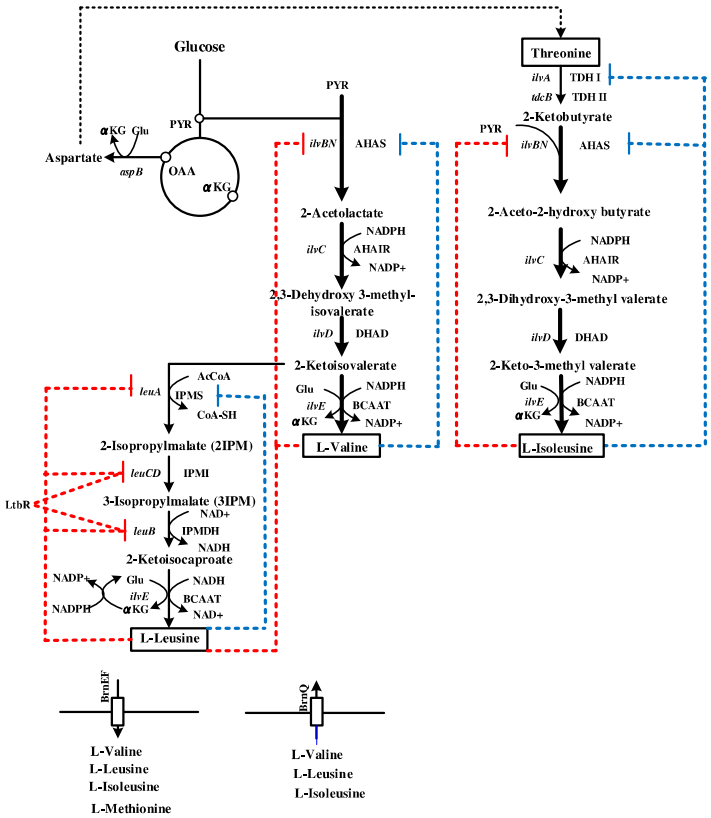

In *C. glutamicum*, only one AHAS (encoded by *ilvBN*) catalyzes the first reaction of condensing two molecules of pyruvate to yield 2-acetolactate. Others are similar as shown in Fig. 8 for *E. coli*.

Appendix 2

Aspartate family amino acid synthetic pathways in *C. glutamicum* (blue line shows enzyme level regulation, while red line shows transcriptional regulation):

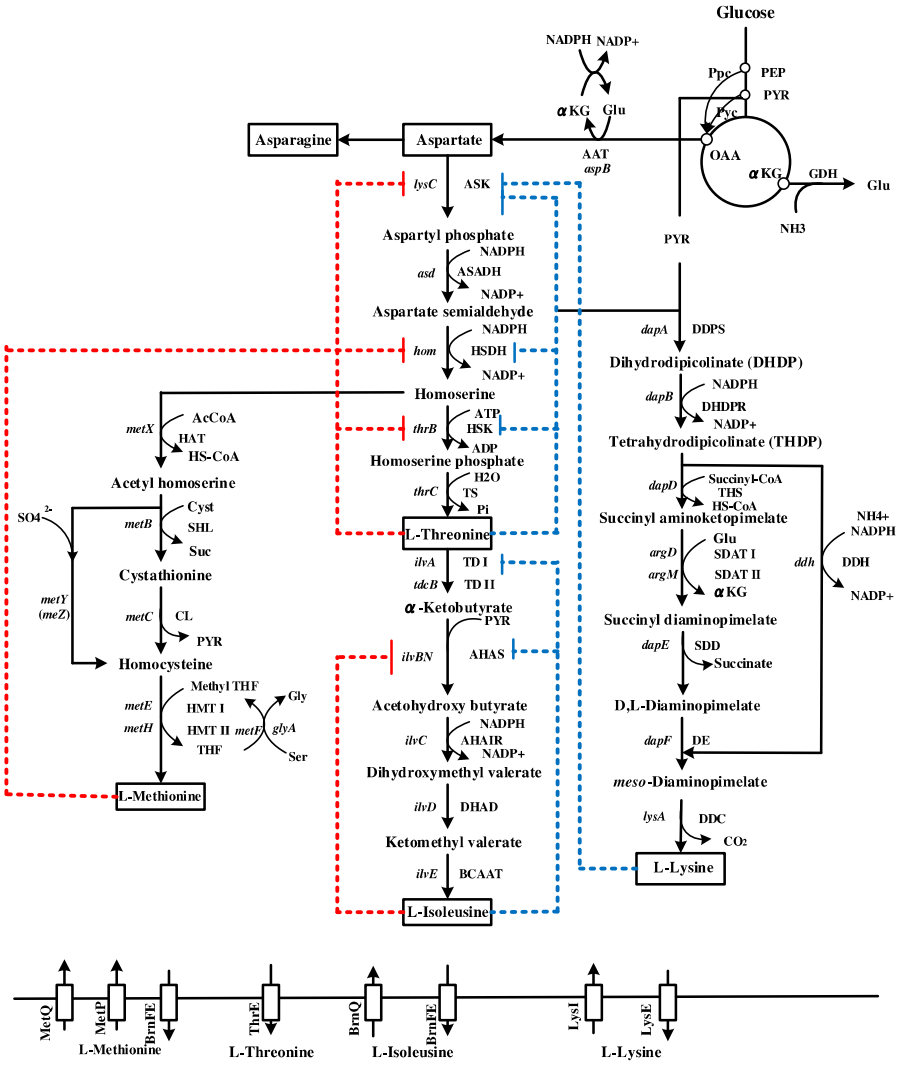

In *C. glutamicum*, aspartate kinase is encoded only by the *lysC* gene, and its activity is synergistically inhibited by L-threonine and L-lysine. The homoserine dehydrogenase is encoded by *hom*, and its expression is slightly feedback repressed by L-methionine, and the activity of homoserine dehydrogenase (HSDH) is feedback inhibited by L-threonine.

The expression of *thrB* is slightly repressed by L-methionine, and the activity of homoserine kinase is feedback inhibited by L-theronine. *C. glutamicum* uses both succinylase and the dehydrogenase variant to synthesize lysine. The last step of lysine synthesis is catalyzed by *meso*-DAP decarboxylase (DDC) encoded by *lysA*. Unlike *E. coli*, the lysine branch is almost free from feedback inhibition in *C. glutamicum*.

In *C. glutamicum*, homoserine is condensed with AcCoA to produce acetyl homoserine by homoserine acetyltransferase (HAT) encoded by *metX*. The methionine synthesis is carried out by two parallel pathways. Acetyl homoserine is converted into homocysteine either by transsulfuration pathway or by direct sulfhydrylation that utilizes inorganic sulfur instead of cysteine. MetR complexed with L-homoserine controls transcription of several genes involved in methionine biosynthesis.

References

Adamson, DN., H.N. Lim. 2013. Rapid and robust signaling in the CsA cascade via RNA-protein interactions and feedback regulation. PNAS USA. 110 (32): 13120-13125.

Agrawal, D.K., R. Marshall, V. Noireaux, E.D. Sontag. 2019. *In vitro* implementation of robust gene regulation in a synthetic biomolecular integral controller. Nat Commun. 10: 5760.

Alifano, P., R. Fani, P. Lio, A. Lazcano, M. Bazzicalupo, M.S. Carlomagno, C.B. Bruni. 1996. Histidine biosynthetic pathway and genes: structure, regulation, and evolution. Microbiol Rev. 60(1): 44-69.

Alvarado, A., W. Behrens, C. Josenhans. 2010. Protein Activity Sensing in Bacteria in Regulating Metabolism and Motility. Front. Microbiol. 10: 3055.

Atkinson, G.C., T. Tenson, V. Hauryliuk. 2011. The RelA/SpoT homologue (RSH) superfamily: distribution and functional evolution of ppGpp synthetase and hydrolases across the tree of life. PLoS One. 6: e23479.

Awano, N., M. Wada, A. Kondoh, T. Oikawa, H. Takagi, S. Nakamori. 2003. Effect of cysteine desulfhydrase gene disruption on L-cysteine overproduction in *Escherichia coli*. Appl Microbiol Biotechnol. 62: 239-243.

Awano, N., M. Wada, H. Mori, S. Nakamori, H. Takagi. 2005. Identification and functional analysis of *Escherichia coli* cysteine desulfhydrase. Appl Environ Microbiol. 71(7): 4149-4152.

Azuma, S., H. Tsunekawa, M. Okabe, R. Okamoto, S. Aiba. 1993. Hyper-production of L-tryptophan via fermentation with crystallization. Appl Microbiol Biotechnol. 39: 471-476.

Barabote, R.D., M.H. Sair, Jr. 2005. Comparative genomic analysis of the bacterial phosphotransferase system. Microbiol Mol Biol Rev. 69(4): 608-634.

Bartek, T. *et al*. 2010. Importance of NADPH supply for improved L-valine formation in *Corynebacterium glutamicum*. Biotechnol Prog. 26: 361–371.

Basan, M., T. Honda, D. Christidoulou, M. Horl, Y.-F. Chang, E. Leoncini, A. Mukherjee, H. Okano, B.R. Taylor, J.M. Silverman, C. Sanchez, J.R. Williamson, J. Paulsson, T. Hwa, U. Sauer. 2020. A universal tradeoff between growth and lag in fluctuating environments. Nature. 584(7821): 470-474.

Becker, J., O. Zelder, S. Hafner, H. Schroder, C. Wittmann. 2011. From zero to hero-Design-based systems metabolic engineering of *Corynebacterium glutamicum* for L-lysine production. Metab Eng. 13: 159-168.

Beisel, C.L., T. Afroz. 2016. Rethinking the Hierarchy of Sugar Utilization in Bacteria. J Bacteriol. J Bacteriol. 198(3): 374–376.

Beljantseva, J., P. Kudrin, S. Jimmy, M. Ehn, R. Pohl, V. Varik, Y. Tozawa, V. Shingler, T. Tenson, D. Rejiman, V. Hauryliuk. 2017. Molecular mutagenesis of ppGpp: turning a RelA activator into an inhibitor. Sci. Rep. 7: 41839.

Bennett, B., E.H. Kimball, M. Gao, R. Osterhout, S.J. van Dien, J.D. Rabinowitz. 2009. Absolute metabolite concentrations and implied enzyme active site occupancy in *Escherichia coli*. Nat Chem Biol. 5(8): 593-599.

Bhatt, S.,A.N. Edwards, H.T. Nguyen, D. Merlin,T. Romeo, D. Kalman. 2009. The RNA binding protein CsrA is a pleiotropic regulator of the locus of enterocyte effacement pathogenicity island of enteropathogenic *Escherichia coli*. Infect Immun.77: 3552–3568.

Bin, Z., W. Fang, Q.Y. Lou, C.X. Lan, T. Li, C.J. Cong, X.Y. Hua. 2015. Increased L-arginine production by site-directed mutagenesis of N-acetyl-L-glutamate kinase and *proB* gene deletion in *Corynebacterium glutamicum*. Biomed Environ Sci. 28(12): 864-874.

Biselli, E., S.J. Schink, U. Gerland. 2020. Slower growth of *Escherichia coli* leads to longer

survival in carbon starvation due to a decrease in the maintenance rate. Mol Syst Biol. 16: e9478.

Bosdriesz, E., D. Molenaar, B. Teusink, F.J. Bruggeman. 2015. How fast-growing bacteria robustly tune their ribosome concentration to approximate growth rate maximization. FEBS J. 282: 2029-2044.

Brauer, M.J., J. Yuan, B.D. Bennet, W. Lu, E. Kimball, D. Botstein, J.D. Rabinowitz. 2006. Conservation of the metabolomic response to starvation across two divergent microbes. PNAS USA. 103(51): 19302-19307.

Briat, C., A. Gupta, M. Khammash. 2016. Antithetic integral feedback ensures robust perfect adaptation in noisy biomolecular networks. Cell Syst. 2: 15-26.

Caldara, M., G. Dupont, F. Leroy, A. Goldbeter, L. De Vuyst, R. Cunin. 2008. Arginine biosynthesis in *Escherichia coli*: Experimental perturbation and mathematical modeling. J Biol Chem. 283(10): 6347-6358.

Caldala, M., D. Charlier, R. Cunin. 2006. The arginine regulon of *Escherichia coli*: whole-system transcriptome analysis discovers new genes and provides an integrated view of arginine regulation. Microbiol. 152: 3343-3354.

Chaix, D., M.L. Ferguson, C. Atmanene, A. Van Dorsselaer, S. Sanglier-Cianférani, C.A. Royer, N. Declerck. 2010. Physical basis of the inducer-dependent cooperativity of the Central glycolytic genes Repressor/DNA complex. Nucleic Acids Res.38(17): 5944–5957.

Charlier, D., P.N. Le Minh, M. Roovers. 2018. Regulation of carbamoylphosphate synthesis in *Escherichia coli*: an amazing metabolite at the crossroad of arginine and pyrimidine biosynthesis. Amino acids. 50: 1647-1661.

Chassagnole, C., B. Rais, E. Quentin, D.A. Fell, J.-P. Mazat. 2001. An integrated study of threonine-pathway enzyme kinetics in *Escherichia coli*. Biochem J. 356: 415-423.

Chavez-Bejar, M.I., A.R. Lara, H. Lopez, G. Hernandez-Chavez, A. Martinez, O.T. Ramirez, F. Bolivar, G. Gosset. 2008. Metabolic engineering of *Escherichia coli* for L-tyrosine production by expression of genes coding for chorismate mutase domain of the native chorismate

mutase-prephenate dehydratase and a cyclohexadienyl dehydrogenase from *Zymomonas mobilis*. Appl Envion Microbiol. 74(10): 3284-3290.

Chen Z, R.R. Bommareddy, D. Frank, S. Rappert, A.P. Zeng. 2014. Deregulation of feedback inhibition of phosphoenolpyruvate carboxylase for improved lysine production in *Corynebacterium glutamicum*. Appl Environ Microbiol. 80: 1388–1393.

Chen, C., Y. Li, J. Hu, X. Dong, X. Wang. 2015. Metabolic engineering of *Corynebacterium glutamicum* ATCC13869 for L-valine production. Metab Eng. 29: 66-75.

Chen, L., M. Chen, C. Ma, A.-P. Zeng. 2018a. Discovery of feed-forward regulation in L-tryptophan biosynthesis and its use in metabolic engineering of *E. coli* for efficient tryptophan bioproduction. Metabolic Eng. 47: 434-444.

Chen, Y., Y. Liu, D. Ding, L. Cong, D. Zhang. 2018b. Rational design and analysis of an *Escherichia coli* strain for high-efficiency tryptophan production. J Ind Microbiol Biotechnol. https://doi.org/10.1007/s10295-018-2020-x.

Chevalier, F., L. Cuyas, J. Jouhet, V. Gros, S. Chiarenza, D. Secco, J. Whelan, K. Seddiki, M.A. Block, L. Nussaume, E. Marechal. 2019. Interplay between Jasmonic Acid, Phosphate Signaling and the Regulation of Glycerolipid Homeostasis in Arabidopsis. Plant Cell Physiol. 60(6): 1260–1273.

Chavez, R.G.,A.F. Alvalez, T. Romeo, D. Georgellis. 2010. The physiological stimulus for the BarA sensor kinase. J Bacteriol. 92: 2009-2012.

Cho, B.-K., S. Federowicz, Y.-S. Park, K. Zengler, B.Ø. Palsson. 2013. Deciphering the transcriptional regulatory logic of amino acid metabolism. Nat Chem Biol. 8: 65.

Cho, B.-K., S.A. Federowicz, M. Embree, Y.-S. Park, D. Kim, B.O. Palsson. 2011. The PurR regulon in *Escherichia coli* K-12 MG1655. Nucleic Acids Res. 39(15): 6456-6464.

Choe, M., Y.-H. Park, C.-R. Lee, Y.-R. Kim, .-J. Seok. 2017. The general PTS component HPr determines the preference for glucose over mannitol. Sci Rep. 7: 43431.

Chubukov, V., L. Gerosa, K. Kochanowski, U. Sauer. 2014. Coordination of microbial

metabolism. Nature Rev Microbiol. 12: 327-340.

Csete, M., J. Doyle.2004. Bow ties, metabolism and disease. Trends Biotechnol. 22(9):446-50.

Dai X, M. Zhu, M. Warren, R. Balakrishnan, H. Okano, J.R. Williamson, K. Fredrick, T. Hwa. 2018. Slowdown of Translational Elongation under Hyperosmotic Stress. MBio. 9(1); e02375-17.

Dai, X., M. Zhu, M. Warren, R. Balakrishnan, V. Patsalo, H. Okano, J.R. Williamson, K. Fredrick, Y.-P. Wang, T. Hwa. 2016. Reduction of translating ribosomes enables *Escherichia coli* to maintain elongation rates during slow growth. Nat Microbiol. 2: 16231.

Deutscher, J. et al. 2014. The bacterial phosphoenolpyruvate: carbohydrate phosphotransferase system: regulation by protein phosphorylation and phosphorylation dependent protein-protein interactions. Microbiol Mol Biol Rev. 78: 231-256.

Ding, D., Y. Liu, Y. Xu, P. Zheng, H. Li, D. Zhang, J. Sun. 2016. Improving the production of L-phenylalanine by identifying key enzymes through multi-enzyme reaction system *in vito*. Sci Rep. 6: 32208.

Dong, X., P.J. Quinn, X. Wang, 2011. Metabolic engineering of *Escherichia coli* and *Corynebacterium glutamicum* for the production of L-threonine. Biotechnol Adv. 29: 11-23.

Dong, X., Y. Zhao, J. Hu, Y. Li, X. Wang. 2016a. Attenuating L-lysine production by deletion of *ddh* and *lysE* and their effect on L-threonine and L-isoleusine production in *Corynebacterium glutamicum*. Enzyme Microbial Technol. 93-94: 70-78.

Dong, X., Y. Zhao, J. Zhao, X. Wang. 2016b. Characterization of aspartate kinase and homoserine dehydrogenase from *Corynebacterium glutamicum* JWJ001 and systematic investigation of L-isoleusine biosynthesis. J Ind Microbiol Biotechnol. 43(6): 873-885.

Doroshenko, V.G., A.O. Lobanov, E.A. Fedorina. 2013. The directed modification of *Escherichia coli* MG1655 to obtain histidine-producing mutants. Appl Biochem Microbiol. 49(2): 130-135.

Doucette, C.D., D.J.Schwab, N.S.Wingreen, J.D.Rawbinowitz. 2011. A-Ketoglutarate

coordinates carbon and nitrogen utilization via enzyme I inhibition. Nature Chem Biol. 7: 894-901.

Du, L. Z. Zhang, Q. Xu, N. Che. 2019. Central metabolic pathway modification to improve L-tryptophan production in *Escherichia coli*. Bioeng. 10 (1): 59–70.

D'Este, M., M. Alvarado-Morales, I. Angelidaki. 2018. Amino acids production focusing on fermentation technologies-a review. Biotechnol Adv.36: 14-25.

Eberhardt, D., J.V.K. Jensen, V.F. Wendisch. 2014. L-Citrulline production by metabolically engineered *Corynebacterium glutamicum* from glucose and alternative carbon sources. AMB Express. 4: 85.

Edwards, A.N., L.M. Patterson-Fortin, C.A. Vakulskas, J.W. Mercante, K. Potrykus, D.Vinella et al. 2011. Circuitry linking the Csr and stringent response global regulatory systems. Mol Microbiol. 80:1561-1580.

Enjalbert, B., F. Letisse, J.-C. Portais. 2013. Physiological and molecular timing of the glucose to acetate transition in *Escherichia coli*. Metabolites. 3: 820-837.

Enjalbert, B., M. Cocaign-Bousquet, J.-C. Portais, F. Letisse. 2015. Acetate exposure determines the diauxic behavior of *Escherichia coli* during the glucose-acetate transition. J Bacteriol. 197(19): 3173-3181.

Fang, Y., J. Wang, W. Ma, J. Yang, H. Zhang, L. Zhao, S. Chen, S. Zhang, X. Hu, Y. Li, X. Wang. 2020. Rebalancing microbial carbon distribution for L-threonine maximization using a thermal switch system. Metab Eng. 61: 33-46.

Feng, B., C.S. Mandava, Q. Guo, J. Wang, W. Cao, N. Li, Y. Zhang, Y. Zhang, Z. Wang, J. Wu, S. Sanyal, J. Lei, N. Gao. 2014. Structural and functional insights into the mode of action of a universally conserved CGTase. PLoS Biol. 1(5): e1001866.

Feng, L.-Y., J.-Z. Xu, W.-G. Zhang. 2018. Improved L-Leucine Production in *Corynebacterium glutamicum* by Optimizing the Aminotransferases. Molecules. 23: 2102.

Ferla, M.P., W.M. Patrick. 2014. Bacterial methionine biosynthesis. Microbiol. 160: 1571-1584.

Folly, B.B., A.D. Ortega, G. Hubmann, S. Bonsing-Vedelaar, H.J. Wijma, P. van der Meulen, A. Milias-Argeitis, M. Heinemann. 2018. Assessment of the interaction between the flux-signaling metabolite fructose-1, 6-bisphosphate and the bacterial transcription factors CggR and Cra. Mol Microbiol. 109(3): 278–290.

Fordjour, E., F.K. Adipah, S. Zhou, G. Du, J. Zhou. 2019. Metabolic engineering of *Escherichia coli* BL21 (DE3) for de novo production of L-DOPA from D-glucose. Micobial Cell Fact. 18: 74.

Francis, V.I., S.L. Porter. 2019. Multikinase networks: two-component signaling networks integrating multiple stimuli. Annu Rev Microbiol. 73: 199–223.

Friedlander, T., A.E. Mayo, T. Tlusty, U. Alon. 2015. Evolution of bow-tie architectures in biology. PLoS Comp Biol. 11(3): e1004055.

Fuentes, D.A.F, P. Manfredi, U. Jenal, M. Zampieri. 2021. Pareto optimality between growth-rate and lag-time couples metabolic noise to phenotypic heterogeneity in *Escherichia coli*. Nat Commun. 12: 3204.

Fujita, Y. 2009. Carbon catabolite control of the metabolic network in *Bacillus subtilis*. Biosci Biotechnol Biochem. 73(2):245-59.

Gao, H., P. Tuyishime, X. Zhang, T. Yang, M. Xu, Z. Rao. 2021. Engineeing of microbial cells for L-valine production: challenges and opportunities. Microb Cell Fact. 20: 172.

Geraskina, N., E.V. Sycheva, V.V. Samsonov, N.E. Eremina, C.D. Hook, V.A. Serebrianyi, N.V. Stoynova. 2019. Engineering *Escherichia coli* for autoinducible production of L-valine: An example of an artificial positive feedback loop in amino acid biosynthesis. PLoS One. 14(4): e0215777.

Gerosa, L., K. Kochanowski, M. Heinemann, U. Sauer. 2013. Dissecting specific and global transcriptional regulation of bacterial gene expression. Mol Syst Biol. 9: 658.

Gerosa, L., R.B. Bart, H. van Rijsewijk, D. Christodoulou, K. Kochanowski, T.S.B. Schmidt, E. Noor, U. Sauer. 2015. Pseudo-transition analysis identifies the key regulators of dynamic

metabolic adaptation from steady-state data. Cell Syst. 1: 270-282.

Ginesy, M., J. Belotserkovsky, J. Enman, L. Isaksson, U. Rova. 2015. Metabolic engineering of *Escherichia coli* for enhanced arginine biosynthesis. Microb Cell Fact. 14: 29.

Giordano, N., F. Mairet, J.L. Gouze, J. Geiselmann, H. de Jong. 2016. Dynamic allocation of cellular resources as an optimal control problem: Novel insights into microbial growth strategies. PLoS Comp Biol. 12(3): e1004802.

Gorke, B. and J. Stulke. 2008. Carbon catabolite repressionin bacteria: many ways to make the most out of nutrients. Nat Microbiol Rev. 6: 613-623.

Grant, G.A. 2012. Contrasting catalytic and allosteric mechanisms for phosphoglycerate dehydrogenases. Arch Biochem Biophys. 519(2): 175-185.

Gu, P., F. Yang, J. Kang, Q. Wang, Q. Qi. 2012. One-step of tryptophan attenuator inactivation and promote swapping to improve the production of L-tryptophan in *Escherichia coli*. Microbial Cell Fact. 11: 30.

Gu, P., F. Yang, T. Su, F. Li, Y. Li, Q. Qi. 2014. Construction of an L-serine producing *Escherichia coli* via metabolic engineering. J Ind Microbiol Biotechnol. 41: 1443-1450.

Gualerzi, C.O., C.L. Pon. 2015. Initiation of mRNA translation in bacteria: structural and dynamic aspects. Cell Mol Life Sci. 72: 4341-4367.

Guedon, E., I. Martin-Vestraete. 2006. Cysteine metabolism and its regulation in bacteria. Microbiol Monogr. DOI.10.1007/7171_2006_060.

Hao, N., J. Mu, N. Hu, S. Xu, M. Yan, Y. Li, K. Guo, L. Xu. 2015. Improvement of L-citrulline production in *Corynebacterium glutamicum* by ornitine acetyltransferase. Metab Eng Synth Biol. 42: 307-313.

Hao, N., Jr. Mu, N. Hu, S. Xu, M. Yan, Y. Li, K. Guo, L. Xu. 2015. Improvement of L-citrulline production in *Corynebacterium glutamicum* by ornithine acetyltransferase. J Ind Microbiol Biotechnol. 42: 307-313.

Hao, Y., Q. Ma, X. Liu, X. Fan, J. Men. H. Wu, S. Jiang, D. Tian, B. Xiong, X. Xie. 2020. High-yield production of L-valine in engineered *Escherichia coli* by a novel two-stage fermentation. Metab Eng. 62: 198-206.

Hauryliuk, V., G.C. Atkinson, K.S. Murakami, T. Tenson, K. Gerdes. 2015. Recent functional insights into the role of (p)ppGpp in bacterial physiology. Nat Rev Microbiol. 13(5): 298-309.

He, F., M.P.H. Stumpf. 2019. Quantifying dynamic regulation in metabolic pathways with nonparametric flux inference. Biophys J. 116: 2035-2046.

He, B., K.Y. Choi, H. Zalkin. 1993. Regulation of *Escherichia coli glnB*, *prsA*, and *speA* by the purine repressor. J Bacteriol. 175(11): 3598-3606.

Hermsen, R., H. Okano, C. You, N. Werner, T. Hwa. 2015. A growth-rate composition formula for the growth of *E. coli* on co-utilized carbon substrate. Mol Syst Biol. 11: 801.

Hogema, B.M. et al. 1998. Inducer exclusion in *Escherichia coli* by non-PTS substrates : the role of the PEP to pyruvate ratio in determining the phosphorylation state of enzyme IIA^{Glc}. Mol Microbiol. 30: 487-498.

Hogg, T., U. Mechold, H. Malke, M. Cashel, R. Hilgenfeld. 2004. Conformational antagonism between opposing active sites in a bifunctional RelA/SpoT homolog modulates (p)ppGpp metabolism during the stringent response. Cell. 117(1): 57-68.

Hollinshead, W.D., S. Rodriguez, H.G. Martin, G. Wang, E.E.K. Baidoo, K.L. Sale, J.D. Keasling, A. Mukhopadhyay, Y.J. Tang. 2016. Examining *Escherichia coli* glycolytic pathways, catabolite repression, and metabolite channeling using Δ*pfk* mutants. Biotechnol Biofuels. 9: 212.

Huang, J.-F., Z.-Q. Liu, L.-Q. Jin, X.-L. Tang, Z.-Y. Shen, H.-H. Yin, Y.-G. Zheng. 2017. Metabolic engineering of *Escherichia coli* for microbial production of L-methionine. Biotechnol Bioeng. 114: 843-851.

Huang, J.-F., Z.-Y. Shen, Q.-L. Mao, X.-M. Zhang, B. Zhang, J.-S. Wu, Z.-Q. Liu, Y.-G. Zheng. 2018. Systematic analysis of bottlenecks in multibranched and multilevel regulated pathway:

The molecular fundamentals of L-methionine biosynthesis in *Escherichia col*. ACS Synth Biol. 7(11): 2577-2589.

Huang, Q., L. Liang, W. Wu, S. Wu, J. Huang. 2017. Metabolic engineering of *Corynebacterium glutamicum* to enhance l-leucine production. Afr. J. Biotechnol. 16: 1048–1060.

Huccetogullari, D., Z.W. Luo, S.Y. Lee. 2019. Metabolic engineering of microorganisms for production of aromatic compounds. Microb Cell Fact. 18: 41.

Huergo, L.F., R.Dixon. 2015. The emergence of 2-oxoglutarate as a master regulator metabolite. Microbiol Mol Biol Rev. 79(4): 419-435.

Ikeda, M., S. Mitsuhashi, K. Tanaka, M. Hayashi. 2009. Reengineering of a *Corynebacterium glutamicum* L-arginine and L-citrulline producer. Appl Environ Microbiol. 75(6): 1635-1641.

Ishii, N., K. Nakahigashi, T. Baba, M. Robert, T. Soga, A. Kanai, T. Hirasawa, M. Naba, K. Hirai, A. Hoque, P.Y. Ho, Y. Kakazu, K. Sugawara, S. Igarashi, S. Harada, T. Masuda, N. Sugiyama, T. Togashi, M. Hasegawa, Y. Takai, K. Yugi, K. Arakawa, N. Iwata, Y. Toya, Y. Nakayama, T. Nishioka, K. Shimizu, H. Mori, M. Tomita. 2007. Multiple high-throughput analyses monitor the response of *E. coli* to perturbations. Science, 316: 593-597.

Jensen, K.F., G. Dandanell, B. Hove-Jensen, M. WillemoEs. 2008. Nucleotides, nucleosides, and nucleobases. EcoSal Plus. 3(1).doi:10.1128/ecosalplus.3.6.2.

Jensen, J.V.K., D. Eberhardt, V.F. Wendisch. 2015. Modular pathway engineering of *Corynebacterium glutamicum* for production of the glutamate-derived compounds ornitine, proline, putrescine, and arginine. J. Biotechnol. 214: 85-94.

Jensen, J.V.K., V.F. Wendisch. 2013. Ornithine cyclodeaminase-based proline production by *Corynebacterium glutamicum*. Micob Cell Fact. 12: 63.

Jiang, M., S.M. Sullivan, P.K. Wout, J.R. Maddock. 2007. G-protein control the ribosome-associated stress protein SpoT. J Bacteriol. 189(17): 6140-6147.

Jing, K., Y. Tang, C. Yao, E.A. del Rio-Chanona, X. Ling, D. Zhang. 2018. Overproduction of L-tryptophan via simultaneous feed of glucose and anthranillic acid from recombinant

Escherichia coli W3110: kinetic modeling and process scale-up. Biotechnol Bioeng. Doi: 10.1002/bit26398.

Jovanovic, M., M. Lilic, D.J. Savic, G. Jovanovic. 2003. The Lys-type tanscriptional regulator CysB controls the repression of *hslJ* transcription in *Escherichia coli*. Microbiol. 149: 3449–3459.

Jung H.-M., D.-K. Im, J.H. Lim, G.Y. Jung, M.-K. Oh. 2019. Metabolic perturbations in mutants of glucose transporters and their applications in metabolite production in *Escherichia coli*. Microb Cell Fact. 18: 170.

Kafri, M., E. Metzl-Raz, G. Jona, N. Barkai. 2016. The Cost of Protein Production. Cell Rep. 14, 22–31.

Kaiser, F., S. Krautwurst, S. Salentin, V.J. Haupt, C. Leberecht, S. Bittrich, D. Labudde, M. Schroeder. 2020. The tructural basis of the genetic code: amino acid recognition by aminoacyl-tRNA synthetases. Sci Rep. 10: 12647.

Keseler I.M., A. Mackie, M. Peralta-Gil, A. Santos-Zavaleta, S. Gama-Castro, C. Bonavides-Martinez, C. Fulcher, A.M. Huerta, A. Kothari, M. Krummenacker, M. Latendresse, L. Muniz-Rascado, Q. Ong, S. Paley, I. Schroder, A.G. Shearer, P. Subhraveti, M. Travers, D. Weerasinghe, V. Weiss, J. Collado-Vides, R.P. Gunsalus, I. Paulsen, P.D. Karp. 2013. EcoCyc: fusing model organism databases with systems biology. Nucleic Acids Res. 41: D605-D612.

Khammash, M. 2016. An engineering viewpoint on biological robustness. BMC Biology. 14: 22.

Kikuchi, G., Y. Motokawa, T. Yoshida, K. Hiraga. 2008. Glycine cleavage system: reaction mechanism, physiological significance, and hyperglycinemia. Proc. Jpn Acad Ser. 84: 246-263.

Kim, B., R. Binkley, H.U. Kim, S.Y. Lee. 2018. Metabolic engineering of *Escherichia coli* for the enhanced production of L-tyrosine. Biotechnol Bioeng. https://doi.org/10.1002/bit26797.

Kim, D., S.W. Seo, Y. Gao, H. Nam, G.I. Guzman, B.-K. Cho, B.O. Palsson. 2018. Systems assessment of transcriptional regulation on central carbon metabolism by Cra and Crp. Nucleic

Acids Res. 46(6): 2901–2917.

Kim, D., Y.K. Kwon, K.H. Cho. 2007. Coupled positive and negative feedback circuits form an essential building block of cellular signaling pathways. Bioassays. 29: 85–90.

Kim, S.C., B.E. Min, H.G. Hwang, S.W. Seo, G.Y. Jung. 2015. Pathway optimization by redesign of untranslated regions for L-tyrosine production in *Escherichia coli*. Sci Rep. 5: 13853.

Kim, S.Y., J. Lee, S.Y. Lee. 2015. Metabolic engineering of *Corynebacterium glutamicum* for the production of L-ornithine. Biotechnol Bioeng. 112: 416–421.

Kitano, H. 2004. Biological robustness. Nature. 5: 826-837.

Kitano, H. 2007. Towards a theory of biological robustness. Mol Syst Biol. 3: 137.

Klumpp, S., M. Scott, S. Pedersen, T. Hwa. 2013. Molecular crowding limits translation and cell growth. PNAS U.S.A. 110, 16754–16759.

Kochanowski, K., L. Gerosa, S.F. Brunner, D. Christoulou, Y.V. Nikolaev, U. Sauer. 2017. Few regulatory metabolites coordinate expression of central metabolic genes in *Escherichia coli*. Mol Sys Biol. 13: 903.

Kochanowski, K., Volkmer, B., Gerosa, L., van Rijsewijk, H.B.R., Schmidt, A., Heinemann, M. 2013. Functioning of a metabolic flux sensor in *Escherichia coli*. PNAS USA 110: 1130–1135.

Koirala, S., X. Wang, C.V. Rao. 2015. Reciprocal regulation of l-arabinose and d-xylose metabolism in *Escherichia coli*. J Bacteriol. 198(3): 386-33.

Kondoh, M., T. Hirasawa. 2019. L-Cysteine production by metabolically engineered *Corynebacterium glutamicum*. Appl Microbiol Biotechnol. 103: 2609-2619.

Kotte, O., B. Volkmer, J.L. Radzikowski, M. Heinemann. 2014. Phenotypic bistability in *Escherichia coli*'s central carbon metabolism. Mol Syst Biol. 10(7): 736.

Kotte, O., J.B. Zaugg, M. Heinemann. 2010. Bacterial adaptation through distributed sensing of

metabolic fluxes. Mol Syst Biol. 6: 355.

Kremling, A., K. Bettenbrock, E.D. Gilles. 2008. A feed-forward loop guarantees robust behavior in *Escherichia coli* carbohydrate uptake. Bioinformatics. 24: 704-710.

Kroner, G.M., M.B. Wolfe, P.L. Freddolino. 2019. *Escherichia coli* Lrp regulates one-third of the genome via direct, cooperative, and indirect routes. J Bacteriol. 201(3): e00411-e00418.

Lange, C., N. Mustafia, J. Frunzke, N. Kennerknecht, M. Wessel, M. Bott, V.F. Wendisch. 2012. Lrp of *Corynebacterium glutamicum* controls expression of the *brnFE* operon encoding the export system for L-methionine and branched-chain amino acids. J Biotechnol. 158: 231– 241.

Lee, H.-W., H.-S. Lee, C.-S. Kim, J.-G. Lee, W.-K. Kim, E.-G. Lee, H.-W. Lee. 2018. Enhancement of L-Threonine Production by Controlling Sequential Carbon-Nitrogen Ratios during Fermentation. J Microbiol Biotechnol. 28(2): 293–297.

Lee, K.H., J.H. Park, T.Y. Kim, H.U. Kim, S.Y. Lee 2007. Systems metabolic engineering of *Escherichia coli* for L-threonine production. Mol Syst Biol. 3: 149.

Lehning, C.E., S. Siedler, M.M.H. Ellabaan, M.O.A. Sommer. 2017. Assessing glycolytic flux alterations resulting from genetic perturbations in *E. coli* using a biosensor. Metab Eng. 42: 194–202.

Lempp, M., N. Farke, M. Kuntz, S.A. Freibert, R. Lill, H. Link. 2019. Systematic identification of metabolites controlling gene expression in *E. coli*. Nat Commun. 10: 4463.

Leng, Y., C.A. Vakulskas, T.R. Zere, B.S. Pickering, P.L. Watnick, P. Babitzke, T. Romeo. 2016. Regulation of CsrB/C sRNA decay by $EIIA^{Glc}$ of the phosphoenolpyruvate carbohydrate phosphotransferase system. Mol Microbiol. 99(4): 627-639.

Li, G., Z. Chen, N. Chen, Q. Xu. 2020. Enhancing the efficiency of L-tyrosine by repeated batch fermentation. Bioengineered. 11(1): 852-861.

Li, H., B. Wang, L. Zhu, S. Cheng. 2016. Metabolic engineering of *Escherichia coli* W3110 for L-homoserine production. Proc Biochem. 51(12): 1973-1983.

Li, M., C. Liu, J. Yang, R. Nian, M. Xian, F. Li, H. Zhang. 2020. Common problems associated with the microbial production of aromatic compounds and corresponding metabolic engineering strategies. Biotechnol Adv. Doi.og/10.1016/j.biotechnoladv.2020.1075-48.

Li, Y., H. Cong, B. Liu, J. Song, X. Sun, J. Zhang, Q. Yang. 2016. Metabolic engineering of *Corynebacterium glutamicum* for methionine production by removing feedback inhibition and increasing NADPH level. Antonie Van Leeuwenhoek. 109(9): 1185-1197.

Li, Y., H. Wei, T. Wang, Q. Xu, C. Zhang, X. Fan, Q. Ma, N. Chen, X. Xie. 2017. Current status on metabolic engineering for the production of L-aspartate family amino acids and derivatives. Bioresour Technol. 245: 1588-1602.

Liang, Q., F. Zhang, Y. Li, X. Zhang, J. Li, P. Yang, Q. Qi. 2015. Comparison of individual component deletions in a glucose-specific phosphotransferase system revealed their different applications. Sci Rep 5: 13200.

Lindner, S.N., D.P. Petrov, C.T. Hagmann, A. Henrich, R. Krämer, B.J. Eikmanns, V.F. Wendisch, G.M. Seibold. 2013. Phosphotransferase System-Mediated Glucose Uptake Is Repressed in Phosphoglucoisomerase-Deficient *Corynebacterium glutamicum* Strains. Appl Environ Microbiol. 79(8): 2588–2595.

Litsios, A., A.D. Ortega, E.C. Wit, M. Heinemann. 2018. Metabolic-flux dependent regulation of microbial physiology. Curr Opin Microbiol. 42: 71-78.

Liu, H., G. Fang, H. Wu, Z. Li, Q. Ye. 2018. L-Cysteine production in *Escherichia coli* based on rational metabolic engineering and modular strategy. Biotechnol J. https://doi.org/10.1002/biot.201700695.

Liu, H., Y. Hou, Y. Wang, Z. Li. 2020. Enhancement of sulfur conversion rate in the production of L-cysteine by engineered *Escherichia coli*. J Agric Food Chem. 68: 250-257.

Liu, J., H. Li, H. Xiong, X. Xie, N. Chen, G. Zhao, Q. Caiyin, H. Zhu, J. Qiao. 2019. Two-stage carbon distribution and cofactor generation for improving L-threonine production of *Escherichia coli*. Biotechnol Bioeng. 116: 110-120.

Liu, L., M. Bilal, H. Luo, Y. Zhao, H.M.N. Iqbal. 2019. Metabolic engineering and fermentation

process strategies for L-tryptophan production by *Escherichia coli*. Processes. 7: 213.

Liu, L., X. Duan, J. Wu. 2016. L-Tryptophan Production in *Escherichia coli* Improved by Weakening the Pta-AckA Pathway. PLoS ONE. doi:10.1371/journal.pone.0158200.

Liu, P., B. Zhang, Z.-H. Yao, Z.-Q. Liu, Y.-G. Zheng. 2020. Multiplex Design of the Metabolic Network for Production of l-Homoserine in *Escherichia coli*. Appl Environ Microbiol. 86: e01477-20.

Liu, R., L. Liang, E.F. Freed, A. Choudhury, G.A. Eckert, R.T. Gill. 2020. Engineering regulatory networks for complex phenotypes in *E. coli*. Nat Commun. 11: 4050.

Liu, W.D. et al. 2015. Structural analysis reveals the substrate-binding mechanism for the expanded substrate specificity of mutant meso-diaminopimelate dehydrogenase. Chembiochem. 16: 924–929.

Liu, Y., Q. Li, P. Zheng, Z. Zhang, Y. Liu, C. Sun, G. Cao, W. Zhou, X. Wang, D. Zhang, T. Zhang, J. Sun, Y. Ma. 2015. Developing a high-throughput screening method for threonine overproduction based on artificial promoter. Microb cell Fact. 14: 121.

Liu, Y., Y. Xu, D. Ding, J. Wen, B. Zhu, D. Zhang. 2018. Genetic engineering of *Escherichia coli* to improve L-phenylalanine production. BMC Biotechnol. 18:5.

Liu, Y.-K., H.-C. Kuo, C.H. Lai, C.-C. Chou. 2020. Single amino acid utilization for bacterial categorization. Sci Rep. 10: 12686.

Locasale, J.W. 2018. New concepts in feedback regulation of glucose metabolism. Curr Opin Systems Biol. 8: 32-38.

Long, M., M. Xu, Z. Ma, X. Pan, J. You, M. Hu, Y. Shao, T. Yang, X. Zhang, Z. Rao. 2020. Significantly enhancing production of *trans*-4-hydroxy-L-proline by integrated system engineering in *Escherichia coli*. Sci. Adv. 6: eaba2383.

Ludwig, H., N. Rebhan, H.□M. Blencke, M. Merzbacher, J. Stülke. 2002. Control of the glycolytic *gapA* operon by the catabolite control protein A in *Bacillus subtilis*: a novel mechanism of CcpA□mediated regulation. Mol Microbiol. 45(2): 543-553.

Lutke-Eversloh, T. , G. Stephanopoulos. 2007. L-Tyrosine production by deregulated strains of *Escherichia coli*. Appl Microbiol Biotechnol. 75: 103-110.

Lux, R., K. Jahreis, K. Bettenbrock, J.S. Parkinson, J. W. Lengeler. 1995. Coupling the phosphotransferase system and the methyl-accepting chemotaxis protein-dependent chemotaxis signaling pathways of *Escherichia coli*. PNAS USA. 92(25): 11583–11587.

Maas, W.K. 1994. The arginine repressor of *Escherichia coli*. Microbiol Rev. 58(4): 631-640.

Malykh, E.A., I.A. Butov, A.B. Ravcheeva, A.A. Krylov, S.V. Mashko, N. Stoynova. 2018. Specific features of L-histidine production by *Escherichia coli* concerned with feedback control of AICAR formation and inorganic phosphate/metal transport. Microb Cell Fact. 17: 42.

Man, Z., M. Xu, Z. Rao, J. Guo, T. Yang, X. Zhang, Z. Xu. 2016. Systems pathway engineering of *Corynebacterium glutamicum* for improved L-arginine production. Sci Rep. 6: 28629.

Mechold, U., K. Potrykus, H. Murphy, K.S. Murakami, M. Cashel. 2013. Differential regulation by ppGpp versus pppGpp in *Escherichia coli*. Nucleic Acids Res. 41(12): 6175-89.

Mercante, J., K. Suzuki, X. Cheng, P. Babitzke, T. Romeo. 2006. Comprehensive alanine-scanning mutagenesis of *Escherichia coli* CsrA defines two subdomains of critical functional importance. J Biol Chem. 281: 31832–31842.

Merill, D.K., J.C. McAlexander, R.W. Guynn. 1981. Equilibrium constants under physiological conditions for the reactions of d-3-phosphoglycerate dehydrogenase and 1-phosphoserine aminotransferase. Arch Biochem Biophys. 212(2): 717-729.

Metzl-Raz, E., M. Kafri, G. Yaakov, I. Soifer, Y. Gurvich, N. Barkai. 2017. Principles of cellular resource allocation revealed by condition-dependent proteome profiling. bioXxiv. Doi: http://dx.doi.org/10.1101/124370.

Mitkevich, V.A., A. Ermakov, A.A. Kulikova, S. Tankov, V. Shyp, A. Soosaar, T. Tenson, A.A. Makarov, M. Ehrenberg, V. Haryliuk. 2010. Thermodynamic characterization of ppGpp binding to EF-G or IF2 and of initiator tRNA binding to free IF2 in the presence of GDP, GTP, or ppGpp. J Mol Biol. 402: 838-846.

Moffatt, B.A., H. Ashihara. 2002. Purine and pyrimidine nucleotide synthesis and metabolism. The Arabidopsis Book: e0018.

Moker, N., M. Brocker, S. Schaffer, R. Kramer, S. Morbach, M. Bott. 2004. Deletion of the genes encoding the MtrA-MtrB two-component system of *Corynebacterium glutamicum* has a strong influence on cell morphology, antibiotics susceptibility and expression of genes involved in osmoprotection. Mol Microbiol. 54: 420–438.

Molchanova, M.L., R.S. Erdagaeva, I. Grigorenko, T.N. Bol'shakova, V.N. Gershanovich. 1992. Role of fructose-1-phosphate kinase in expression of PEP-synthase in *Escherichia coli* K-12. Genetika 28: 46–51.

Monteiro, F., G. Hubmann, V. Takhaveev, S.R. Vedelaar, J. Norder, J. Hekelaar, J. Saldida, A. Litsios, H.J. Wijma, A. Schmidt, M. Heinemann, 2019. Measuring glycolytic flux in single yeast cells with an orthogonal synthetic biosensor. Mol Syst Biol. 15: e9071

Morbach, S., C. Junger, H. Sahm, L. Eggeling. 2000. Attenuation control of *ilvBNC* in *Corynebacterium glutamicum*: evidence of leader peptide formation without the presence of a ribosome binding site. J Biosci Bioeng. 90:501–507.

Morgan, G.J., D.H. Burkhardt, J.W. Kelly, E.T. Powers. 2018. Translation efficiency is maintained at elevated temperature in *Escherichia coli*. J Biol Chem. 293(3): 777–793.

Morin, M., D. Ropers, F. Letisse, S.Laguerre, J.-C. Portais, M. Cocaign-Bousquet, B. Enjalbert. 2016. The post-transcriptional regulatory system CSR controls the balance of metabolic pools in upper glycolysis of *Escherichia coli*. Mol. Microbiol. 100 (4): 86700.

Morin, M., D. Ropers, E. Cinquemani, J.C. Portais, B. Enjalbert, M. Cocaign-Bousquet. 2017. The Csr system regulates *Escherichia coli* fitness by controlling glycogen accumulation and energy levels. mBio. 8: e01628-17.

Mundhada, H., J.M. Seoane, K. Schneider, H.B. Christensen, A. Koza, M. Herrgard, A. Feist, A.T. Nielsen. 2016. Increased production of L-serine in *Escherichia coli* through adaptive laboratory evolution. Metab Eng. 39: 141-150.

Mundhada, H., K. Schneider, H.B. Christensen, A.T. Nielsen. 2015. Engineering of high yield production of L-serine in *Escherichia coli*. Biotechnol Bioeng. 113(4): 807-816.

Neumann, S., K. Grosse, V. Sourjik. 2012. Chemotactic signaling via carbohydrate phosphotransferase systems in *Escherichia coli*. PNAS USA. 109(30): 12159–12164.

Nguyen, J, V. Fernandez, S. Pontrelli, U. Sauer, M. Achermann, R. Stocker. 2021. A distinct growth physiology enhances bacterial growth under rapid nutrient fluctuations. Nat Commun. 12: 3662.

Niu, H., R. Li, Q. Liang, Q. Qi, Q. Li, P. Gu. 2019. Metabolic engineering for improving l-tryptophan production in *Escherichia coli*. J Ind Microbiol Biotechnol. 46:55–65.

Noh, M., S.M. Yoo, W.J. Kim, S.Y. Lee. 2017. Gene expression knockdown by modulating synthetic small RNA expression in *Escherichia coli*. Cell Syst. 5: 418-426.

Nonaka, G., K. Takumi. 2017. Cysteine degradation gene *yhaM*, encoding cysteine desulfidase, serves as a genetic engineering target to improve cysteine production in *Escherichia coli*. AMB Expr. 7: 90.

Panickkin, V.B., V.A. Livshits, I.V. Biryukova, S.V. Mashko. 2016. Metabolic engineering of *Escherichia coli* for L-tryptophan production. Appl Biochem Microbiol. 52(9): 783-809.

Pannuri, A., C.A. Vakulskas, T. Zere, L.C. McGibbon, A.N. Edwards, D. Georgellis, P. Babitzke, T. Romeo. 2016. Circuitry Linking the Catabolite Repression and Csr Global Regulatory Systems of *Escherichia coli*. J Bacteriol. 198(21): 3000-3015.

Park, S.-D., J.-Y. Lee, S.-Y. Sim, Y. Kim, H.-S. Lee. 2007. Characteristics of methionine production by an engineered Corynebacterium glutamicum strain. Metab Eng. 9(4): 327-336.

Park, J.H., J.E. Oh, K.H. Lee, J.Y. Kim, S.Y. Lee. 2012. Rational design of *Escherichia coli* for L-isoleusine production. ACS Synth Biol. 11: 532-540.

Park, J.H., S.. Lee. 2010. Fermentative production of branched chain amino acids: a focus on metabolic engineering. Appl Microbiol Biotechnol. 85: 491-506.

Park, S.-D., J.-Y. Lee, S.-Y. Sim, Y. Kim, H.-S. Lee. 2017. Characteristics of methionine production by an engineered *Corynebacterium glutamicum* strain. Metab Eng. 9(4): 327-336.

Park, S.H., H. U. Kim, T.Y. Kim, J.S. Park, S.-S. Kim, S.Y. Lee. 2014. Metabolic engineering of *Corynebacterium glutamicum* for L-arginine production. Nat Commun. 5: 4618.

Patange, O., C. Schwall, M. Jones, C. Villava, D.A. Griffice, A. Phillips, J.C.W. Locke. 2018. *Escherichia coli* can survive stress noisy growth modulation. Nat Commun. 9: 5333.

Pereira, B., H. Zhang, M. De Mey, C.G. Lim, Z.J. Li. G. Stephanopoulos. 2016. Engineering a novel biosynthetic pathway in *Escherichia coli* for production of renewable ethylene glycol. Biotechnol Bioeng. 113(2): 376-383.

Persky, N.S., D.J. Ferullo, D.L. Cooper, H.R. Moore, S.T. Lovettet. 2009. The ObgE/CgtA GTPase influences the stringent response to amino acid starvation in *Escherichia coli*. Mol Microbiol. 73:253–66.

Petit, C., Y. Kim, S.-W. Lee, J. Brown, E. Larsen, D.R. Ronning, J.-W. Suh, C.-M. Kang. 2018. Reduction of feedback inhibition in homoserine kinase (ThrB) of *Corynebacterium glutamicum* enhances L-threonine biosynthesis. ACS Omega. 3: 1178-1186.

Polen, T., M. Kramer, J. Bongaerts, M. Wubbolts, V.F. Wendisch. 2005. The global gene expression response of *Escherichia coli* to L-phenylalanine. J Biotechnol. 115: 221-237.

Potrykus, K., M. Cashel. 2018. Growth at best and worst of times. Nat Microbiol. 3(8): 862-863.

Potts, A.H., C.A. Vakulskas, A. Pannuri, H. Yakhnin, P. Babitzke, T. Romeo. 2017. Global role of the bacterial post-transcriptional regulator CsrA revealed by integrated transcriptomics. Nat Commun. 8: 1596.

Potts, A.H., Y. Guo, B.M.M. Ahmer, T. Romeo. 2019. Role of CsrA in stress responses and metabolism important for *Salmonella* virulence revealed by integrated transcriptomics. PLoS One. 14: e0211430.

Pourciau, C., A. Pannuri, A. Potts, H. Yakhnin, P. Babitzke, T. Romeo. 2019. Regulation of Iron

Storage by CsrA Supports Exponential Growth of *Escherichia coli*. mBio. 10(4): e01034-19.

Qin, T., X. Hu, J. Hu, X. Wang. 2015. Metabolic engineering of *Corynebacterium glutamicum* strain ATCC13032 to produce L-methionine. Biotechnol Appl Biochem. 62(4): 563-73.

Ramseier, T.M., D. Nègre, J.C. Cortay, M. Scarabel, A.J. Cozzone, M.H. Saier, Jr. 1993. In vitro binding of the pleiotropic transcriptional regulatory protein, FruR, to the *fru*, *pps*, *ace*, *pts* and *icd* operons of *Escherichia coli* and *Salmonella typhimurium*. J. Mol. Biol. 234:28-44.

Raskin, D.M., N. Judson, J.J. Mekalanos. 2007. Regulation of the stringent response is the essential function of the conserved bacterial G protein CgtA in *Vibrio cholerae*. PNAS USA. 104(11): 4636-4641.

Revelles, O., P. Millard, J.-P. Nougayrede, U. Dobrindt, E. Oswald, F. Letisse, J.-C. Portais. 2013. The carbon storage regulator (Csr) system exerts a nutrient-specific control over central metabolism in *Escherichia coli* strain Nissle 1917. PLoS One. 8(6): e66386.

Rodionova, I.A., Z. Zhang, J. Mehla, N. Goodacre, M. Babu, A. Emili, P. Uetz, M.H. Saier Jr. 2017. The phosphocarrier protein HPr of the bacterial phosphotransferase system globally regulates energy metabolism by directly interacting with multiple enzymes in *Escherichia coli*. J Biol Chem. Doi: 10.1074/jbc.M117/795294.

Rodriguez, A., J.A. Martnez, N. Flores et al. 2014. Engineering *Escherichia coli* to overproduce aromatic amino acids and derived compounds. Microb Cell Fact. 13: 126.

Romeo, T., M. Gong, M.Y. Liu, A.M. Brun-Zinkernagel. 1993. Identification and molecular characterization of *csrA*, a pleiotropic gene from *Escherichia coli* that affects glycogen biosynthesis, gluconeogenesis, cell size, and surface properties. J Bacteriol 175: 4744–4755.

Ronneau, S., R. Hallez. 2019. Make and break the alarmone: regulation of (p)ppGpp synthetase/hydrolase enzymes in bacteria. FEMS Microbiol Rev. 43: 389-400.

Ross, W. et al. 2016. ppGpp binding to a site at the RNAP-DksA interface accounts for its dramatic effects on transcription initiation during the stringent response. Mol Cell. 62: 811-823.

Sander, T., N. Farke, C. Diehl, M. Kuntz, T. Glatter, H. Link. 2019. Allosteric feedback inhibition enables robust amino acid biosynthesis in *E. coli* by enforcing enzyme overabundance.

Cell Syst. 8: 66-75.

Sabnis, N.A., H. Yang, T. Romeo. 1995. Pleiotropic regulation of central carbohydrate metabolism in *Escherichia coli* via the gene csrA. J. Biol. Chem., 270: 29096-29104.

Seier, Jr., M.H., T.M. Ramseier. 1996. The Catabolite Repressor/Activator (Cra) Protein of Enteric Bacteria. J Bacteriol. 178(12): 3411-3417.

Santos, C.N.S., W. Xiao, G. Stephanopoulos. 2012. Rational, combinatorial, and genomic approaches for engineering L-tyrosine production in *Escherichia coli*. PNAS USA. 109(34): 13538-13543.

Santos-Zavaleta, A. et al. 2019. Regulon DB v 10.5: tackling challenges to unify classic and high throughput knowledge of gene regulation in *E. coli* K-12. Nucleic Acids Res. 47: D212-D220.

Sanyal, R., R. Harinarayanan. 2020. SpoT and GppA hydrolases prevent the gratuitous activation of RelA by pppGpp in *Escherichia coli*. Bioxiv. Doi: https:// doi.org/10.1101/350843.

Schinck, S., D. Christidoulou, A. Mukherjee, E. Athaide, U. Sauer, M. Basan. 2021. Trade-offs in adaptation to glycolysis and gluconeogenesis result in a preferential flux direction in central metabolism. bioRxiv. doi: https://doi.org/10.1101/2021.05.07.443112.

Schmidt, A., K. Kochanowski, S. Videlaar, E. Ahrne, B. Volkmer, L. Callipo, K. Knoops, M. Bauer, R. Aebersold, M. Heinemann. 2016. The quantitative and condition-dependent *Escherichia coli* proteome. Nat Biotechnol. 34(1): 104-110.

Schwentner, A., A. Feith, E. Munch, T. Busche, C. Ruckert, J. Kalinowski, R. Takors, B. Blombach. 2018. Metabolic engineering to guide evolution-creating a novel mode for L-valine production with *Corynebacterium glutamicum*. Metab Eng. 47: 31-41.

Schwentner, A., A. Feith, E. Münch, J. Stiefelmaier, I. Lauer, L. Favilli et al. 2019. Modular Systems Metabolic Engineering Enables Balancing of Relevant Pathways for L-Histidine Production with *Corynebacterium glutamicum*. Biotechnol. Biofuels. 12: 65.

Scott, M., C.W. Gunderson, E.M. Mateescee, Z. Zhang, T. Hwa. 2010. Interdependence of cell

growth and gene expression: origins and consequences. Science 330: 1099-1102.

Shiio I., R. Miyajima. 1969. Concerted inhibition and its reversal by end products of aspartate kinase in *Brevibacterium flavum*. J Biochem. 65:849-859.

Shimada, T., N. Fujita, K. Yamamoto, A. Ishihama. 2011a. Novel roles of cAMP receptor protein (CRP) in regulation of transport and metabolism of carbon sources. PLoS One: 6: e20081.

Shimada T, K. Yamamoto, A. Ishihama. 2011b. Novel members of the Cra regulon involved in carbon metabolism in *Escherichia coli*, J Bacteriol. 193 (3): 649-659.

Shimada, T., N. Saito, M. Maeda, K. Tanaka, A. Ishihama. 2015. Expanded roles of leusine-responsive regulatory protein in transcription regulation of the *Escherichia coli* genome: genomic SELEX screening of the regulation targets. Microb Genomics. http://mgen.sgmjournals.org.

Shimizu, K. 2017. Metabolic regulation and metabolic engineering for biofuel and biochemical production. CRC press. Taylors and Francis group, New York USA.

Shimizu, K., Y. Matsuoka. 2019a. Regulation of glycolytic flux and overflow metabolism depending on the source of energy generation for energy demand. Biotechnol Adv. 37(2): 284-305.

Shimizu, K., Y. Matsuoka. 2019b. Redox rebalance against genetic perturbations and modulation of central carbon metabolism by the oxidative stress regulation. Biotechnol Adv. 37(8): 107441.

Shin, J.H., S.Y. Lee. 2014. Metabolic engineering of microorganisms for the production of L-arginine and its derivatives. Microb Cell Fact. 13: 166.

Shin, Y., M..Z. Qayyum, D. Pupov, D. Esyunina, A. Kulbachinskiy, K.S. Murakami. 2021. Structural basis of ribosomal RNA transcription regulation. Nat Commun. 12: 528.

Shu, Q., M. Xu, J. Li, T. Yang, X. Zhang, Z. Xu, Z.Rao. 2018. Improved L-ornithine production

in *Corynebacterium glutamicum* by introducing an artificial linear transacetylation pathway. Metab Eng. 45: 393-404.

Shyp, V., S. Tankov, A. Ermakov, P. Kudrin, B.P. English, M. Ehrenberg, T. Tenson, J. Elf, V. Hauryliuk. 2012. Positive feedback regulation of the stringent response enzyme RelA by its product. EMBO Rep. 13(9): 835-839.

Simic, P. J. Willuhm, H. Sahm, L. Eggling. 2002. Identification of *glyA* (encoding serine hydroxymethyltransferase) and its use together with the exporter ThrE to increase L-threonine accumulation by *Corynebacterium glutamicum*. Appl Environ Microbiol. 68(7): 3321-3327.

Singh, D., M.S. Fairlamb, K.S. Harrison, C. Weeramange, S. Meinhardt, S. Tungtur, B.F. Rau, P. Scott Hefty, A.W. Fenton, L. Swint-Kruse. 2017. Protein-protein interactions with fructose-1-kinase alter function of the central *Escherichia coli* transcription regulator, Cra. BioRxiv. Doi: https://doi.org/10.1101/201277.

Somavanshi, R., B. Ghosh, V. Sourjik. 2016. Sugar influx sensing by the phosphotransferase system of *Escherichia coli*. PLoS Biol. 14(8): e2000074.

Sprenger, G. 2007. Aromatic Amino Acids. In Wendisch VF (ed.) Amin Acid Biosynth - Pathways, Regul Metab Eng. Berlin, Heidelberg: Springer.

Steinchen, W., G. Bange. 2016. The magic dance of the alarmones (p)ppGpp. Mol Microbiol. 101(4): 531-44.

Stelling, J., U. Sauer, Z. Szallasi, F.J. Doyle, III, J. Doyle. 2004. Robustness of cellular functions. Cell. 118: 675-685.

Suzuki, K., X. Wang, T. Weilbacher, A.K. Pernestig, O. Merefors, D. Georgellis, P. Babitzke, T. Romeo. 2002. Regulatory circuitry of the CsrA/ CsrB and BarA/UvrY systems of *Escherichia coli*. J Bacteriol. 184: 5130-5140.

Suzuki, K., P. Babitzke, S.R. Kushner, T. Romeo. 2006. Identification of a novel regulatory protein (CsrD) that targets the global regulatory RNAs CsrB and CsrC for degradation of RNase E. Genes Dev. 20: 2605-2617.

Takagi, H., I. Ohtsu. 2016. L-Cysteine metabolism and fementation in micooganisms. Adv Biochem Eng/Biotechnol. 159. 129-151

Takumi, K., G. Nonaka. 2016. Bacterial Cysteine-inducible resistance systems. J. Bacteriol. 198(9): 1384-1392.

Takumi, K., M.K. Ziyatdinov, V. Samsonov, G. Nonaka. 2017. Fermentative production of cysteine by *Pantoea ananatis*. Appl Environ Microbiol. 83(5): e02502-16.

Timmermans, J., L. van Melderen. 2010. Post-transcriptional global regulation by CsrA in bacteria. Cell Mol Life Sci. 67: 2897-2908.

Tollerson II, R., M. Ibba. 2020. Translational regulation of environmental adaptation in bacteria. J Biol Chem. 295(30):10434-10445.

Towbin, B.D., Y. Korem, A. Bren, S. Doron, R. Sorek, U. Alon. 2017. Optimality and sub-optimality in a bacterial growth law. Nat Commun. 8: 14123.

Traxler, M.F., S.M. Summers, H.-T. Nguyen, V.M. Zacharia, G.A. Hightower, J.T. Smith, T. Conway. 2008. The global, ppGpp-mediated stringent response to amino acid starvation in *Escerichia coli*. Mol Microbiol. 68(5): 1128-1148.

Traxler, M.F., V.M. Zacharia, S. Marquardt, S.M. Summers, H.T. Nguyen, S.E. Stark, T. Conway. 2011. Discretely calibrated regulatory loops controlled by ppGpp partition gene induction across the 'feast to famine' gradient in *Escherichia coli*. Mol Microbiol. 79: 830–845.

Tribe, D.E., H. Camakaris, J. Pittard. 1976. Constitutive and repressivle enzymes of the common pathway of aromatic biosynthesis in *Escherichia coli* K-12: regulation of enzyme synthesis at different growth rates. J Bacteriol. 127(3): 1085-1097.

Trondle, J., K. Schoppel, A, Bleidt, N. Trachtmann, G.A. Sprenger, D. Weuster-Botz. 2020. Metabolic control analysis of L-tryptophan production with *Escherichia coli* based on data from short-term perturbation experiments. J Biotechnol. 307: 15-28.

Udaka, S. 1966. Pathway-specific pattern of control of arginine biosynthesis in bacteria. J Bacteriol. 91: 617-621.

Usuda, Y., O. Kurahashi. 2005. Effects of deregulation of methionine biosynthesis on methionine excretion in *Escherichia coli*. Appl Environ Microbiol. 71: 3228-3234.

Utagawa, T. 2004. Production of arginine by fermentation. American Soc Nutr Sci. 2854S-2857S.

Vadia, S., J.L. Tse, R. Lucena, Z. Yang, D.R. Kellogg, J.D. Wang, P.A. Levin. 2017. Fatty Acid Availability Sets Cell Envelope Capacity and Dictates Microbial Cell Size. Curr Biol. 27(12):1757-1767.

Vakulskas, C.A., Y. Leng, H. Abe, T. Amaki, A. Okayama, P. Babitzke, K. Suzuki, T. Romeo. 2016. Antagonistic control of the turnover pathway for the global regulatory sRNA CsrB by the CsrA and CsrD proteins. Nucleic Acids Res. Doi: 10.1093/nar/gkw484.

van Heerden, J.H., M.T. Wortel, F.J. Bruggeman, J.J. Heijnen, Y.J.M. Bollen, R. Plamque, J. Hulshof, T.G. O'Toole, S.A. Wahl, B. Teusink. 2014. Lost in transition: Start-up of glycolysis yields subpopulations of nongrowing cells. Science. 343: 1245114 (1-9)

Venditti, V., R. Ghirlando, G.M. Clore. 2013. Strucural basis for enzyme I inhibition by α-ketoglutarate. ACS Chem Biol. 8: 1232-1240.

Venditti, V., V. Tugarinov, C.D. Schwieters, A. Grishaev, M. Clore. 2015. Large interdomain rearrangement triggered by suppression of micro- to millisecond dynamics in bacterial enzyme I. Nat Commun. 6: 5960

Vogt, M., S. Haas, S. Klaffl, T. Polen, L. Eggeling, J.V. Ooyen et al. 2014. Pushing product formation to its limit: metabolic engineering of *Corynebacterium glutamicum* for L-leusine overproduction. Metab Eng. 22: 40-52.

Wang, C., J. Wu, B. Shi, J. Shi, Z. Zhao. 2020. Improving L-serine formation by *Escherichia coli* by reduced uptake of produced L-serine. Microb Cell Fact. 19: 66.

Wang, J., L.K., Cheng, J. Wang, Q. Liu, T. Shen, N. Chen. 2013. Genetic engineering of *Escherichia coli* to enhance production of L-tryptophan. Appl Microbiol Biotechnol. 97: 7587–7596.

Wang, X. 2019. Strategy for improving L-isoleusine production efficiency in *Corynebacterium glutamicum*. Appl Microbiol Biotechnol. 103(5): 2101-2111.

Wang, X., H. Zhang, P.L. Quinn. 2018. Production of L-valine from metabolically engineered *Corynebacterium glutamicum*. Appl Microbiol Biotechnol. 102: 4319-4330.

Wang, X., K. Xia, X. Yang. X. Yang, C. Tang. 2019. Growth strategy of microbes on mixed carbon sources. Nat Commun. 10: 1279.

Wang, Y.-Y., F. Zhang, J.-Z. Xu, W.-G. Zhang, X.-L. Chen, L.-M. Liu. 2019. Improvement of l-Leucine Production in *Corynebacterium glutamicum* by Altering the Redox Flux. Int J Mol Sci. 20: 2020.

Wei, B.L., AM. Brun-Zinkernagel, J.W. Simecka, B.M. Pruss, P. Babitzke, T. Romeo, T. 2001. Positive regulation of motility and *flhDC* expression by the RNA-binding protein CsrA of *Escherichia coli*. Mol Microbiol. 40: 245–256.

Westfall, C., P.A. Levin. 2018. Comprehensive analysis of central carbon metabolism illuminates connections between nutrient availability, growth rate, and cell morphology in *Escherichia coli*. PLoS Genetics. 14(2): e1007205.

White, D., M.E. Hart, T. Romeo. 1996. Phylogenetic distribution of the global regulatory gene *csrA* among eubacteria. Gene 182: 221–223.

Whitacre, J.M. 2012. Biological robustness: paradigms, mechanisms, and systems principles. Front Genet. 3: 67.

Winkler, M.E., S. Ramos-Montanez. 2009. Biosynthesis of histidine. EcoSal Plus. 3(2): doi: 10.1128/ecosalplus.3.6.1.9.

Wout, P., K. Pu, S.M. Sullivan, V. Reese, S. Zhou, B. Lin, J.R. Maddock. 2004. The *Escherichia coli* GTPase CgtA cofractionates with the 50S ribosomal subunit and interacts with SpoT, a ppGpp synthetase/hydrolase. J Bacteriol. 186(16): 5249-5257.

Wu, H., D. Tian, X. Fan, W. Fan, Y. Zhang, S. Jiang, C. Wen, Q. Ma, N. Chen, X. Xie. 2020.

Highly efficient production of L-histidine from glucose by metabolically engineered *Escherichia coli*. ACS Synth Biol. 9(7): 1813-1822.

Wu, J., Y. Liu, S. Zhao, J. Sun, Z. Jin, D. Zhang. 2019. Application of dynamic regulation to increase L-phenylalanine production in *Escherichia coli*. J Microbiol Biotechnol. 29(6): 923-932.

Wu, W., Y. Zhang, D. Liu, Z. Chen. 2019. Efficient mining of natural NADH-utilizing dehydrogenases enables systematic cofactor engineering of lysine synthesis pathway of *Corynebacterium glutamicun*. Metab Eng. 52: 77-86.

Wu, X.-Y., X.-Y. Guo, B. Zhang, Y. Jiang, B.-C. Ye. 2020. Recent advances L-ornitine biosynthesis in metabolically engineered *Corynebacterium glutamicum*. Front Bioeng Biotechnol. 7: 440.

Xie, X.X., Y. Liang, H. Liu, Y. Liu, Q. Xu, C. Zhang, N. Chen. 2014. Modifcation of glycolysis and its effect on the production of l-threonine in *Escherichia coli*. J Ind Microbiol Biotechnol. 41: 1007–1015.

Xu Q, F. Bai, N. Chen, G. Bai. 2017. Gene modification of the acetate biosynthesis pathway in *Escherichia coli* and implementation of the cell recycling technology to increase L-tryptophan production. PLoS ONE. 12(6): e0179240.

Xu, G., Q. Zhu, Y. Luo, X. Zhang, W. Guo, W. Dou, H. Li, H. Xu, X. Zhang, Z. Xu. 2015. Enhanced production of l-serine by deleting *sdaA* with modifying and overexpressing *serA* in a mutant of *Corynebacterium glutamicum* SYPS-062 from sucrose. Biochem Eng J. 103: 60-67.

Xu, J.-Z., H.-Z. Ruan, H.-B. Yu, L.-M. Liu, W. Zhang. 2020. Metabolic engineering of cabrohydrate metabolism systems in *Corynebacterium glutamicum* for improving the efficiency of L-lysine production from mixed sugar. Microb Cell Fact. 19: 39.

Xu, J.-Z., H.-Z. Ruan, L.-M. Liu, L.-P. Wang, W.-G. Zhang. 2019a. Overexpression of thermostable *meso*-diaminopimelate dehydrogenase to redirect diaminopimelate pathway for increasing L-lysine production in *Escherichia coli*. Sci Rep. 9: 2423.

Xu, J.-Z., H.-B. Yu, M. Han, L.-M. Liu, W.-G. Zhang. 2019b. Metabolic engineering of glucose

uptake systems in *Corynebacterium glutamicum* for improving the efficiency of L-lysine production. Metab Eng & Synthetic Biol. 46: 937-949.

Xu, J.-Z., Z.-H. Wu, S.-L. Gao, W. Zhang. 2018. Rational modification of tricarboxylic acid cycle for improving L-lysine production in *Corynebacterium glutamicum*. Microbial Cell Fact. 17: 105.

Xu, M., P. Liu, J. Chen, A. Peng, T. Yang, X. Zhang, Z. Xu, Z. Rao. 2020. Development of a novel biosensor-driven mutation and selection system via in situ growth of *Corynebacterium crenatum* for the production of l-arginine. Frontiers Bioeng Biotechnol. 8: 175.

Xu, M., Z. Rao, W. Dow et al. 2012. Site-directed mutagenesis studies on the L-arginine-binding sites of feedback inhibition in N-acetyl-L-glutamate kinase (NAGK) from *Corynebacterium glutamicum*. Curr Microb. 64: 164-172.

Xu, Y.-F., D. Amador-Noguez, M.L. Reaves, X.-J. Feng, J.D. Rabinowitz. 2012. Ultrasensitive regulation of anaplerosis via allosteric activation of PEP carboxylase. Nat Chem Biol. 8: 562-568.

Yakhnin, A.V., C.S.Baker, CA. Vakulskas, H. Yakhnin, I. Berezin, T.Romeo, P. Babitzke 2013. CsrA activates *flhDC* epression by protectting *flhDC* mRNA from RNase E-mediated cleavage. Mol Microbiol. 87(4): 81-866.

Yakhnin, H., R. Aichele, S.E. Ades, T. Romeo, P. Babitzke. 2017. Circuitry linking the global Csr- and σ^E-dependent cell envelope stress response systems. J Bacteriol. 199(23): e008-17.

Yang, H., M.Y. Liu, T. Romeo. 1996. Coordinate genetic regulation of glycogen catabolism and biosynthesis in *Escherichia coli* via the CsrA gene product. J Bacteriol. 178(4): 1012–1017.

Yang M., K.H. Vousden. 2016. Serine and one-carbon metabolism in cancer. Nat Rev Cancer. 16: 650-662.

Yang, J., Y. Fang, J. Wang, C. Wang, L. Zhao, X. Wang. 2019. Deletion of regulator-encoding genes *fadR*, *fabR*, and *iclR* to increase L-threonine production in *Escherichia coli*. Appl Micob Cell Phys. 103: 4549-4564.

Yanofsky, C. 1981. Attenuation in the control of expression of bacterial operons. Nature. 289: 751–758.

Yin, L., F. Shi, X. Hu, C. Chen, X. Wang. 2013. Increasing L-isoleusine production in *Corynebacterium glutamicum* by overexpressing global regulator Lrp and two-component export system BrnFE. Appl Microbiol. 114: 1369-1377.

Yin, L., J. Zhao, C. Chen, X. Hu, X. Wang. 2014. Enhancing the carbon flux and NADPH supply to increase L-isoleusine production in *Corynebacterium glutamicum*. Biotechnol Bioproc Eng. 19: 132-142.

Yokota, A., M. Ikeda (Eds.). 2017. Amino Acid Fermentation. Adv Biochem Eng/Biotechnol. 159. DOI: 10.1007/10_2016_27

You, C., H. Okano, S. Hui, Z. Zhang, M. Kim, C.W. Gunderson, Y.P. Wang, P. Lenz, D. Yan, T. Hwa. 2013. Coordination of bacterial proteome with metabolism by cAMP signaling. Nature 500: 301-306.

Zampieri, M., M. Horl, F. Hotz, N.F. Muller, U. Sauer. 2019. Regulatory mechanisms underlying coordination of amino acid and glucose catabolism in *Escherichia coli*. Nat Commun. 10: 3354.

Zaslaver, A., A.E. Mayo, R. Rosenberg, P. Bashkin, H. Sberro, M. Tsalyuk, M.G. Surette, U. Alon. 2004. Just-in-time transcription program in metabolic pathway. Nat Genetics. 36(5): 486-491.

Zere, T.R., C.A. Vakulskas, Y. Leng, A. Pannuri, A.H. Potts et al. 2015. Genomic targets and features of BarA-UvrY (-SirA) signal transduction systems. PLoS One 10:e0145035.

Zhan, M., B. Kan, J. Dong, G. Xu, R. Han, Y. Ni. 2019. Metabolic engineering of *Corynebacterium glutamicum* for improved L-arginine synthesis by enhancing NADPH supply. J Ind Microbiol Biotechnol. 46: 45-54.

Zhang, B., M. Yu, W.-P. Wei, B.-C. Ye. 2018a. Optimization of L-ornitine production in recombinant *Corynebacterium glutamicum* S9114 by *cg3035* overexpression and manipulating

the central metabolic pathway. Microb Cell Fact. 17: 91.

Zhang, B., M. Yu, Y. Zhou, B.-C. Ye. 2018b. Improvement of L-ornitine production by attenuation of *argF* in engineered *Corynebacterium glutamicum* S9114. AMB Express. 8: 26.

Zhang, B., M. Yu, Y. Zhou, Y. Li, B.-C. Ye. 2017. Systematic pathway engineering of *Corynebacterium glutamicum* S9114 for L-ornitine production. Microb Cell Fact. 16: 158.

Zhang, W., M. Zhang, C. Gao, Y. Zhang, Y. Ge, S. Guo, X. Guo, Z. Zhou, Q. Liu, Y. Zhang, C. Ma, F. Tao, P. Xu. 2017. Coupling between D-3-phosphoglycerate dehydrogenase and D-2-hydroglutarate dehydrogenase drives bacterial L-serine synthesis. PNAS USA. E7574-E7582.

Zhang, X., G. Xu, J. Shi, M.A.G. Koffas, Z. Xu. 2018. Microbial production of L-serine from renewable feedstocks. Trends Biotechnol. 36(7): 700-712.

Zhang, X., Y. Gao, Z. Chen, G. Xu, X. Zhang, H. Li, J. Shi, M.A.G. Koffas, Z. Xu. 2020. High-yield production of L-serine though a novel identified exporter combined with synthetic pathway in *Corynebacterium glutamicum*. Microb Cell Fact. 19: 115.

Zhang, X., Z.W. El-Hajj, E. Newman. 2010. Deficiency in L-serine deaminase interferes with one-carbon metabolism and cell wall synthesis in *Escherichia coli* K-12. J Bacteriol. 192(20): 5515-5525.

Zhang, Y., E. Zbornikova, D. Rejman, K. Gerdes. 2018. Novel (p)ppGpp binding and metabolizing proteins of *Escherichia coli*. mBio. 9(2): e02188-17.

Zhao, H., Y. Fang, X. Wang, L. Zhao, J. Wang, Y. Li. 2018. Increasing L-threonine production in *Escherichia coli* by engineeringthe glyoxylate shunt and the L-threonine biosynthesis pathway. Appl Microbiol Biotechnol. 102: 5505–5518.

Zhao, L., Y. Lu. J. Yang, Y. Fang, L. Zhu, Z. Ding, C. Wang, W. Ma, X. Hu, X. Wang. 2020. Expression regulation of multiple key genes to improve l-threonine in *Escherichia coli*. Microb Cell Fact. 19:46.

Zhu, M., Y. Pan, X. Dai. 2019. (p)ppGpp: the magic governor of bacterial growth economy.

Curr Genetics. https://doi.org/10.1007/s00294-019-00973-z.

Zhu, Q., X. Zhang, Y. Luo, W. Guo, G. Xu, J. Shi, Z. Xu. 2015. L-Serine overproduction with minimization of by-products by engineered *Corynebacterium glutamicum*. Appl Microbiol Biotechnol. 99: 1665-1673.

Zorrilla, S.,D. Chaix, A. Ortega, C. Alfonso, T. Doan, E. Margeat, G. Rivas, S. Aymerich, N. Declerck, C. A Royer. 2007. Fructose-1,6-bisphosphate acts both as an inducer and as a structural cofactor of the central glycolytic genes repressor (CggR). Biochem. 46(51):14996-5008.

Figure captions

Figure 1. Three routes of affecting the cAMP level via Cya: ① Reduction of PEP level by the feed-forward activation of Pyk and Ppc by FBP, ② Modulation of Cya via inhibition of EI of PTS by αKG, ③ Direct inhibition of Cya by αKG. Feedback regulation scheme is shown in the box.

Figure 2. (a) Phosphorylation of EIIA (EIIA-P) (%) for PTS sugars (Open symbol), and non-PTS carbohydrates (filled black symbol) (Bettenbrock et al 2007, Kremling et al 2008). (b) LacZ expression (as a reporter of cAMP-Crp activity) with respect to the cell growth rate. Open and filled black symbols for the wild-type *E. coli* strain and grey symbols for Δ*pts* strain (You et al 2010, Hermsen et al 2015).

Figure 3. The positive feedback regulation of glycolysis by the modulation of Cra by FBP via F1P in *E. coli*. Feedback regulation scheme is shown in the box.

Figure 4. Activation of CsrD by the unphosphorylated EIIA, and activation of glycolysis by the active CsrA via lower CsrB/C activities (red lines). This forms the positive feedback regulation for the glycolysis by CsrA as shown in the box. A variety of regulation by CsrA and cAPM-Crp is also shown.

Figure 5. One carbon metabolism and cysteine metabolism (blue line shows enzyme level regulation, while red line shows transcriptional regulation): L-serine is synthesized from 3-phosphoglycerate (3PG) in the glycolysis, where 3PG is oxidized to yield 3-phosphohydroxypyruvate (3PHP) catalyzed by 3-phosphoglycerate dehydrogenase (PHGDH) encoded by *serA*, in which PHGDH is allosterically inhibited by L-serine. Subsequent transamination leads to the formation of 3-phosphoserine (3PS) catalyzed by 3-phosphoserine aminotrasferase (PSAT) encoded by *serC*. The 3-phosphoserine is then dephosphorylated to yield L-serine by phosphoserine phosphatase (PSPH) encoded by *serB*. L-Serine is further converted to L-glycine by serine hydroxymethyltransferase (SHMT) encoded by *glyA*, and L-serine is also converted to pyruvate by serine dehydratase (SEDH) encoded by *sdaA*.

The 1st step in the cysteine biosynthesis (from serine) involves the serine acetyltransferase (SAT), encoded by *cysE*, where SAT is strictly inhibited by L-cysteine. CysE catalyzes the reaction of serine and AcCoA to give O-acetylserine (OAS). The 2nd step involves OAS-sulfhydrylase (OASS), which converts OAS and sulfide into cysteine and acetate. The cysteine level is detected by the master regulator CysB, which controls the transcription of most of the genes that encode proteins involved in sulfur assimilation.

Figure 6. Histidine biosynthetic pathway (blue line shows enzyme level regulation, while red line shows transcriptional regulation): The 1st key step in the histidine biosynthetic pathway, the condensation of PRPP and ATP to form phosphoribosyl-ATP, is catalyzed by the ATP-PR transferase (HisG). Allosteic feedback inhibition of HisG by histidine is made by the competitive inhibition by AMP and ADP, and competitive product inhibition by PR-ATP. HisG is also allosterically inhibited by AICAR. HisG, ATP phosphoribosyltransferase; PR-ATP, phosphoribosyl-ATP; HisE, phosphoribosyl-ATP pyrophosphatase, PR-AMP, phosphoribosyl-AMP; HisI, phosphoribosyl-AMP cyclohydrolase; HisN, histidinol phosphate phosphatase; 5'-ProFAR, 1-(5-phosphoribosyl)-5-[(5-phosphoribosylamino) methylideneamino] imidazol-4-carboxamide; HisA, 5'-ProFAR isomerase, PR-FAR, 5-[(5-phospho-1-deoxyribulose-1-ylamino) methylideneamino]-1-(5-phosphoribosyl) imidazol-4-carboxamid; HisF, synthase subunit of IGP synthase; HisH, glutaminase subunit of IGP synthase; IGP, imidazole-glycerol phosphate; HisB, imdazoleglycerol phosphate dehydratase; IAP, imidazole-acetol phosphate; HisC, histidinol phosphate aminotransferase; Hol-P, L-histidinol phosphate; HisN, histidinol phosphate phosphatase; His-ol, histidinol; HisD, histidinol dehydrogenase; AICAR, 1-(5'-phosphoribosyl)-5-amino-4-imidazolecarboxamide; PurH, bifunctional AICAR formyltransferase/IMP cyclohydrolase; FAICAR, 5-formamidoimidazole-4- carboxamide ribotide; PurA, adenylosuccinate synthase; IMP, inosine

monophosphate; AS, adenylosuccinate; PurB, adenylosuccinate lyase; Adk, adenylate kinase; PRPP, phosphoribosyl pyrophosphate; Prs, PRPP synthetase.

Figure 7. Glutamate family amino acid biosynthetic pathways (blue line shows enzyme level regulation, while red line shows transcriptional regulation): (a) In *E. coli*, N-acetylglutamate (NAG) is first synthesized from glutamate and AcCoA by NAG synthase (NAGS) (encoded by *argA*). NAG is phosphorylated by NAG kinase (NAGK) (encoded by *argB*) to form N-acetylglutamyl phosphate (NAGP). NAGP is converted to N-acetylglutamate semialdehyde (NAGSA) by *argC*-encoded N-acetylglutamate 5-semialdehyde dehydrogenase (NAGSDH) (with NADPH), and NAGSA is in turn converted to N-acetylornithine (NAO) by *argD*-encoded N-acetylornithine aminotransferase (NAOAT). NAO is then converted to L-ornithine by ornithine acetyltransferase (OAT). Citrulline is then produced by *argFI*-encoded ornithine carbamoyltransferase (OCT) from ornithine. N-argininosuccinate (NAS) is in turn produced from citrulline by argininosuccinate synthase (ASS) encoded by *argG*, and then L-arginine is produced by *argH*-encoded argininosuccinate lyase (ASL). The proline biosynthetic pathway starts from glutamate by the phosphorylation of glutamate by γ-glutamyl kinase (GK) (encoded by *proB*), followed by reduction to glutamate-γ-semialdehyde by γ-glutamyl phosphate reductase (GPR) (encoded by *proA*), a spontaneous cyclisation, and finally the reduction to proline by pyrroline-5-carboxylate reductase (P5CR) (encoded by *proC*).
(b) In *C. glutamicum*, ornithine acetyltransferase (OAT)/N-acetylglutamate synthase (NAGS) (encoded by *argJ*) catalyzes the conversion of N-acetylornithine (NAO) and glutamate to ornithine and N-acetylglutamate (NAG), and the ornithine biosynthetic pathway is cyclic. NAG kinase (NAGK) (encoded by *argB*) then phosphorylates it (by ATP) to form N-acetylglutamyl phosphate (NAGP). NAGP is converted to N-acetylglutamate semialdehyde (NAGSA) by *argC*-encoded N-acetylglutamate 5-semialdehyde dehydrogenase (NAGSDH) (or N-acetyl-gamma-glutamyl-phosphate reductase, NAGPR) (with NADPH), and NAGSA is in turn converted to N-acetylornithine (NAO) by *argD*-encoded N-acetylornithine aminotransferase (NAOAT). NAO is then converted to L-ornithine by OAT. Citrulline is in turn produced by *argF*-encoded ornithine carbamoyltransferase (OCT) from ornithine. L-arginine is produced from citrulline by ornithine carbamoyltransferase and *argGH*-encoded argininosuccinate synthase (ASS) and arginiosuccinate lyase (ASL) via N-arginino-succinate (NAS).

Figure 8. Branched chain amino acid biosynthetic pathways (blue line shows enzyme level regulation, while red line shows transcriptional regulation): In *E. coli*, acetohydroxy acid synthase (AHAS) catalyzes the condensation of two molecules of pyruvate to form

2-acetolactate, where three isoenzymes such as AHAS I, II, and III are encoded by *ilvBN*, *ilvGM*, and *ilvIH*, respectively. The expression of the *ilvGMEDA* operon is controlled by the transcriptional attenuation by all three amino acids, whereas the *ilvBN* operon is controlled by the attenuation mediated only by L-valine and L-leusine.

The 2-acetolactate is converted (with NADPH) to 2,3-dehydroxyisovalerate by acetohydroxy acid isomeroreductase (AHAIR) encoded by *ilvC*, and in turn 2,3-dehydoxyisovalerate is converted to 2-ketoisovalerate by dihydroxyacid dehydratase (DHADH) encoded by *ilvD*. The expression of the *ilvC* gene is induced by acetolactate, mediated by the positive transcriptional activator IlvY.

The 1st step specific to L-leusine biosynthesis is the conversion of 2-ketoisovalerate and AcCoA to 2-isopropylmalate (2IPM) and CoA by 2-isopropylmalate syntase (IPMS) (encoded by *leuA*), which is feedback-inhibited by L-leusine. The two further enzymes unique to leusine synthesis are IPM dehydratase (IPMD) encoded by *leuCD* to yield 3-isopropylmalate (3IPM), and IPM dehydrogenase (IPMDH) encoded by *leuB* to yield 2-ketoisocaproate. L-leusine is then synthesized by the branched-chain amino acid transaminase (BCAAT).

On the other hand, the 1st step of L-isoleusine biosynthesis is the deamination of L-threonine by threonine dehydratase, encoded by *ilvA*. This enzyme is sensitive to feedback inhibition by L-isoleusine, and this inhibition is reversed by L-valine. The 2-aceto-2-hydroxybutyrate is converted to 2,3-dehydroxy-3-methylvalerate (for L-isoleusine biosynthesis).

Figure 9. Aspartate family amino acid biosynthetic pathways (blue line shows enzyme level regulation, while red line shows transcriptional regulation): In *E. coli*, the 1st step is the conversion of aspartate to aspartyl phosphate catalyzed by aspartate kinase (Ask) in the synthesis of all aspartate family amino acids (AFAAs), which are subject to feedback inhibition. In *E. coli*, three Ask isoenzymes, Ask I, II, and Ⅲ, differ in their regulation mechanisms. The expression of *thrA* is repressed by L-threonine and L-isoleusine in a covalent manner, and Ask I is feedback inhibited by L-threonine. Ask II (encoded by *metL*), and the expression of *metL* is repressed by L-methionine. Ask Ⅲ is the product of *lysC* gene, of which expression is repressed by L-lysine, and the activity of Ask Ⅲ is allosterically inhibited by also L-lysine.

In both *E. coli* and *C. glutamicum*, aspartyl semialdehyde dehydrogenase (ASADH) is encoded by the *asd* gene. It catalyzes deoxidation of aspartyl-phosphate (Asp-P) to form aspartyl semialdehyde. Expression of *asd* in *E. coli* is subjected to multivalent repression by L-lysine, L-threonine, and L-methionine.

Homoserine dehydrogenase (HSDH) is the 2nd key enzyme of the pathway, controlling the carbon flux toward L-homoserine synthesis. In *E. coli*, the two isoenzymes of HSDH are present (HSDH I and II), where HSDH I is subject to inhibition by L-threonine. Homoserine kinase is the 3rd key enzyme of the pathway, where it controls carbon flux toward L-threonine synthesis. In *E. coli*, *thrB* and *thrC* are clustered with *thrA* in the *thr* operon, and their expression is subject to covalent repression by L-threonine and L-isoleusine. The activity of homoserine kinase (HSK) is inhibited by L-threonine and L-isoleusine.

The 1st step of lysine synthesis is the condensation of aspartate semialdehyde (ASA) with pyruvate by dihydrodipicolinate synthase (DDPS) encoded by the *dapA* gene, where the DDPS activity is inhibited by L-lysine. The 2nd step is the reduction of dihydrodipicolinate (DHDP) to tetrahydodipicolinate (THDP) catalyzed by dihydrodipicolinate reductase (DHDPR) encoded by *dapB*. At this step, the diaminopimelate (DAP) pathway is at variance. Namely, *E. coli* uses the succinylase variant with its four specific reactions to make the lysine precursor *meso*-DAP.

Methionine biosynthesis competes the precursor with the formation of threonine (and subsequently isoleusine) at the homoserine branch point. In *E. coli*, homoserine undergoes condensation with succinyl-CoA and produce succinyl homoserine by homoserine succinyl transferase (HST) encoded by *metA*.

Figure 10. Aromatic amino acid biosynthetic pathways (blue line shows enzyme level regulation, while red line shows transcriptional regulation): DAHP (3-deoxy-D-arabino-heptulosonate 7-phosphate) is synthesized from PEP and E4P in the CCM by DAHP synthase (DAHPS) encoded by *aroF*, *aroG*, and *aroH*. DAHP is then converted to DHQ (3-dehydroquinate) by DHQ synthase encoded by *aroB*. DHQ is in turn converted to DHS (3-dehydoshikimate) by DHQ dehydratase encoded by *aroD*. DHS is then converted to shikimic acid (SA) by shikimate dehydrogenase encoded by *aroE* and shikimate dehydrogenase/quinate dehydrogenase encoded by *ydiB*. SA is then converted to S3P (shikimate 3-phosphate) by shikimic acid kinase (SHK) encoded by *aroK* and *aroL*. S3P is further converted to EPSP (5-enolpyruvate-shikimate 3-phosphate) by 3-phosphoshikimate 1-carboxyvinyltransferase (EPSPS) encoded by *aroA*. EPSP is then converted to chorismic acid (CHA) by CHA synthase (CHAS) encoded by *aroC*.

In the L-tryptophan biosynthesis, additional precursors such as PRPP, L-glutamine, and L-serine are required. The 1st step towards L-tryptophan biosynthesis, anthranillate synthase, AS (encoded by *trpED*) is allosteically inhibited by L-tryptophan. Anthanilate is then converted to phosphoribosyl-anthanilate (PRA) by PRA (encoded by *trpD*), and then PRA is converted to carboxyphenylamino deoxyribulose phosphate (CDRP) by indole glycerol phosphate synthase (IGPS) (encoded by *trpC*) to yield indole glycerol phosphate (IGP). IGP is then converted to

L-tryptophan via indole by two steps catalyzed by two enzymes (encoded by *trpA* and *trpB*).

In *C. glutamicum*, two types of DAHPSs exist. One is an L-tyrosine sensitive, while another one (Type II) is L-phenylalanine and L-tyrosine sensitive. Others are similar as stated above for *E. coli*.

Fig. 11 Purine and pyrimidine synthetic pathways (Blue line shows enzyme level regulation, while red line shows transcriptional regulation.): (a) Purine biosynthetic pathway together with L-histidine synthetic pathway and C_1 metabolic pathway: *purF* encoding amidophosphoribosyltransferase, *purD* encoding PRA-glycine ligase, *purN* encoding phosphoribosylglycinamide formyltransferase, *purL* encoding phosphoribosylformylglycinamide synthase, *purM* encoding phosphoribosylformylglycinamide cycloligase, *purK* encoding phosphoribosylaminoimidazole carboxylase, *purE* encoding phosphoribosylaminoimidazole mutase, *purC* encoding phosphoribosylaminoimidazole succininocarboxamide synthase, *purH* encoding bifunctional AICAR formyltransferase/IMP cyclohydrolase, *purA* encoding adenylo succinate synthase, *purB* encoding adenylo succinate lyase. PRPP: phosphoribosyl pyrophoshate, PRA: phosphoribosylamine; GAR: glycinamide ribonucleotide; FGAR: phosphoribosyl N-fomylglycineamide; FGAM: 5'-phosphoribosyl formylglycineamidine; AIR: 5-aminoimidazole ribotide; CAIR: carboxy-5-aminoimidazole; SAICAR: phosphoribosyl-aminoimidazole succininocarboxamide; AICAR: 5-amino 4-imidazole 4-carboxamide ribonucleotide; FAICAR: 5-formamidoimidazole 4-carboxamide ribotide; IMP: inosine monophosphate; AS: adenylosuccinate; XMP: xanthosine monophosphate; GMP: guanosine monophosphate; Adk: adenylate kinase. Others are given in the histidine synthetic pathway (**Fig. 6**).
(b) Pyrimidine biosynthetic pathway together with arginine synthetic pathway: *carAB* encoding carbamoylphosphate synthase (CPSase), *pryI/pyrB* encoding aspartate carbamoyltransferase (ACTase), *pyrC* encoding dihydroorotase, *pyrD* encoding dihydroorotate dehydrogenase, *pyrE* encoding phosphoribosyltransferase, *pyrF* encoding orotidine 5'-phosphate decarboxylase. Others are given in the synthesis of arginine (glutamate family amino acids) (**Fig. 7**).

Figure 12. (a) Fraction of the ribosomal protein (in the total protein) with respect to the cell growth rate in *E. coli* (Scott et al 2010, Dai et al 2016). (b) The change in the ppGpp level with respect to the specific growth rate, μ, where the parameter values are as follows: φ_0=0.093 and

1/ϒ=0.221 (obtained from **Fig. 12a**), and $K_{i,ppGpp}$=1.5 [μM] and k_r=7.0.

Figure 13. Positive feedback regulation of (p)ppGpp synthesis by RelA, compensated by the hydrolase activity of SpoT, and the repression of the protein synthesis by ppGpp.

Figure 14. The mechanism of hydrolyzing (p)ppGpp by SpoT in response to its increase by RelA via CgtA by sensing the available enegy.

Figure 15. Overall feedback regulation systems of amino acid biosyntheses by (allosteric) enzyme level regulation (blue line) and transcriptional regulation (red line) (together with aminotransferase reactions).

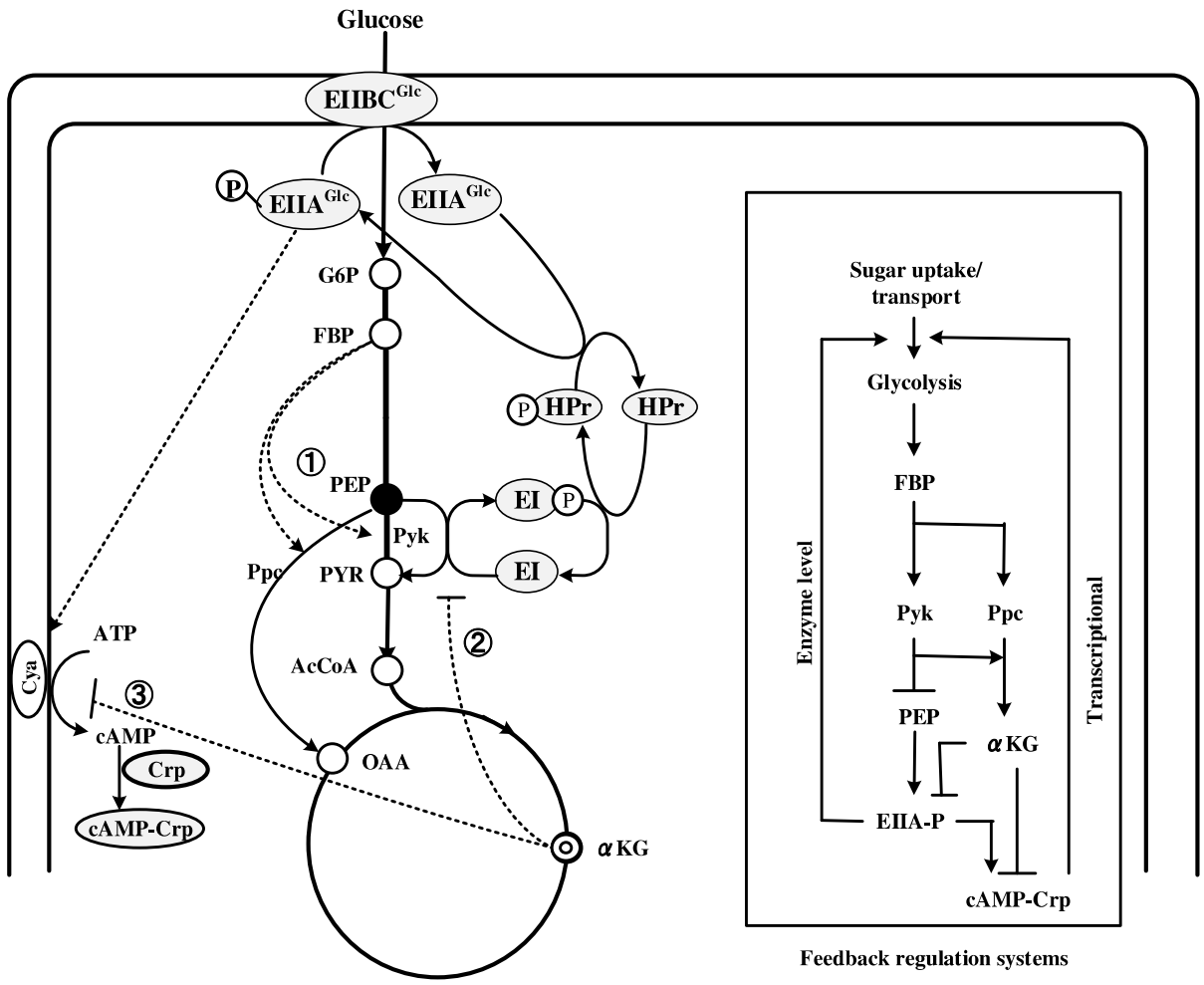
Glucose
EIIBC^Glc
P
EIIA^Glc
EIIA^Glc
G6P
FBP
P
HPr
HPr
①
PEP
EI
P
Pyk
Ppc
PYR
EI
②
ATP
Cya
③
cAMP
Crp
cAMP-Crp
AcCoA
OAA
αKG
Sugar uptake/
transport
Glycolysis
FBP
Pyk
Ppc
PEP
αKG
EIIA-P
cAMP-Crp
Enzyme level
Transcriptional
Feedback regulation systems

Fig.1

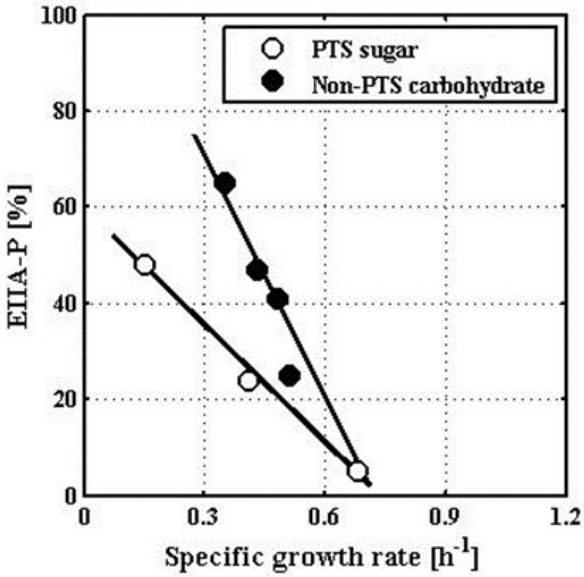
PTS sugar
Non-PTS carbohydrate
EIIA-P [%]
Specific growth rate [h^-1]
0
20
40
60
80
100
0
0.3
0.6
0.9
1.2

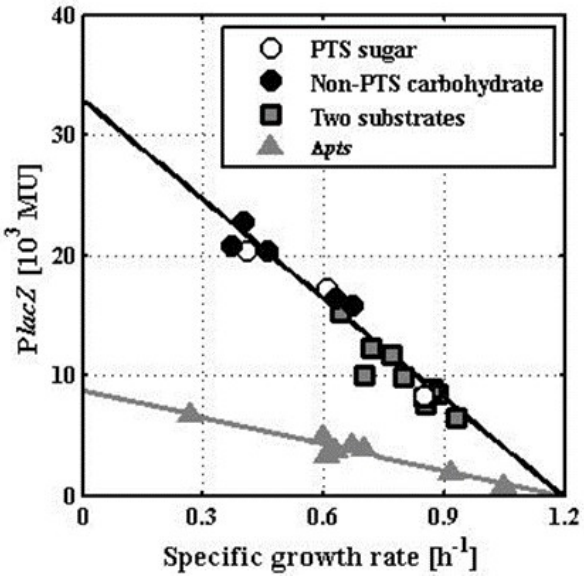
PTS sugar
Non-PTS carbohydrate
Two substrates
Δpts
PlacZ [10^3 MU]
Specific growth rate [h^-1]
0
10
20
30
40
0
0.3
0.6
0.9
1.2

Fig.2 (a) (b)

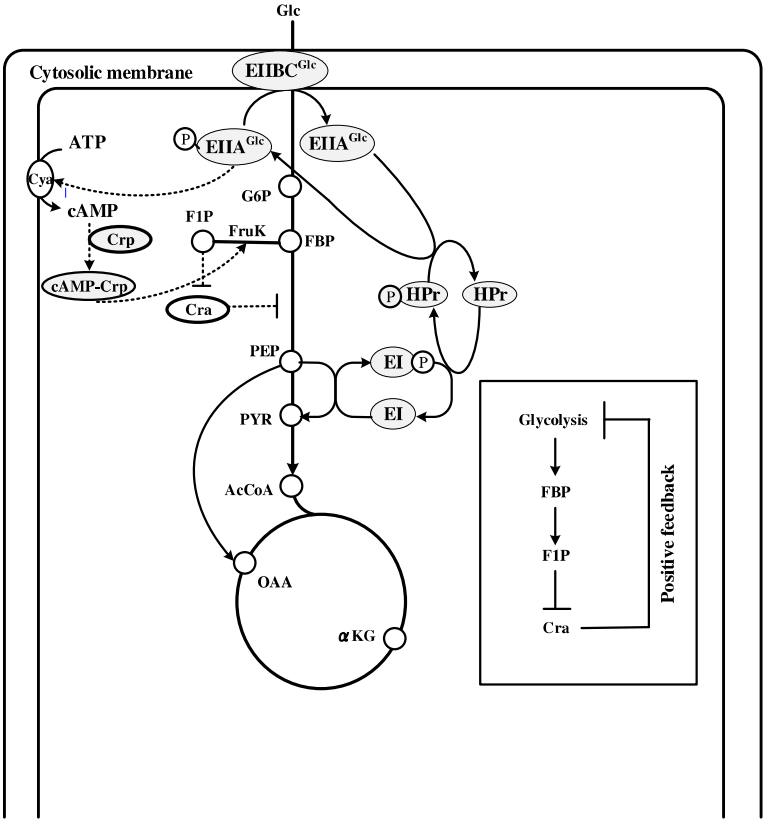
Glc
Cytosolic membrane
EIIBC^Glc
ATP
P
EIIA^Glc
EIIA^Glc
Cya
cAMP
G6P
F1P
FruK
FBP
Crp
cAMP-Crp
Cra
P
HPr
HPr
PEP
EI
P
EI
PYR
AcCoA
OAA
αKG
Glycolysis
FBP
F1P
Cra
Positive feedback

Fig.3

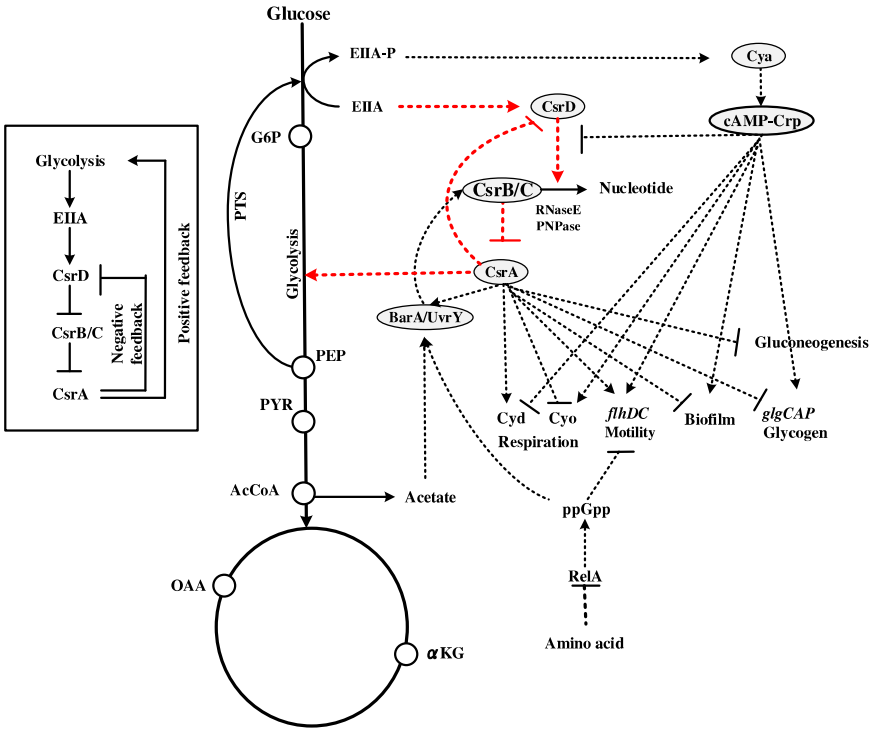
Glucose
EIIA-P
Cya
EIIA
CsrD
cAMP-Crp
G6P
CsrB/C
Nucleotide
RNaseE
PNPase
PTS
Glycolysis
CsrA
BarA/UvrY
Gluconeogenesis
PEP
PYR
Cyd
Cyo
Respiration
flhDC
Motility
Biofilm
glgCAP
Glycogen
AcCoA
Acetate
ppGpp
RelA
Amino acid
OAA
αKG
Glycolysis
EIIA
CsrD
CsrB/C
CsrA
Negative feedback
Positive feedback

Fig.4

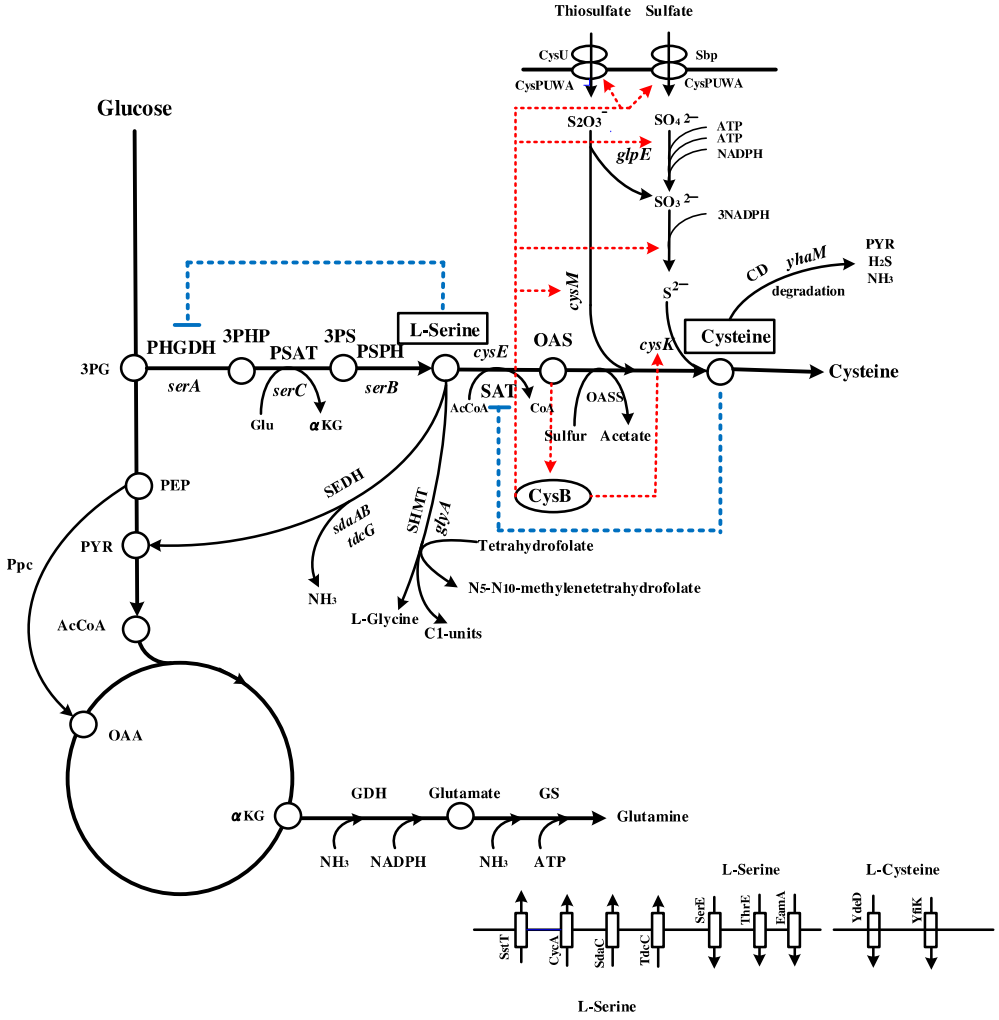
Thiosulfate
Sulfate
CysU
Sbp
CysPUWA
CysPUWA
Glucose
S2O3
SO4 2−
ATP
ATP
NADPH
glpE
SO3 2−
3NADPH
PYR
H2S
NH3
CD
yhaM
degradation
S2−
cysM
L-Serine
Cysteine
3PG
PHGDH
3PHP
PSAT
3PS
PSPH
cysE
OAS
cysK
Cysteine
serA
serC
serB
SAT
OASS
Glu
αKG
AcCoA
CoA
Sulfur
Acetate
CysB
PEP
SEDH
sdaAB
tdcG
SHMT
glyA
Tetrahydrofolate
PYR
Ppc
NH3
N5-N10-methylenetetrahydrofolate
L-Glycine
C1-units
AcCoA
OAA
αKG
GDH
Glutamate
GS
Glutamine
NH3
NADPH
NH3
ATP
L-Serine
L-Cysteine
SstT
CycA
SdaC
TdcC
SerE
ThrE
EamA
YdeD
YfiK
L-Serine

Fig.5

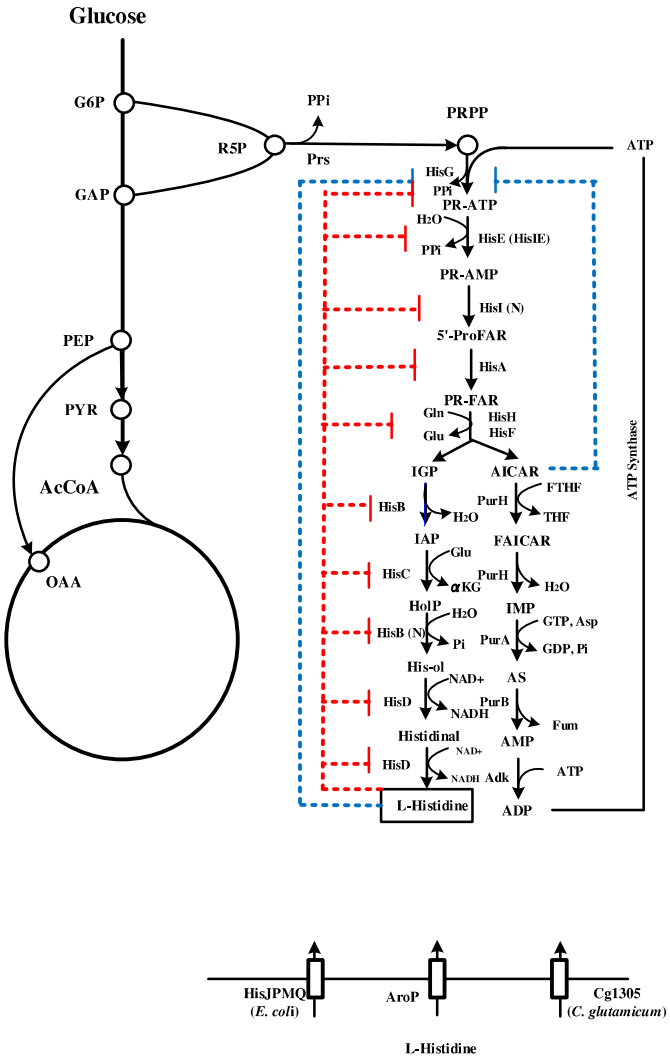
Glucose
G6P
GAP
R5P
PPi
Prs
PRPP
ATP
HisG
PPi
PR-ATP
H2O
PPi
HisE (HisIE)
PR-AMP
HisI (N)
5'-ProFAR
HisA
PR-FAR
Gln
Glu
HisH
HisF
IGP
AICAR
FTHF
PurH
THF
HisB
H2O
IAP
FAICAR
Glu
HisC
αKG
PurH
H2O
HolP
H2O
IMP
GTP, Asp
HisB (N)
Pi
PurA
GDP, Pi
His-ol
NAD+
AS
HisD
NADH
PurB
Fum
Histidinal
AMP
NAD+
HisD
NADH
Adk
ATP
L-Histidine
ADP
ATP Synthase
PEP
PYR
AcCoA
OAA
HisJPMQ
(E. coli)
AroP
Cg1305
(C. glutamicum)
L-Histidine

Fig.6

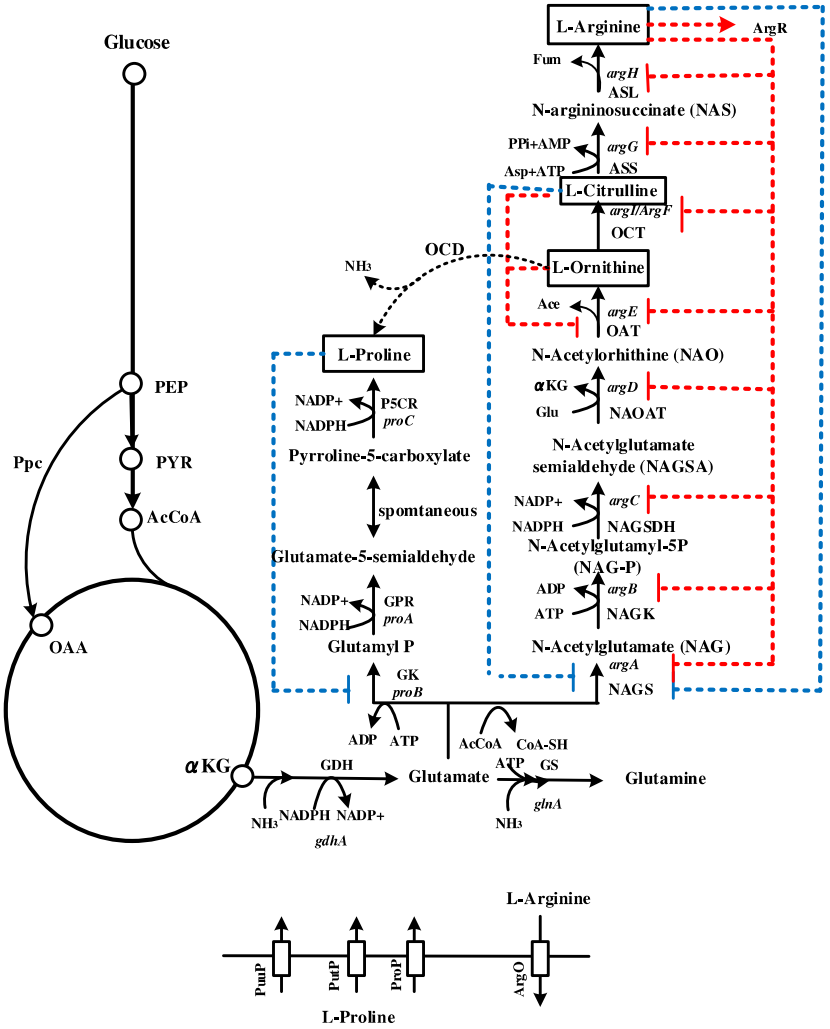
Glucose
PEP
PYR
AcCoA
Ppc
OAA
αKG
L-Arginine
ArgR
Fum
argH
ASL
N-argininosuccinate (NAS)
PPi+AMP
argG
ASS
Asp+ATP
L-Citrulline
argI/ArgF
OCT
OCD
NH3
L-Ornithine
Ace
argE
OAT
N-Acetylorhithine (NAO)
αKG
argD
Glu
NAOAT
N-Acetylglutamate
semialdehyde (NAGSA)
NADP+
argC
NADPH
NAGSDH
N-Acetylglutamyl-5P
(NAG-P)
ADP
argB
ATP
NAGK
N-Acetylglutamate (NAG)
argA
NAGS
L-Proline
NADP+
P5CR
NADPH
proC
Pyrroline-5-carboxylate
spomtaneous
Glutamate-5-semialdehyde
NADP+
GPR
NADPH
proA
Glutamyl P
GK
proB
ADP
ATP
AcCoA
CoA-SH
ATP
GS
GDH
Glutamate
Glutamine
NH3
NADPH
NADP+
gdhA
glnA
NH3
L-Arginine
PutP
PutP
ProP
ArgO
L-Proline

(a)

Fig.7

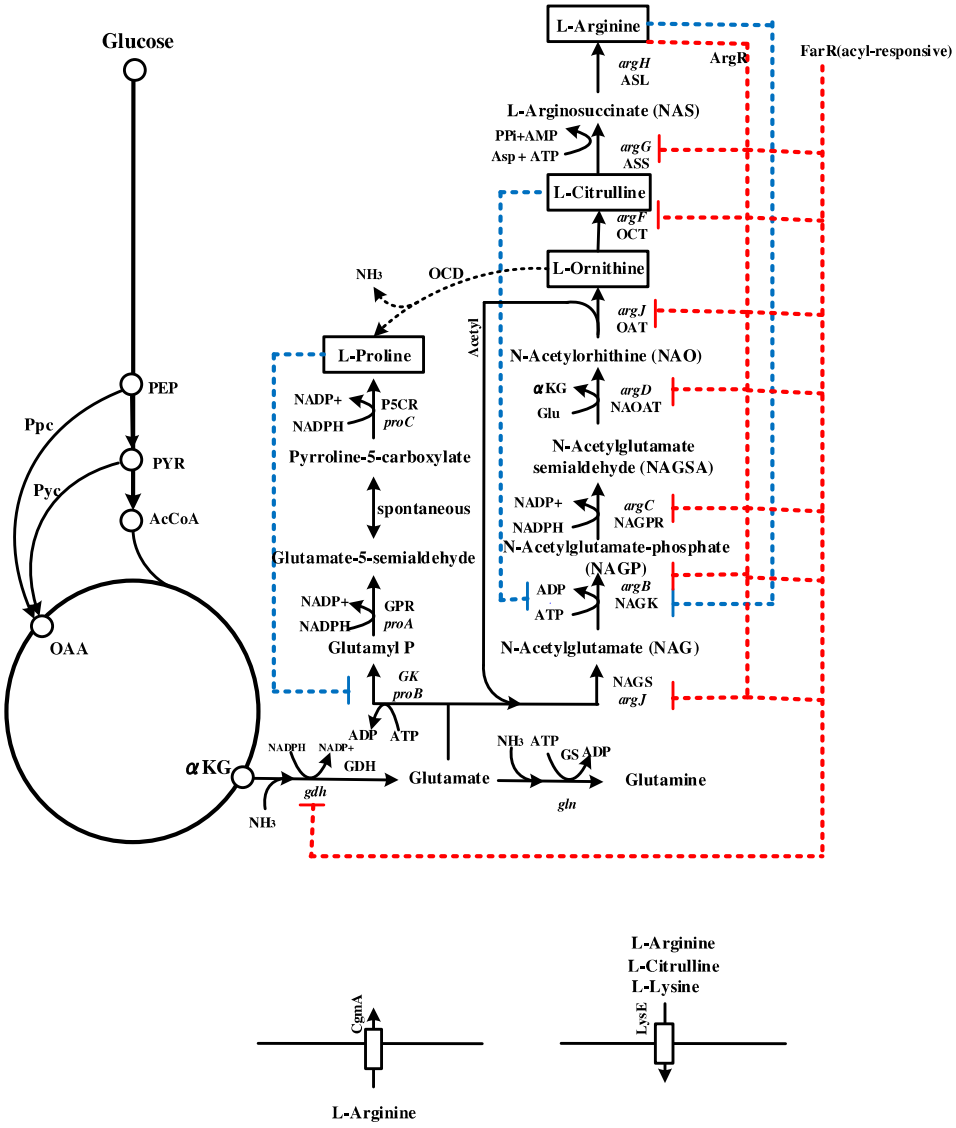
Glucose
PEP
Ppc
PYR
Pyc
AcCoA
OAA
αKG
NH3
GDH
gdh
NADPH
NADP+
Glutamate
GS
ADP
ATP
gln
Glutamine
L-Proline
NADP+
NADPH
P5CR
proC
Pyrroline-5-carboxylate
spontaneous
Glutamate-5-semialdehyde
GPR
proA
Glutamyl P
GK
proB
OCD
L-Arginine
argH
ASL
ArgR
FarR(acyl-responsive)
L-Arginosuccinate (NAS)
PPi+AMP
Asp + ATP
argG
ASS
L-Citrulline
argF
OCT
L-Ornithine
argJ
OAT
Acetyl
N-Acetylorhithine (NAO)
Glu
argD
NAOAT
N-Acetylglutamate
semialdehyde (NAGSA)
argC
NAGPR
N-Acetylglutamate-phosphate
(NAGP)
argB
NAGK
N-Acetylglutamate (NAG)
NAGS
argJ
CgmA
L-Arginine
L-Arginine
L-Citrulline
L-Lysine
LysE

(b)

Fig.7

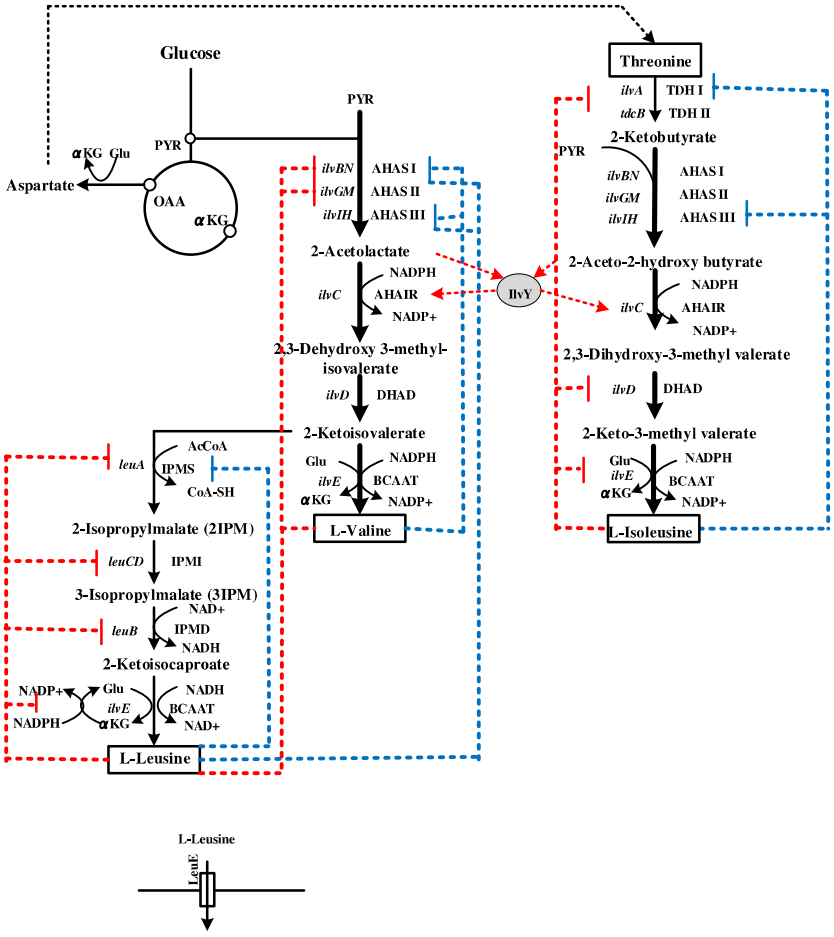
Glucose
PYR
αKG Glu
Aspartate
OAA
αKG
Threonine
ilvA
TDH I
tdcB
TDH II
2-Ketobutyrate
PYR
ilvBN
ilvGM
ilvIH
AHAS I
AHAS II
AHAS III
2-Acetolactate
NADPH
ilvC
AHAIR
NADP+
IlvY
2-Aceto-2-hydroxy butyrate
2,3-Dehydroxy 3-methyl-isovalerate
ilvD
DHAD
2,3-Dihydroxy-3-methyl valerate
2-Ketoisovalerate
Glu
ilvE
BCAAT
L-Valine
2-Keto-3-methyl valerate
L-Isoleusine
leuA
AcCoA
IPMS
CoA-SH
2-Isopropylmalate (2IPM)
leuCD
IPMI
3-Isopropylmalate (3IPM)
NAD+
leuB
IPMD
NADH
2-Ketoisocaproate
L-Leusine
L-Leusine
LeuE

Fig.8

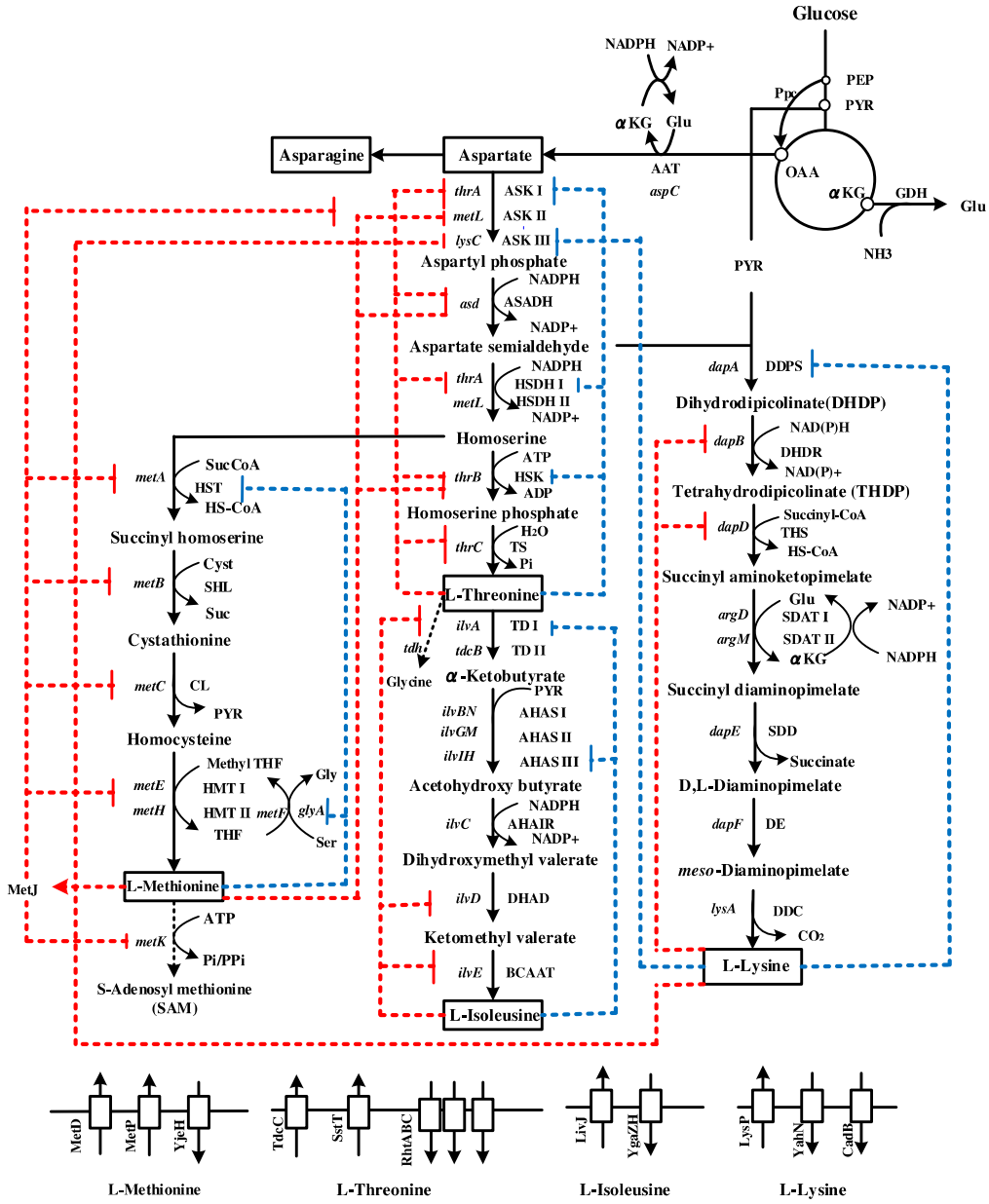
Glucose
NADPH
NADP+
PEP
Ppc
PYR
αKG
Glu
AAT
aspC
Asparagine
Aspartate
OAA
αKG
GDH
Glu
NH3
PYR
thrA
metL
lysC
ASK I
ASK II
ASK III
Aspartyl phosphate
NADPH
asd
ASADH
NADP+
Aspartate semialdehyde
NADPH
thrA
HSDH I
metL
HSDH II
NADP+
Homoserine
ATP
thrB
HSK
ADP
Homoserine phosphate
H2O
thrC
TS
Pi
L-Threonine
ilvA
TD I
tdh
tdcB
TD II
Glycine
α-Ketobutyrate
PYR
ilvBN
ilvGM
ilvIH
AHAS I
AHAS II
AHAS III
Acetohydroxy butyrate
NADPH
ilvC
AHAIR
NADP+
Dihydroxymethyl valerate
ilvD
DHAD
Ketomethyl valerate
ilvE
BCAAT
L-Isoleusine
dapA
DDPS
Dihydrodipicolinate(DHDP)
NAD(P)H
dapB
DHDR
NAD(P)+
Tetrahydrodipicolinate (THDP)
Succinyl-CoA
dapD
THS
HS-CoA
Succinyl aminoketopimelate
Glu
argD
SDAT I
NADP+
argM
SDAT II
αKG
NADPH
Succinyl diaminopimelate
dapE
SDD
Succinate
D,L-Diaminopimelate
dapF
DE
meso-Diaminopimelate
lysA
DDC
CO2
L-Lysine
metA
SucCoA
HST
HS-CoA
Succinyl homoserine
Cyst
metB
SHL
Suc
Cystathionine
metC
CL
PYR
Homocysteine
Methyl THF
metE
HMT I
metH
HMT II
THF
metF
glyA
Gly
Ser
L-Methionine
MetJ
ATP
metK
Pi/PPi
S-Adenosyl methionine
(SAM)
MetD
MetP
YjeH
L-Methionine
TdcC
SstT
RhtABC
L-Threonine
LivJ
YgaZH
L-Isoleusine
LysP
YahN
CadB
L-Lysine

Fig.9

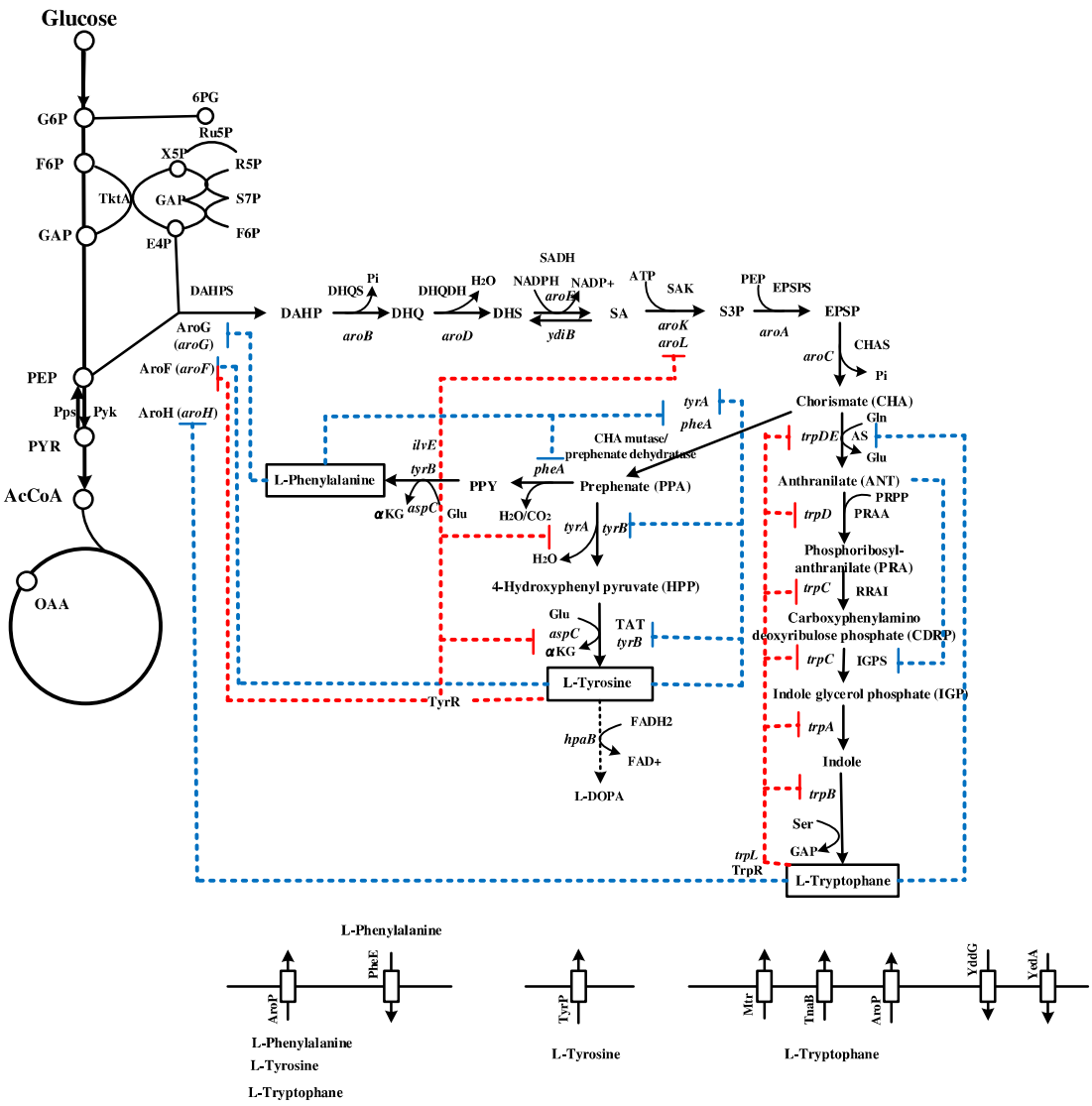
Glucose
G6P
6PG
Ru5P
F6P
X5P
R5P
TktA
GAP
S7P
GAP
E4P
F6P
DAHPS
DAHP
DHQS
Pi
DHQ
aroB
DHQDH
H2O
DHS
aroD
SADH
NADPH
NADP+
aroE
ydiB
SA
ATP
SAK
aroK
aroL
S3P
PEP
EPSPS
aroA
EPSP
aroC
CHAS
Pi
Chorismate (CHA)
AroG
(aroG)
AroF (aroF)
AroH (aroH)
PEP
Pps
Pyk
PYR
AcCoA
OAA
tyrA
pheA
CHA mutase/
prephenate dehydratase
ilvE
tyrB
L-Phenylalanine
PPY
pheA
Prephenate (PPA)
αKG
aspC
Glu
H2O/CO2
tyrA
tyrB
H2O
4-Hydroxyphenyl pyruvate (HPP)
Glu
aspC
αKG
TAT
tyrB
L-Tyrosine
TyrR
FADH2
hpaB
FAD+
L-DOPA
Gln
trpDE
AS
Glu
Anthranilate (ANT)
PRPP
trpD
PRAA
Phosphoribosyl-
anthranilate (PRA)
trpC
RRAI
Carboxyphenylamino
deoxyribulose phosphate (CDRP)
trpC
IGPS
Indole glycerol phosphate (IGP)
trpA
Indole
trpB
Ser
GAP
trpL
TrpR
L-Tryptophane
L-Phenylalanine
AroP
PheE
L-Phenylalanine
L-Tyrosine
L-Tryptophane
TyrP
L-Tyrosine
Mtr
TnaB
AroP
YddG
YedA
L-Tryptophane

Fig.10

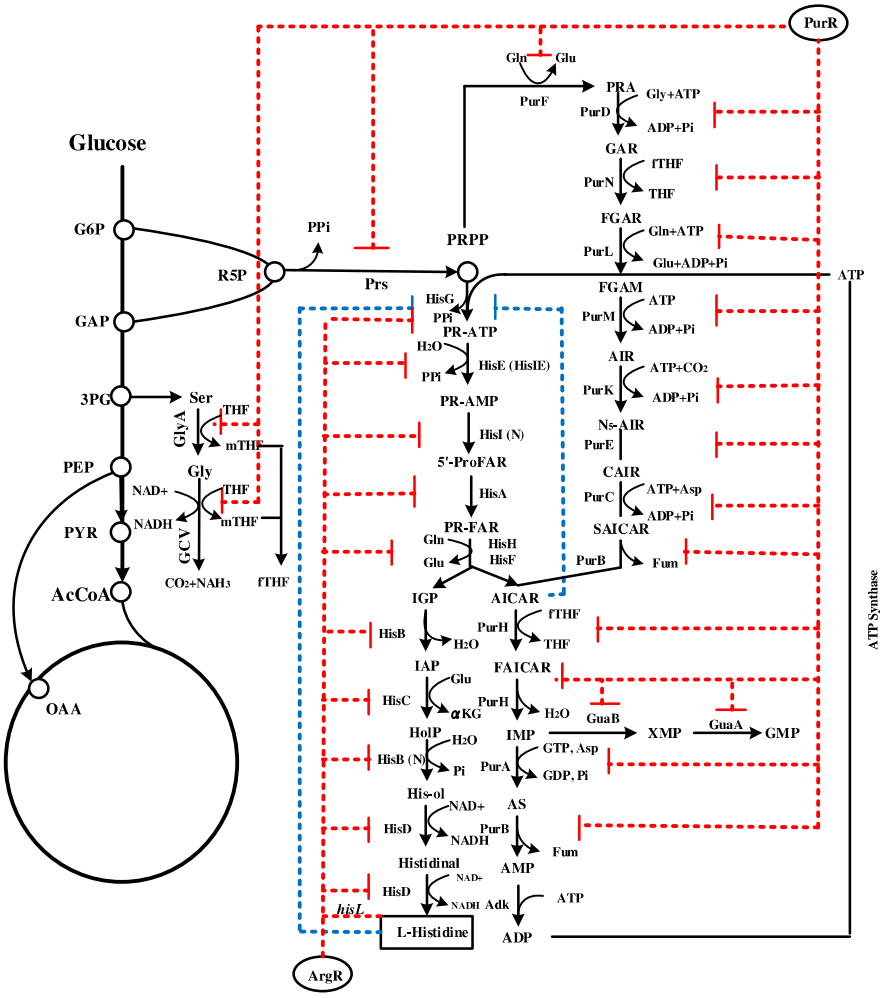
PurR
Glucose
G6P
GAP
3PG
PEP
PYR
AcCoA
OAA
R5P
PPi
Prs
PRPP
Gln
Glu
PurF
PRA
PurD
Gly+ATP
ADP+Pi
GAR
PurN
fTHF
THF
FGAR
PurL
Gln+ATP
Glu+ADP+Pi
FGAM
PurM
ATP
ADP+Pi
AIR
PurK
ATP+CO2
ADP+Pi
N5-AIR
PurE
CAIR
PurC
ATP+Asp
ADP+Pi
SAICAR
PurB
Fum
AICAR
PurH
fTHF
THF
FAICAR
PurH
H2O
IMP
GTP, Asp
GDP, Pi
PurA
AS
PurB
Fum
AMP
ATP
ADP
Adk
XMP
GuaB
GMP
GuaA
ATP
ATP Synthase
HisG
PPi
PR-ATP
H2O
HisE (HisIE)
PPi
PR-AMP
HisI (N)
5'-ProFAR
HisA
PR-FAR
Gln
Glu
HisH
HisF
IGP
HisB
H2O
IAP
Glu
HisC
αKG
HolP
H2O
HisB (N)
Pi
His-ol
NAD+
HisD
NADH
Histidinal
NAD+
HisD
NADH
hisL
L-Histidine
ArgR
Ser
GlyA
THF
mTHF
Gly
NAD+
THF
NADH
mTHF
GCV
CO2+NAH3
fTHF

(a)

Fig.11

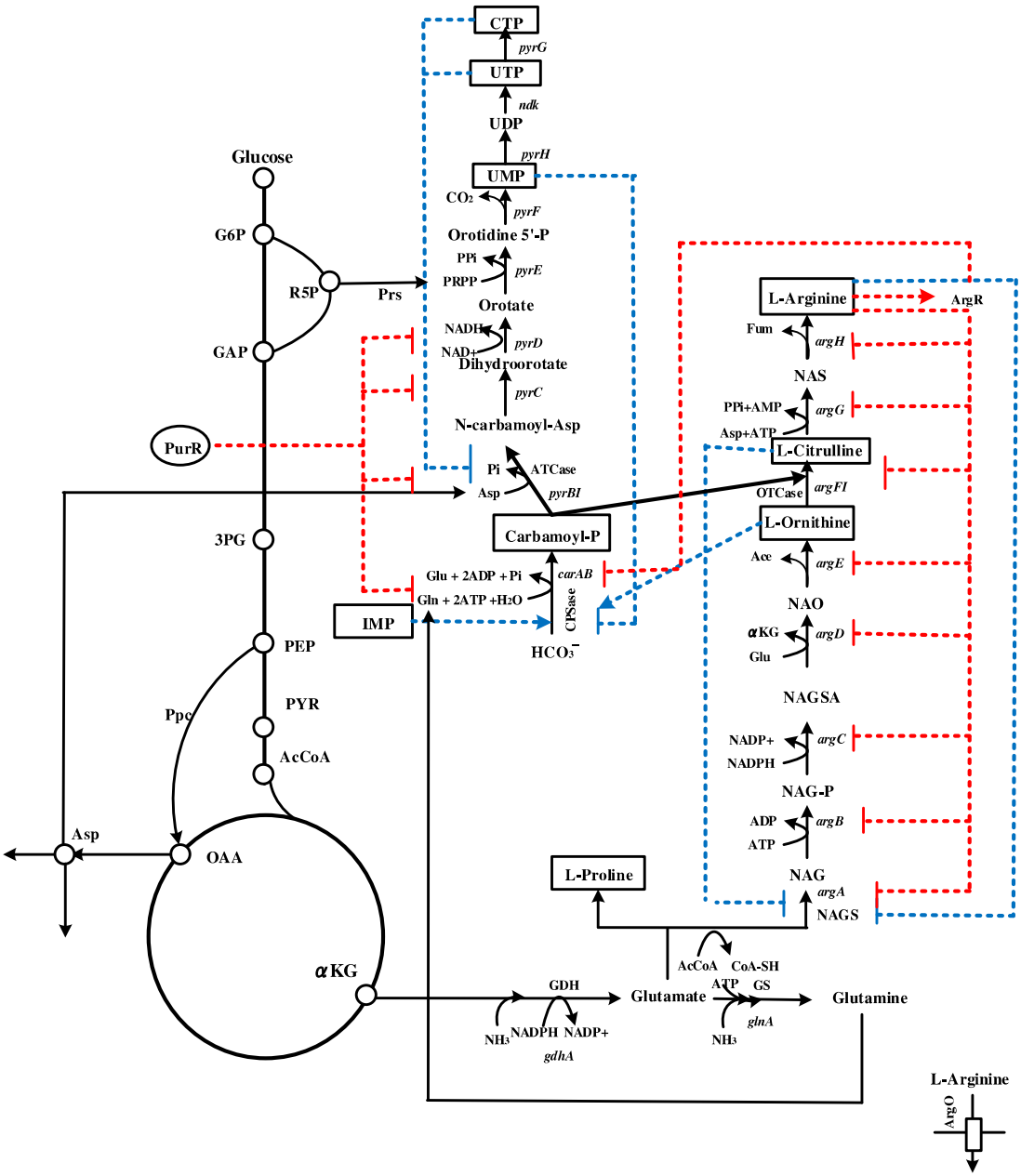
CTP
pyrG
UTP
ndk
UDP
pyrH
UMP
CO2
pyrF
Orotidine 5'-P
PPi
PRPP
pyrE
Orotate
NADH
NAD+
pyrD
Dihydroorotate
pyrC
N-carbamoyl-Asp
Pi
ATCase
Asp
pyrBI
Carbamoyl-P
Glu + 2ADP + Pi
carAB
Gln + 2ATP +H2O
CPSase
HCO3-
IMP
Glucose
G6P
R5P
Prs
GAP
PurR
3PG
PEP
Ppc
PYR
AcCoA
Asp
OAA
αKG
L-Arginine
ArgR
Fum
argH
NAS
PPi+AMP
argG
Asp+ATP
L-Citrulline
OTCase
argFI
L-Ornithine
Ace
argE
NAO
αKG
argD
Glu
NAGSA
NADP+
argC
NADPH
NAG-P
ADP
argB
ATP
NAG
argA
NAGS
L-Proline
AcCoA
CoA-SH
ATP
GS
GDH
Glutamate
Glutamine
NH3
NADPH
NADP+
gdhA
glnA
NH3
L-Arginine
ArgO

(b)

Fig.11

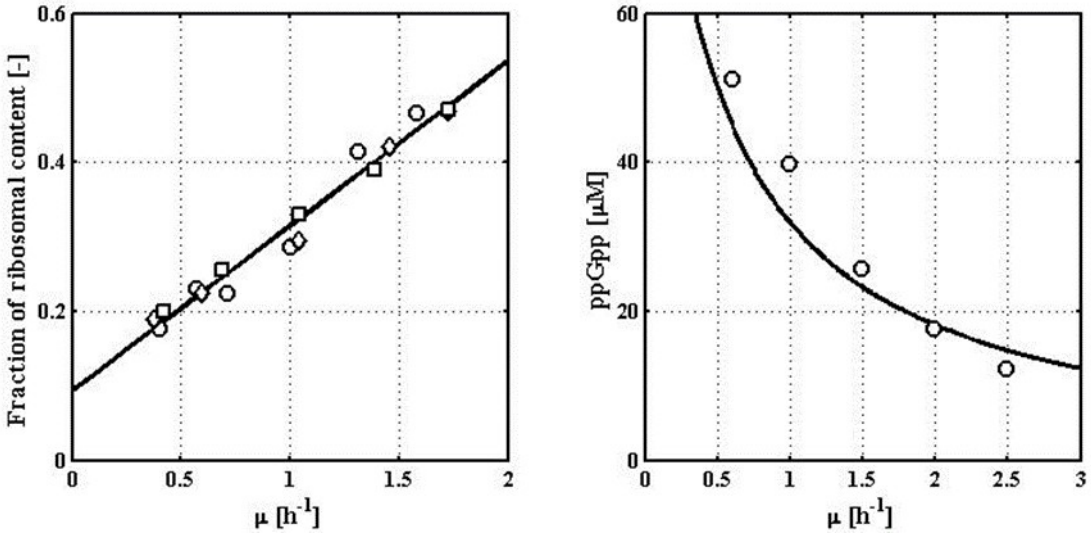
Fraction of ribosomal content [-]
0.6
0.4
0.2
0
0
0.5
1
1.5
2
μ [h-1]
ppGpp [μM]
60
40
20
0
0
0.5
1
1.5
2
2.5
3
μ [h-1]

Fig.12

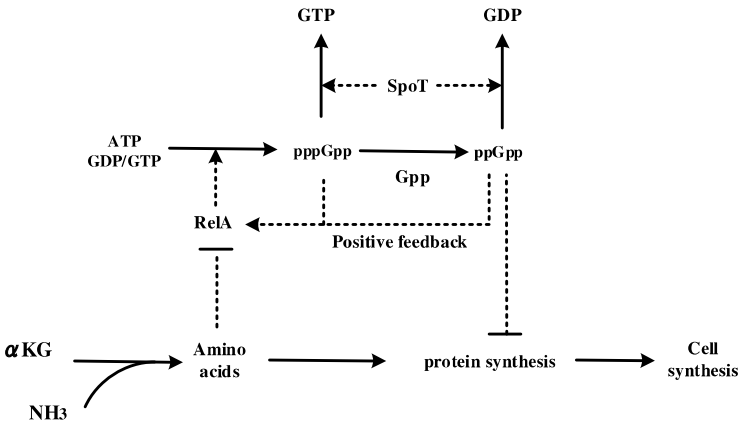
GTP
GDP
SpoT
ATP
GDP/GTP
pppGpp
ppGpp
Gpp
RelA
Positive feedback
αKG
Amino
acids
protein synthesis
Cell
synthesis
NH3

Fig.13

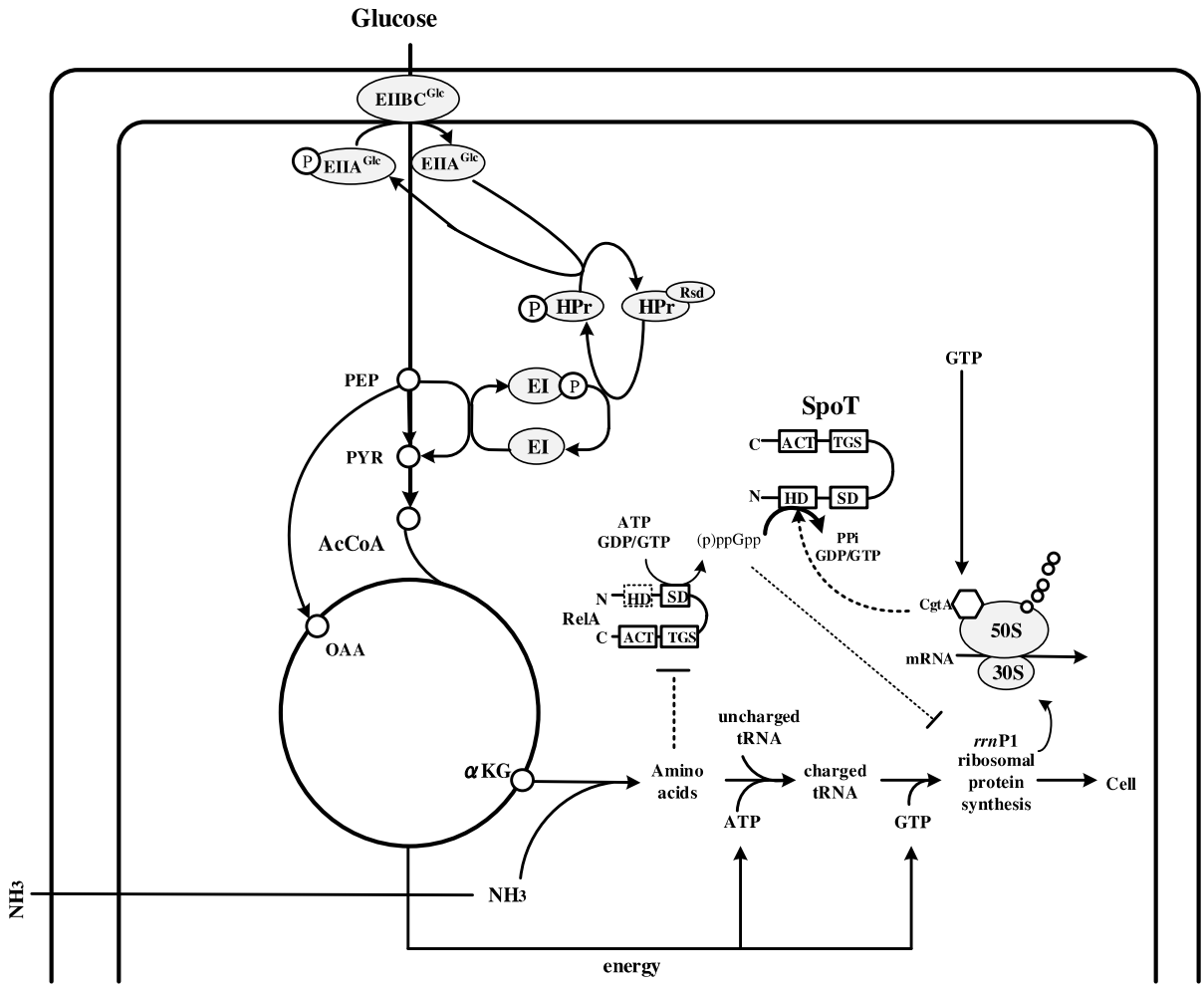
Glucose
EIIBC^Glc
P EIIA^Glc
EIIA^Glc
P HPr
HPr
Rsd
PEP
EI P
EI
PYR
AcCoA
OAA
αKG
SpoT
C ACT TGS
N HD SD
ATP
GDP/GTP
(p)ppGpp
PPi
GDP/GTP
N HD SD
RelA
C ACT TGS
GTP
CgtA
50S
mRNA
30S
uncharged
tRNA
Amino
acids
charged
tRNA
ATP
GTP
rrnP1
ribosomal
protein
synthesis
Cell
NH3
NH3
energy

Fig.14

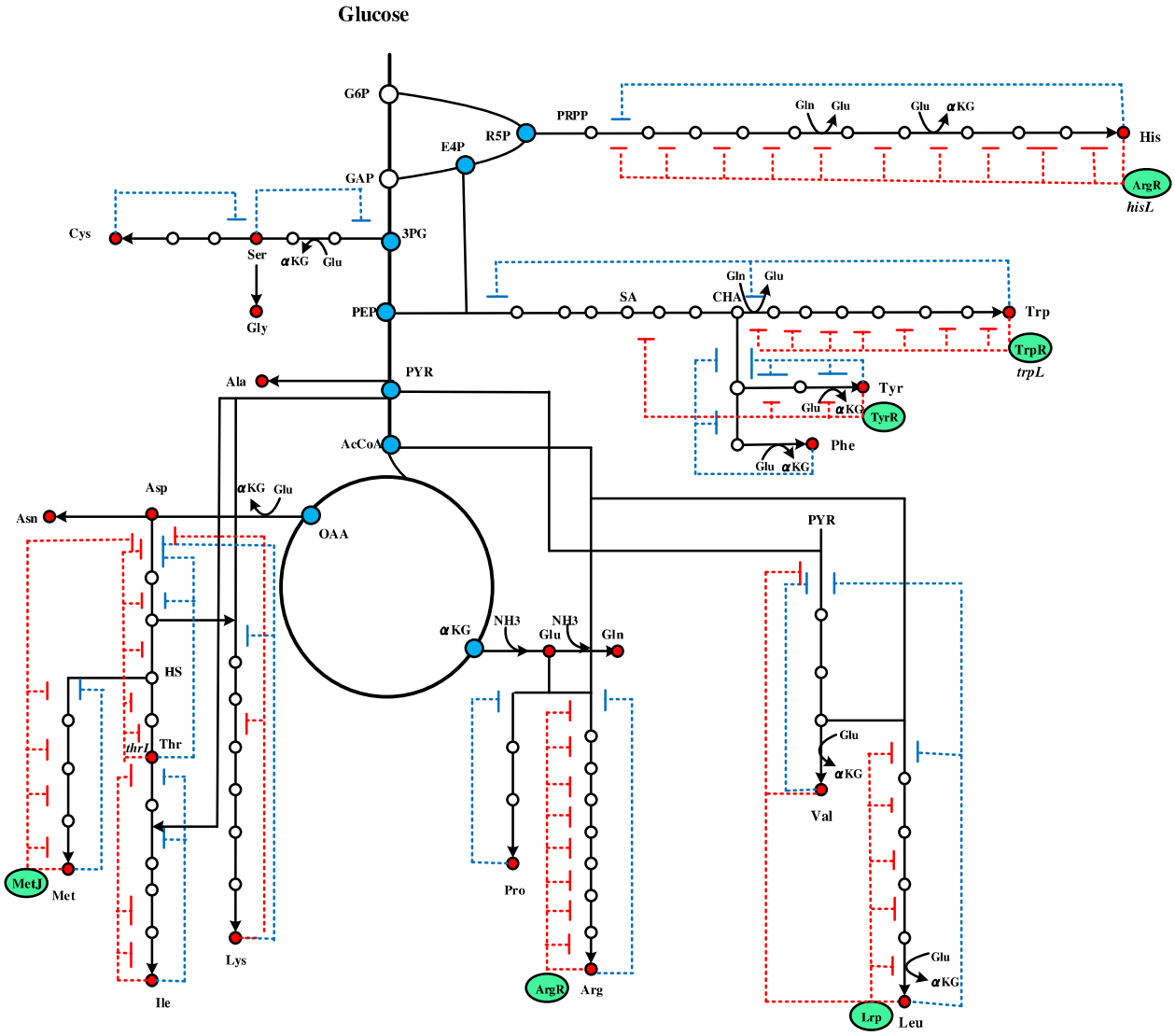
Glucose
G6P
GAP
E4P
R5P
PRPP
Gln
Glu
Glu
αKG
His
ArgR
hisL
Cys
Ser
αKG
Glu
3PG
Gly
PEP
SA
CHA
Gln
Glu
Trp
TrpR
trpL
Ala
PYR
Tyr
Glu
αKG
TyrR
AcCoA
Phe
Glu
αKG
Asp
αKG
Glu
Asn
OAA
PYR
αKG
NH3
Glu
NH3
Gln
HS
thrL
Thr
Glu
αKG
Val
MetJ
Met
Pro
Lys
Glu
αKG
ArgR
Arg
Ile
Lrp
Leu

Fig.15

Table 1 Performances of L-amino acid fermentation by bacteria							
Product	**Strains**	**Main genotypes**	**Cultivation**	**Titer** [g/l]	**Yield** [g/g-Glc]	**Productivity** [g/l.h]	**Reference**
Serine	*E. coli* MG1655	*serA**(fbr), *serB**,*serC**,*eamA**,Δ*sdaA*, Δ*sdaB*, Δ*tdcG*, Δ*glyA*	fed-batch	11.7	0.43	-	Mundhada et al 2015
〃	*E. coli* ALE-5(DE3)	*serA**(fbr), *serB**,*serC**,*eamA**,Δ*sdaA*, Δ*sdaB*, Δ*tdcG*, Δ*glyA*,*thrA**(ALE)	fed-batch	37	0.24	0.83	Mundhada et al 2016
〃	*E. coli* ES-134	*serA**(fbr), *serB**,*serC**, Δ*glyA*, Δ*sdaA*, Δ*sstT*,Δ*cycA*, Δ*sdaC*, Δ*tdcC*	fed-batch	34.8	0.32	0.97***	Wang et al 2020
〃	*C. glutamicum* SYPS-062-33aΔSS	Δ*alaT*,Δ*avtA*,Δ*ilvN*	fed-batch	42.62	0.21 [g/g-S]	0.44	Zhu et al 2015
〃	*C. glutamicum* A36	*serA**(Δ197), *serC*, serB*,serE**	batch	43.9	0.44 [g/g-S]	0.37***	Zhang et al 2020
Cysteine	*P. ananatis* AJ13355	Δ*ccdA, cefA*,cefB**	batch	2.2	-	0.1***	Takumi et al 2017
〃	*E. coli* JM109	*serA**, *serB**, *serC**, *cysE**(fbr)	fed-batch	5.1	-	0.16***	Liu et al 2018
〃	*E. coli* JM109	*cysB**, *serACB**, *cysM**, *nrdH**, Δ*yhaM*, Δ*tnaA*, Δ*sdaA*, Δ*decR*	fed-batch	7.5	-	0.34***	Liu et al 2020
Histidine	*E. coli* HW6-3	Δ*purF*,Δ*mazG*,Δ*amn*,Δ*ygdH*,Δ*yjjG*,Δ*yrfG*,Δ*ushA*,Δ*surE* *hisG**(fbr),*hisDCBHAFI**, *purHAB*,*gdh**(*B. subtilis*), *tdcD**(*C. glutamicum*)	fed-batch	66.5	0.23	1.5	Wu et al 2020
Arginine	*C. glutamicum* ATCC21831	Δ*argR*,Δ*farR*,*pgi***,*tkt**,*tal**,*zwf**,*opcA**,*pgl**,ΔNCgl1221, *carAB**,*argGH**	fed-batch	92.5	0.4	1.28	Park et al 2014

〃	*C. glutamicum* SNK118	Δ*argR*Δ*farR*Δ*ldh*,/*ppnK**,*pntAB**	fed-batch	67	0.35	0.89	Zhan et al 2019
〃	*C. crenatum* SYPA 5-5	Δ*argR*Δ*proB*/Peftu-*argB**(fbr),*argCJBDFR**,*argGH**, *iolT1**,*ppgK**,*pyc**,*gltA**,*icd**,*gdh**,*odhA**,*lysC**	fed-batch	87.3	0.431	1.21	Man et al 2016
〃	*C. cenatum* DArg36	Δ*argR*: atmospheric and room temperature plasma (ARTP) mutagenesis	fed-batch	95.5	0.73	0.99	Xu et al 2020
Citrulline	*C.glutamicum* CIT1	Δ*argF*,Δ*argG*, Δ*argR*,*argFB**(fbr)	batch	7.7	0.38	0.32	Eberhardt et al 2014
〃	*C. glutamicum* ATCC130321	Δ*argG*,Δ*argR*,*argJ**	batch	8.51	-	-	Hao et al 2015
Ornithine	*E. coli* YW06	Δ*argF*, Δ*proB*,Δ*argR*	fed-batch	51.5	0.24	-	Kim et al 2015
〃	*C. glutamicum* S026	Δ*argF*,ΔNCｇｌ１221,Δ*argR*,Δ*putP*,Δ*mscCG2*,Δ*iolR* *odhA***,*proB***,*ncgl2228***, *pta***,*cat***,*pgi***,*lysE**, *gdh**,*Cg3035**,*pfkA**, *tkt**,*argCJBD**,*glt**,*gdh2**	fed-batch	43.6	0.34	-	Zhang et al 2018, 2019
〃	*C. crenatum*	Δ*proB*, Δ*argF*,*argB**,*argA**(*E. coli*),*argE**(*S.marcescens*)	batch	40.4	0.27	0.673	Shu et al 2018
Proline	*E. coli* M6	Δ*proP*,Δ*putP*,Δ*putA*,Δ*aceA*,*proB*(fbr)*	batch	37.5	-	0.938	Long et al 2020
〃	*E. coli* NMH26	Δ*argl*,Δ*putA*,Δ*speCF*,Δ*speE*,Δ*puuA*,Δ*speG*,Δ*puuP*,Δ*putP*, Δ*proP*, *argE**, *argC**, *argB**, *argH**, *argD**	fed-batch	33.8	-	-	Noh et al 2017
〃	*C. glutamicum* ORN1	Δ*argR*,Δ*argF*, *argB*(fbr)*, *ocd**(*P. putida*)	batch	12.7	0.31	0.42***	Korgaard et al 2013
〃	*C.acetoacidophilum* RYU3161	mutation by NTG and UV irradiation	fed-batch	42	-	1.4	Ahn et al 2004
Valine	*E. coli* K12	Δ*ilvGM*,Δ*ilvIH*,Δ*ilvY*,*ilvY**,*ilvC**,*ilvBN*(fbr)*	batch	6.1	-	-	Geraskina et al 2019
〃	*E. coli* W3110	Δ*ldhA*,Δ*pflB*,Δ*adhE*,*alsS* *(*B. subtilis*),*ilvEC**(*B. subtilis*),	fed-batch	84	0.41	2.33	Hao et al 2020

	VHY18	*brnFE**(*C. glutamicum*),*spoT*[R290,K292D]					
〃	*C.glutamicum* ATCC13032	Δ*ppc*,Δ*pyc,icd***,*ilvBNCE**	batch	8.9	0.22	0.018***	Schwentner et al 2018
〃	*C.glutamicum* WCC003	*ilvBNC1**,*lrp1**,*brnFE**,Δ*aceE*,Δ*alaT*,Δ*ilvA*	fed-batch	51	0.473 [m/m]	0.533	Chen et al 2015
Leusine	*C. glutamicum* ML1-9	Δ*ilvA*,Δ*alaT*,Δ*ldh*,Δ*panBC*,Δ*ltbR*, *leuA*(fbr)*	fed-batch	38.1	0.26	0.87***	Huang et al 2017
〃	*C. glutamicum* XQ-9	Δ*ltbR*,*ilvC*(M),Δ*ilvE*::*leuDH**(*L. sphaericus*), Δ*gdh*::*rocG**(*B. subtilis*)	batch	23.31	0.191	0.32***	Wang et al 2019
〃	*C. glutamicum* FA-1	Δ*ilvE*,Δ*aspB*,tyr*B**	batch	18.55	-	0.26***	Feng et al 2018
Threonine	*E. coli* TH27C	*thrA*(fbr)*,*lysC*(fbr)*,*thrABC*(fbr)*,*rhtABC**,*ppc**,*acs**,Δ*lysA*, *ilA***,Δ*tdh*,Δ*tdcC*,Δ*iclR*	fed-batch	82.4	0.393	1.65	Lee et al 2007
〃	*E. coli B57*TWF04	Δ*fadR*,Δ*fabR*,Δ*iclR*,*ppnk**,*thrA*(fbr)*,*thrBC**,*rhtC**,*aspC**,*ppc**	fed-batch	103.9	-	2.2***	Yang et al 2019
〃	*E. coli* TWF083	TWF001/*iclR***,*aspC**,*arcA***,*cpxR***,*gadE***,*pykF***	fed-batch	116.6	0.486	2.43	Zhao et al 2020
Isoleusine	*E. coli* ILE03	*thrABC**,*ilvA*(fbr)*,*ilvIH*(fbr)*,*ygaZH**,*ilvCED**,*lrp**	fed-batch	9.46	0.14	-	Park et al 2012
〃	*C. glutamicum* IWJ001	*ilvBN*1*,*ilvA*1*,*ppnk*1*	fed-batch	32.3	-	0.45***	Yin et al 2014
Methionine	*E. coli* W3110	Δ*metJ*,Δ*metI*,Δ*lysA*,*metA**,*yjeH**	fed-batch	16.86	-	0.35	Huang et al 2018
〃	*E. coli* MET-3	*metA*(fbr)*,*yjeH**,*serA**	fed-batch	12.8	0.13 [m/m]	0.261	Zhou et al 2019
〃	*C. glutamicum* MH20-22B	*hom*(fbr),Δ*thrB*	batch	2.9	-	-	Park et al 2007

〃	*C. glutamicum* LY-5	Δ*metD*,Δ*thrB*, *dapA***,*lysC**,*pyc**,*zwf**,*pgl**	fed-batch	6.85	-	0.10***	Li et al 2016
Homoserine	*E. coli* W3110	Δ*lysA*,Δ*metA*,Δ*thrBC*,Δ*tdcC*,*metL**,*rhtA**	fed-batch	39.54	-	-	Li et al 2016
〃	*E. coli* W3110	*thrA**,Δ*metA*,Δ*thrB*,Δ*iclR*,Δ*lysA*,Δ*ptsG*,Δ*galR*,*rhtA**,*eamA**, *glk**,*gltB**	fed-batch	37.57	0.31	0.42***	Liu et al 2020
Lysine	*E. coli* LATR12-2	Δ*dapD*,Δ*rpiB*::*ddh*(*Symbiobacterium thermophilum*)	fed-batch	119.5	0.49	2.99	Xu et al 2019
〃	*C. glutamicum* LYS-12	Δ*pck*,*icd***,*hom***,*pyc**,*lysC**,*dapB**,*ddh**,*lysA**,*fbp**, *tkt-tal-zwf-opcA-pgl**	fed-batch	120	0.55	4	Becker et al 2011
〃	*C. glutamicum* JL-69	Δ*pck*::*ppc**, Δ*odx*::*pyc**, *gdh**	fed-batch	181.5	-	3.78	Xu et al 2018
〃	*C. glutamicum* ATCC21543	*aspdh**(*P.aeruginosa*),*asd**(*T. mobilis*),*dapB**(*E. coli*)	batch	27.7	0.35	0.46	Wu et al 2019
〃	*C. glutamicum* ZL-92	Δ*ptsG*,*iolT1**,*iolT21**,*ppgK**	fed-batch	201.6	0.65	5.04	Xu et al 2019
〃	*C. glutamicum* K-8	Δ*pck*::*ppc**, Δ*odx*::*pyc**, Δ*gltA.gdh**, Δ*ptsG*, Δ*ptsF*, *iolT1**, *ioT2**, *glk**, *ndh**, Δ*sigH*	fed-batch	221.3	0.71	5.53	Xu et al 2020
Phenylalanine	*E. coli* HD-A2	*aroF**,*pheA*(fbr)*,*aroA**(*aroL**)	fed-batch	62.47	0.236	1.30***	Ding et al 2016
〃	*E. coli* Xllp21	*aroF**,*aroD**,*pheA*(fbr)*,Δ*tyrR*, Δ*pts*,*galP**,*glk**	fed-batch	72.9	0.26	1.40***	Liu et al 2018
〃	*E. coli* Xllp3	*aroK**(dnamic regulation for *tyrP*)	fed-batch	61.3	0.22	1.28***	Wu et al 2019
Tyrosine	*E. coli* T2	Δ*tyrR*,*aroG**(fbr),*tyrA**(fbr),*ppsA**,*tktA**	fed-batch	9.7	0.102	-	Lutke-Eversloh et al 2007
〃	*E. coli* JM101	Δ(*ptsHI*,*crr*),*glk**,*aroG**(fbr),*pheA**, *tyrC* *(*Z. mobilis*)	batch	3	0.066	0.111	Chavez-Bejar et al 2008

〃	*E. coli* P2	Δ*tyrR*,*aroG**(fbr),*tyrA**(fbr),*rpoA*/*rpoD*(global mutation)	fed-batch	13.8	0.12	2.1	Santos et al 2012
〃	*E. coli* SCK5	Δ*tyrR*,*aroG**(fbr),*tyrA**(fbr),*tktA**,*aroA**,*aroB**,*aroC**,*aroD**, *aroE**, *aroL**,*tryB**,*ppsA**	batch	3	0.102	0.0354	Kim et al 2015
〃	*E. coli* BTY2.13	Δ*tyrR*,*aroG**(fbr),*tyrA**(fbr),*aroL**/*tyrC**(*Z. mobilis*)	fed-batch	43.1	-	-	Kim et al 2018
Tryptophan	*E. coli* AGX1757	Δ*trpR*,Δ*tnaA*,*trpE*(fbr)*	fed-batch	54.5	0.23	0.683	Azuma et al 1993
〃	*E. coli* GPT1017	Δ*trpR*,Δ*tnaA*,Δ*ptsG*,Δ*aroP*, Δ*tnaB*,*aroG*(fbr)*,*trpE*(fbr)*,*tktA**	fed-batch	16.3	-	0.25***	Gu et al 2013
〃	*E. coli* TRTH0709	Δ*trpR*,Δ*tnaA*,Δ*pta*,Δ*tyrA*,Δ*mtr*,*aroG*(fbr)*,*trpE*(fbr)**trpDCBA**, *serA**,*tktA**,*ppsA**,*yddG**	fed-batch	48.7	0.219	-	Wang et al 2013
〃	*E. coli* FB-04	Δ*trpR*,Δ*tnaA*,Δ*pheA*,Δ*tyrA*, *aroF*(fbr)*,*trpE*(fbr)*D**	fed-batch	44	0.13	0.82	Liu et al 2016
〃	*E. coli* S028	Δ*aroF*,Δ*aroG*,Δ*mtr*,Δ*tnaA*,Δ*tnaB*,*trpEDCBA**	fed-batch	40	0.15	0.6	Chen et al 2017
〃	*E. coli* S028	Δ*aroF*,Δ*aroG*,Δ*mtr*,Δ*tnaA*,Δ*tnaB*,*trpEDCBA**,*trpC**(*A. niger*)	fed-batch	29	0.18	0.69***	Chen et al 2018
〃	*E. coli* KW03	Δ*pykF*,Δ*ptsH*,Δ*trpR*,Δ*pta*,*aroG*(fbr)*,*trpEDCBA**,*galP**,*glk**	fed-batch	39.7	0.167	1.6	Chen et al 2018
〃	*E. coli* TRTHB	*trpEDCBA**, Δ*tnaA*,Δ*gltB*,Δ*pta*,Δ*ackA*	fed-batch	47.18	0.178	1.18***	Xu et al 2017
〃	*E. coli* TRP07	Δ*lacI*,Δ*tnaA*,Δ*mtr*,*trpE**::*trpLE*,*aroG**::*tyrR*,Δ*pykA*,Δ*ppc* *pck*::*ycjV*,*citT*::*poxB*,*acnBA*-*icd*::*yghx*,*pyc*(*C. glutamicum*)::*yjiV*	batch	49	0.186	1.36***	Du et al 2019

Note *: overexpression including heterologous expression, **: attenuation, ***: computed from fermentation data, [g/g-Glc]: glucose as a carbon source, [g/g-S]: sucrose as a carbo source, [m/m] molar yield, (fbr): feedback-inhibition-resistant, ALE: adaptive laboratory evolution, - : not available.

Table 2 Metabolic engineering strategies for L-amino acid fermentation

Serine	The PHGDH reaction is thermodynamically unfavorable to proceed due to the high positive free energy in *E. coli* (Grant 2012, Merrill et al 1981). This can be overcome by coupling with the reaction of heterologous αhydroxyglutarate dehydogenase (HGDH) (from *Pseudomonas* sp.), which converts αhydroxyglutarate (HG) to αKG, in which αKG can be converted to HG by PHGDH reaction (Zhang, W. et al 2017). The overexpression of *serA*^{fbr}, as well as *serB*, *serC*, and *eamA* (encoding cysteine/homoserine transporter), and the deletion of (serine) degradation genes such as *sdaA*, *sdaB*, and *tdcG* as well as *glyA*, followed by random mutagenesis (to increase the tolerance towards serine) gave the titer of 11.7 g/l by the fed-batch cultivation of *E. coli* (Mundhada et al 2015) (**Table 1**). High intracellular serine concentration becomes toxic to the cell, and serine inhibits homoserine dehydrogenase (encoded by *thrA*), and thus the adaptive evolution may be useful to overcome the product inhibition, thereby improving the L-serine production up to 37 g/l in *E. coli* (Mundhada et al 2016) (Table 1). Moreover, the overexpression of *serA*^{fbr} (as well as *serB* and *serC*) and deletion of *glyA* and *sdaA* (as well as *sstT*, *cycA*, *sdaC*, and *tdcC*) gave the titer of 34.8 g/l in 36 h in *E. coli* (Wang et al 2020) (Table 1). The *serE* (NCg10589) gene encoding the exporter of L-serine (and L-threonine) and its positive regulator NCg10581 were identified in *C. glutamicum*, and its overexpression combined with the serine synthetic pathway genes (*serA*^{fbr} *serC*, and *serB*) gave the titer of 43.9 g/l from sucrose (**Table 1**) (Zhang et al 2020). In order to reduce the by-product formation, deletion of *alaT* and *avtA* (encoding transaminases), and introduction of attenuated mutation of AHAS contributed to L-serine production in *C. glutamicum* (Zhu et al 2015) (**Table 1**).
Cysteine	As the sulfur source, thiosulfate ($S_2O_3^{2-}$) is much more effective than sulfate (SO_4^{2-}) for L-cysteine production, because the latter requires NADPH and ATP in its assimilation pathway (Takagi and Ohtsu 2016). The assimilation pathway of thiosulfate depends on O-acetyl-serine sulfhydrylase (encoded by *cysM*), while sulfate is first converted to sulfite (SO_3^{2-}), which is in turn converted to sulfide (S^{2-}), and then to L-cysteine (by the cysteine synthase encoded by *cysK*) (**Fig. 5**). A major cysteine desulfhydrase gene, *ccdA* involved in cysteine degradation, and the cysteine efflux pump genes *cefA* and *cefB* are responsive for L-cysteine production in *Pantoea ananatis*, and thus the deletion of *ccdA* gene and the overexpression of *cefA* and *cefB* genes gave 2.2 g/l of L-cysteine production in 22 h (Takumi et al 2017) (**Table 1**). The overexpression of *cysE*^{fbr} and *serA*^{fbr} and disruption of *aecD* (encoding cysteine desulfhydrase) and NCg12463 gene (encoding a possible cysteine import gene) may be effective for L-cysteine production by *C. glutamicum* (Kondoh and Hirasawa 2019). The overexpression of *serA*, *serB*, *serC*, *cysE*^{fbr}, and *ydeD*, and the deletion of *tnaA* and *sdaA* genes in *E. coli* gave 5.1 g/l in 32 h by the fed-batch fermentation of *E. coli* (Liu, H. et al 2018). Moreover, the overexpression of *cysB*, *serACB*, *cysM*, (and *nrdH*) and the deletion of *yhaM*, *tnaA*, *sdaA* (and *decR*) gave 7.5 g/l of cysteine production in 22 h in *E.*

	coli (Liu, H. et al 2020) (**Table 1**).
Histidine	For the efficient L-histidine production, the primal target is to remove the histidine-mediated feedback inhibition and transcriptional attenuation (by *hisL*), in which the expression levels of *hisDCBHAFI* may be optimized. Then the enhanced PRPP supply and rerouting the purine nucleotide synthetic pathway may improve the L-histidine production. Moreover, the expression of NADH-dependent *gdh* from *B. subtilis* and lysine exporter from *C. glutamicum* enabled the recombinant strain to produce 11.8 g/l of histidine in *E. coli*. This performance could be further improved by the fed-batch cultivation, yielding 66.5 g/l of histidine production (Wu et al 2020) (**Table 1**).
Arginine	The deletion of *argR* and the feedback-resistant *argB* ($argB^{fbr}$) in *C. glutamicum* gave 52 g/l of L-arginine production (Ikeda et al 2009). Plasmid-based overexpression of $argB^{fbr}$ and *argCJBDFRGH* operon in *C. crenatum* led to 45.6 g/l of L-arginine production (Xu, M. et al 2012). Further metabolic engineering of *C. glutamicum* by the removal of the regulatory repressors of L-arginine operon, and disruption of L-glutamate exporter with the flux optimization of the biosynthetic pathway reactions gave 92.5 g/l of L-arginine production by fed-batch fermentation (Shin et al 2014, Park et al 2014) (**Table 1**). In the arginine biosynthetic pathway, GDH and NAGPR (encoded by *argC*) are NADPH-dependent, and thus the overproduction of NADPH in CCM is useful for the efficient L-arginine production. Since the main site of NADPH production is at the oxidative PP pathway, the inactivation of Pgi may be considered (Man et al 2016) (Table 1). Another approach for increasing the availability of NADPH is the overexpression of NAD^+ kinase or $NAD(P)^+$ transhydrogenase. Therefore, deletion of *argR* and *farR* as well as the overexpression of *pntAB* (from *E. coli*) and *ppnK* enabled 67.0 g/l of L-arginine production in *C. glutamicum* (Zhan et al 2019) (Table 1). The atmospheric and room temperature plasma (ARTP) mutagenesis on Δ*argR* mutant gave 95.5 g/l of L-arginine production (Xu, M. et al 2020) (**Table 1**).
Citrulline	For the citrulline production, *argG* gene must be deleted to prevent the conversion from citrulline to L-arginine in addition to Δ*argR*. Thus, Δ*argG* and Δ*argR* with overexpression of *argJ* gave 8.51 g/l of citrulline production in *C. glutamicum* (Hao et al 2015) (**Table 1**). Moreover, the feedback resistant *argB* with heterologous overexpression of *argF* yielded 7.7 g/l of L-citrulline production in *C. glutamicum* (Eberhardt et al 2014) (**Table 1**).
Ornithine	Deletion of *argF*, *argR*, and *proB* and the enhancement of the feedback-inhibition-resistant enzyme (with enhanced PP pathway) gave 51.5 g/l of ornithine production in *E. coli* (Kim, S.Y. et al 2015) (**Table 1**). Moreover, the cyclic pathway in *C. glutamicum* can be changed to linear pathway by introducing the heterologous expression of *argA* and *argE* (from *E. coli*) with the mutation of *argB* (with the deletion of *proB* and *argF*), giving 40.4 g/l of L-ornithine production in *C. glutamicum* (Shu et al 2018) (Table 1). Additional mutation gave 43.6 g/l of L-ornithine production (Zhang, B. et al 2018a, 2018b, 2017) (**Table 1**).
Proline	Proline is typically synthesized via GK (encoded by *proB*), GPR (encoded by *proA*), and P5CR (encoded by *proC*) (**Fig. 7**). An alternative route involves ornithine

	cyclodeaminase (OCD), which catalyzes the conversion of ornithine to proline and ammonia (**Fig. 7**). However, *E. coli* does not possess this enzyme, while several other bacteria possess such enzyme (Jensen and Wendisch 2013, Bin et al 2015). The ornithine overproducing *C. glutamicum* strain with deletion of *argR* and *argF* (called as ORN1) can be used to produce proline by the heterologously produced OCD (from *P. putida* etc.), allowing the conversion of ornithine to proline (**Fig. 9**) (Jensen and Wendisch 2013). The heterologous *ocd* gene (from *P. putida*) was expressed in *C. glutamicum*, giving 12.7 g/l of L-proline production in 30 h (Jensen et al 2013) (**Table 1**). For the efficient proline production, L-proline utilization pathway may be removed by deleting *putA* gene (encoding L-proline dehydrogenase), as well as the L-proline importer genes, *proP* and *putP* in *E. coli*. Moreover, the branched pathway in which L-ornithine is converted to putrescine may be removed by deleting *speC* and *speF* genes (encoding ornithine decarboxylase and its isozyme). The genes *glnA* and *argF* can be also removed to increase the ornithine production, but the cell growth is depressed, and therefore, fine tuning of knockdown of such genes by synthetic small RNA (sRNA) allows 33.8 g/l of L-proline production (and 42.3 g/l of putrescine production) (Noh et al 2017) (**Table 1**). Moreover, deletion of *proP*, *putP*, *putA*, and *aceA* (encoding isocitrate lyase, Icl), together with the mutation of *proB* (*proB*^{fbr}), and codon optimization gave 37.5 g/l of L-proline production (and 54.8 g/l of trans-4-hydroxy-L-proline) in 60 hours in *E. coli* (Long et al 2020) (**Table 1**).
Valine	Except for enterobacteria (such as *E. coli*), most prokaryotes have single AHAS, where the small subunit of AHAS encoded by *ilvN* is responsible for the feedback inhibition by all three BCAAs, and the expression of the *ilvBNC* opeon is also controlled by the trarnscriptional attenuation mediated by all three BCAAs (Morback et al 2000). The elimination of feedback inhibition of AHAS by L-valine (by *ilvBN*^{fbr}) together with the positive feedback loop by autoinducibility of 2-acetolactate synthesis by the replacement of *ilvBN*^{fbr} regulatory region with an *ilvC*-P_{ilvC} (promoter of the *ilvC* gene) unit enabled the increased AHAS synthesis, resulting in the enhanced L-valine production of 6.1 g/l in *E. coli* (Geraskina et al 2019) (**Table 1**). In *C. glutamicum*, the four enzymes, AHAS, AHAIR, DHAD, and BCAAT are used for L-valine production. AHAS is encoded by *ilvB* and *ilvN*, while AHAIR, DHAD, and BCAAT are encoded by *ilvC*, *ilvD*, and *ilvE*, respectively (**Appendix 1**). These enzymes also catalyze the reactions for the biosynthesis of L-isoleusine, and thus L-isoleusine is the major by-product in the L-valine fermentation. Intracellular L-valine is exported via BrnFE, responsible for the export of BCCAs and L-methionine (**Appendix 1**), in which the expression of *brnFE* is activated by Lrp (Lange et al 2012). Pyruvate is the precursor for L-valine synthesis. Therefore, several strategies have been attempted to increase L-valine production in *C. glutamicum*. For example, the deletion of *leuA* (to reduce L-leusine biosynthesis) and *panB* (encoding 3-methyl-2-oxobutanoate hydroxymethyl transferase) (to block pantothenate

	biosynthesis) (Bartek et al 2010). The overexpression of *ilvBNC*, *lrp*1 (for enhancing BrnFE), *brnFE*, and deletion of *aceE*, *alaT*, and *ilvA* (to reduce the L-isoleusine production) gave 51 g/l of L-valine production by the fed-batch fermentation of *C. glutamicum* in 96 h (Chen et al 2015) (**Table 1**). The efficient L-valine fementation can be also made using *E. coli* by the heterologous introduction of a feedback inhibition-resistant *alsS* (encoding AHAS from *B. subtilis*), and overexpression of *ilvCE,* as well as the heterologous introduction of L-valine exporter *brnFE* (from *C. glutamicum*) and the *spot*$^{[R290E,K292D]}$ to enhance the glucose uptake rate (Hao et al 2020). Moreover, NADPH-dependent branched chain amino acid aminotransferase was replaced by NADH-dependent leusine dehydrogenase (from *B. subtilis*), and the metabolic pathway genes such as *pflB*, *ldhA*, and *adhE* were knocked out. Then, the two-phase culture was employed to enhance the cell growth (under aerobic condition), followed by L-valine production under oxygen limited condition (Hao et al 2020).
Leusine	Overexpression of the feedback resistant *leuA* (*leuA*^{fbr}), deletion of *ltbR*, *araT* (to reduce alanine production from pyruvate), *ilvA* (to reduce isoleusine production), and *panBC* (to prevent the production of D-pantothenate from 2-ketopropylmalate) gave 38.1 g/l of L-leusine production in *C. glutamicum* (Huang et al 2017) (**Table 1**). In addition to the disruption of *ltbR* and the overexpression of *leuA* and *ilvBNCE* in *C. glutamicum*, *ilvC* and *gdh* may be modified by inserting NAD-specific leusine dehydrogenase (encoded by *leuCD*) from *Lysinibacillus sphaericus* and the glutamate dehydrogenase (encoded by *rocG*) from *B. subtilis* to improve the redox flux by utilizing NADH (instead of NADPH), resulting in 23.31 g/l of L-leusine production (Wang, X.-Y. et al 2019) (**Table 1**). In addition to *ilvE* (encoding BCAAT), there are several types of aminotransferases (in which the affinity for substrates is different): *tyrB* and *aspC* in *E. coli*, *B. subtilis*-derived aminotransferase gene *ywfG* and *ybgE*, and *C. acetobutyricum*-derived *CaIlvE* (Feng et al 2018). The deletion of *ilvE* gene allows the significant decrease in L-valine production, making the flux toward L-leusine production in *C. glutamicum*. Moreover, the deletion of *aspB* may be considered to reduce the by-product formation, but Δ*ilvE*Δ*aspB* double mutant becomes auxotrophic for the three BCAAs. Thus, another aminotransferase, *tyrB* gene was overexpressed in Δ*ilvE*Δ*aspB* mutant *C. glutamicum*, which gave 18.55 g/l of L-leusine production (Feng et al 2018) (**Table 1**).
Threonine	The degradation of L-threonine may be prevented by the deletion of *tdh* gene (encoding threonine dehydrogenase to produce glycine) and mutation of *ilvA*. In addition, *metA* and *lysA* genes may be removed to avoid by-product formation. The overexpression of the threonine exporter genes *rhtABC* and the deletion of the threonine transport gene, *tdcC* may be also useful for the increase in the yield of L-threonine. Moreover, the overexpression of *ppc* and *acs* genes, and the deletion of *iclR* gene (or *fadR* and *fabR* genes) (to activate the glyoxylate pathway) may be also useful to increase the precursor metabolite, OAA in *E. coli* (Lee et al 2007, Zhao et al 2018, Yang et al 2019) (**Table 1**). In order to reduce the acetate formation, and increase NADPH, the threonine producing strain, *E. coli* THRD was further modified by Δ*pfkB*Δ*pykF*, yielding

	111.37 g/l of L-threonine production with 7.42 g/l of acetate production (Xie et al 2014). Moreover, the deletion of *fadR*, *fabR*, and *iclR* genes to reduce acetate formation, while increasing OAA pool size together with the overexpression of *ppnK*, *thrA*^{fbr}, *thrBC*, *rhtC*, *aspC*, and *ppc* gene in *E. coli* (TWF044) gave 103.89 g/l of L-threonine production in 48 h by the fed-batch fermentation (Yang et al 2019). In order to increase the NADPH availability, the overexpression of *gdh*, *fdh* (formate dehydrogenase), and pyridine nucleotide transhydrogenase was considered in the two-stage fermentation using *E. coli* THRD strain (Liu et al 2019). A thermal switch system for the two-stage (growth and production) system was considered by rebalancing between pyruvate and OAA by controlling the heterologous expression of *pyc* and OAA decarboxylase, while deleting *ldhA*, *pfkB*, *poxB*, *pta*, *adhE*, and *tdcC*/*sstT* (transporter of threonine), giving about 47 g/l of L-threonine production in 27 h by the fed-batch cultivation of *E. coli* TWF113 (Fang et al 2020). Recently, the *thrL* leader regulator elements were applied to regulate the expression of *iclR*, *arcA*, *cpxR*, *gadE*, *fadR*, and *pykF*, while the threonine-activating promoters were applied to regulate the expression of *aspC* gene in *E. coli* TWF001, resulting in 116.62 g/l of L-threonine production in 48 h of fed-batch fermentation (Zhao et al 2020) (**Table 1**). In the fermentative production of L-threonine and L-isoleusine by *C. glutamicum*, the production of by-products, L-lysine and L-methionine must be reduced by inactivating *dapA* and *metX* genes in *C. glutamicum*. However, diaminopimelate (the direct precursor for L-lysine biosynthesis) is a component of peptidoglycan, essential for the cell wall synthesis. Thus, the deletion of *ddh* and *lysE* (encoding L-lysine exporter) may be considered (Dong et al 2016b).
Isoleucine	Metabolic engineering of *E. coli* for isoleusine production may be made by enhancing *thrABC*, *ilvA*^{fbr}, *ilvIH*^{fbr}, *ygaZH* (encoding BCAA exporter) genes, as well as *ilvCED* and *lrp*, giving 9.46 g/l of L-isoleusine production in *E. coli* (Park et al 2012) (**Table 1**). The similar strategy of improving the L-isoleusine production can be made by *C. glutamicum* (Wang, X. et al 2019). The L-isoleusine producer, *C. gltamicum* IWJ001 (Yin et al 2013) could be improved by the overexpression of *ilvA*1, *ilvBN*1, *lrp*, *brnFE*, *ppnk*1, giving 32.3 g/l of L-isoleusine production in 72 h of fed-batch fermentation (Yin et al 2014) (**Table 1**).
Methionine	For the efficient L-methionine production, deletion of *metJ*, *metI*, and *lysA*, and the overexpression of methionine synthetic pathway genes, *metA* and *yieH* gave 9.75 g/l of L-methionine production in *E. coli* (Huang et al 2017) (Table 1). Moreover, the L-methionine biosynthetic pathway was modulated by uncovering the multiple layers of limitations, giving 16.86 g/l of L-methionine production by 48 h of fed-batch fermentation (Huang et al 2018) (**Table 1**). Overexpression of the heterologous *metX* and *metY* genes in a lysine producing *C. glutamicum* gave 16 g/l of L-methionine production (Mocker et al 2004). In addition to the inactivation of MetJ and McbR, the mutation of *lysC*^{T3111} and *hom*^{G377E} were employed to increase the methionine precursor supply in *C. glutamicum* (Park et al 2007, Qin et al 2015, Li, Y. et al 2016). A methionine-producing strain can be constructed from a lysine-producing *C. glutamicum*

	(Mlf20-22B) by deregulation of *hom* gene (*hom*^{fbr}), and deletion of the *thrB* gene (Δ*thrB*), giving 2.9 g/l of methionine production by batch culture (Park et al 2007) (**Table 1**). In the metabolic engineering of *C. glutamicum*, *metD* (encoding L-methionine uptake system) was deleted, and then random mutagenesis was performed to remove feedback inhibition by end-products. Then, the branched pathway genes *thrB* and *dapA* were deleted, followed by point mutation of *lysC*, and *pyc*, as well as by the mutation of G6PDH and 6PGDH, giving 6.85 g/l of L-methionine production in 72 h of fed-batch cultivation of *C. glutamicum* (Li, Y. et al 2016) (**Table 1**).
Homoserine	The primary target is to inactivate the expression of *thrBC* genes and *metA*, as well as *lysA* gene. Moreover, the overexpression of *thrA*, *metL*, and *lysC* genes is effective. Thus, these together with the overexpression of *rhtA* gene (encoding L-homoserine exporter) and inactivation of *tdcC* gene gave 39.54 g/l of L-homoserine production by the fed-batch culture of recombinant *E. coli* (Li, H. et al 2016) (**Table 1**). Moreover, further modulation of the glucose transport system (by inactivating *ptsG* and *galR*, while overexpressing the expression of *glk* gene) and the glutamate production system (by activating *gltB*) gave 37.57 g/l of L-homoserine production (Liu, P. et al 2020) (**Table 1**).
Lysine	Earlier metabolic engineering approach was made by the step-by-step improvement in *C. glutamicum* by overexpressing the lysine biosynthetic pathway genes, *lysC*, *dapB*, *ddh*, *lysA*, as well as *pyc*, *fbp*, and *tkt* operon, while repressing the expression of *home* gene, *icd* gene with *pck* gene knockout (to increase the OAA pool size), giving 120 g/l of L-lysine production by the fed-batch fermentation with the productivity of 4.0 g/l.h (Becker et al 2011) (**Table 1**). Since Ask is subject to allosteric inhibition by L-lysine and L-threonine in *C. glutamicum*, the feedback inhibition resistant mutation of *lysC* is effective. Moreover, since Ppc is strongly inhibited by malate, the point mutation of *ppc* gave 211.3 mmol/mol of lysine production in 21 h (Chen et al 2014). Since 4 moles of NADPH are required for the synthesis of one mol of lysine in *C. glutamicum*, the initial attempt was to enhance the oxidative PP pathway. The heterologous NADH-utilizing dehydrogenases may be introduced to save the NADPH usage. For example, aspartate dehydrogenase was introduced from *Pseudomonas aeruginosa*, aspartate-semialdehyde dehydrogenase from *Tistrella mobilis*, and dihydrodipicolinate reductase from *E.coli*, giving 27.7 g/l of L-lysine production (Wu, W. et al 2019) (**Table 1**). Although it is effective to express *ddh* gene (from *C. glutamicum*) in *E. coli*, the optimal temperature for *E. coli* (37 °C) is different from that of *C. glutamicum* (30 °C). Thus, the overexpression of *ddh* from *Symbiobacterium thermophilum* in *E. coli* is effective for L-lysine production (Xu, J.-Z. et al 2019a). Since the dehydrogenase pathway converts THDPA to *meso*-DAP in a single step by DDH (encoded by *ddh*), the knockout of *dapD* gene, and the replacement of the natural *rpiB* gene by *ddh* gene in *E. coli* gave 119.5 g/l of L-lysine production by fed-batch fermentation (Xu, J.-Z. et al 2019a) (**Tables 1**).

	The feedback-inhibition resistant *ppc* and *pyc* genes were inserted in the *pck* and *odx* loci, and the P1 promoter of the TCA cycle gene *gltA* was deleted, and the natural promoter of GDH-encoding *gdh* was replaced by $P_{tac\text{-}M}$ promoter (to increase glutamate for the reaction of aspartate aminotransferase, AAT), which gave 181.5 g/l of L-lysine production in the fed-batch culture by adding 2.4 g/l of biotin (to enhance Pyc activity) (Xu et al 2018). The modulation of the glucose transport system by PTS may also contribute to L-lysine production. In particular, the overexpression of the glucose transport genes such as *ioT1* and *ioT2*, as well as *ppgk* in Δ*pgi* mutant could produce 201.6 g/l of L-lysine production by the fed-batch culture of *C. glutamicum* (Xu, J.-Z. et al 2019b) (**Table 1**). In order to overcome the shortage of ATP generation, co-expression of bifunctional ADP-dependent Glk and NADH dehydrogenase as well as inactivation of sigma H factor (thus reducing the consumption of ATP and increasing the ATP generation), gave 221.3 g/l of L-lysine production in *C. glutamicum* (Xu et al 2020) (**Table 1**).
Phenylalanine	Noting that AroL and AroA are the limiting pathway enzymes for the phenylalanine biosynthesis, the overexpression of *aroF*, $pheA^{fbr}$, and *aroA* (and *aroL*) gave 62.47 g/l of L-phenylalanine production in 48 h by the fed-batch cultivation of *E. coli* (Ding et al 2016) (**Table 1**). Then, the overexpression of *aroF*, *aroD*, and $pheA^{fbr}$, and inactivation of TyrR gave 72.9 g/l of L-phenylalanine production in 52 h, where the PTS system was inactivated, while the expression of *galP* and *glk* was enhanced to increase the PEP pool size (Liu, Y. et al 2018) (Table 1). The dynamic regulation strategy was attempted by constructing phenylalanine-inducible promoters that inhibit different strength through modification of the promoter region of *tyrP*. Then, the dynamically controlled expression of AroK gave 61.3 g/l of L-phenylalanine production in 48 h (Wu, I. et al 2019) (**Table 1**).
Tyrosine	Initial attempt of metabolic engineering for the L-tyrosine production has been focused on the transcriptional deregulation of the *tyrR* (and *trpR*) regulon, followed by removing the feedback inhibition of L-Tyrosine on AroG and TyrA (Lutke-Eversloh and Stephanopoulos 2007). Co-expression of the rate-limiting enzymes, shikimate kinase (AroK or AroL) and quinate/shikimate dehydrogenase (YdiB), and deletion of the L-phenylalanine branch has been shown to increase L-tyrosine production (Lutke-Eversloh and Stephanopoulos 2008). In addition to the deletion of *tyrR* gene and the overexpression of $aroG^{fbr}$ and $tyrA^{fbr}$, the overexpression of *ppsA* and *tktA* is useful, resulting in 9.7 g/l of L-tyrosine production by the fed-batch cultivation of recombinant *E. coli* (Lutke-Versloh and Stephanopoulos 2007) (**Table 1**). In addition to such strategy, significant improvement can be made through the use of combinatory approaches by generating strains from two mutagenesis libraries (*rpoA* and *rpoD*). In *E. coli*, the mutation of two plasmid-encoded components of RNA polymerase, *rpoD* (encoding the principal sigma factor, σ^{70}) and *rpoA* (encoding the α subunit) led to the improvement of cellular traits, as well as the transcription rate, making them important knobs for modulating global transcriptional profiles, resulting in 13.8 g/l of L-tyrosine production after 36 h, where the cell growth rate was 0.405 h^{-1} in *E. coli* (Santos et al 2012) (**Table 1**).

	In addition to the typical strategy for L-tyrosine production by disrupting *tyrR* gene and the overexpression of *aroG*^{fbr} and *tyrA*^{fbr}, a synthetic constitutive promoter was introduced to enhance the Pps activity (to increase PEP pool size), giving 3.0 g/l of L-tyrosine production (Kim, S.C. et al 2015) (**Table 1**). Since the enzymes for the pathway from chorismate to L-tyrosine production is inhibited by L-tyrosine (**Fig. 10**), the overexpression of heterologous *tyrC* gene (from *Zymomonas mobilis*) encoding the feedback-inhibition-insensitive enzyme, cyclohexadienyl dehydrogenase (TyrC), and the chorismate mutase (CM) domain from native *pheA* from *E. coli* increased the carbon flow towards L-tyrosine production (in which PTS was disrupted and *aroG*^{fbr} was also overexpressed), giving 3 g/l of L-tyrosine production (Chavez-Bejar et al 2008) (**Table 1**). This strategy together with the removal of L-tyrosine specific transporter (TyrP) gave 43.14 g/l of L-tyrosine production by the fed-batch cultivation of *E. coli* using the exponential feeding followed by DO-stat feeding method (Kim, B. et al 2018) (**Table 1**) The efficient production of L-tyrosine can be also extended for the production of 3,4-dihydroxyphenyl-L-alanine (L-DOPA), which can be used for Parkinson's disease (Fordjour et al 2019).
Tryptophan	The primary approach for L-tryptophan production is to increase the concentrations of the precursor metabolites, PEP and E4P (by Δ*ptsG* and the overexpression of *tktA* gene, respectively) as well as the overexpression of the feedback resistant *aroG* and *trpE*, and the inactivation of the attenuation by TrpR and TnaA. This strategy allowed the production of 10.15 g/l of L-tryptophan in 48 h in *E. coli* (Gu et al 2012). This performance can be improved by further inactivating three permease genes, *aroP*, *tnaB*, and *mtr*, giving 16.3 g/l of L-tryptophan production in 66 h by *E. coli* (Gu et al 2012) (**Table 1**). In addition to the decrease in acetate production by *pta* gene knockout, the knockout of the high affinity transporter gene, *mtr* and the overexpression of the aromatic amino acid exporter gene *yddG* allow the lower 'intracellular' concentration of L-tryptophan but higher 'extracellular' L-tryptophan production, yielding 48.7 g/l of L-tryptophan production by the fed-batch cultivation of *E. coli* (Wang et al 2013) (**Table 1**). In addition to Δ*trpR*Δ*tnaA*Δ*pheA*Δ*tyrA*, and the overexpression of *aroF*^{fbr} and *trpE*^{fbr}*D*, the disruption of *pta* (as well as *ackA*) contributes to reducing the acetate production (down to 2.1 g/l), while increasing the L-tryptophan production, giving 44 g/l of L-tryptophan production (Liu et al 2016) (**Table 1**). This performance can be further increased by the cell recycling to 55.12 g/l of L-tryptophan production (Xu et al 2017). Moreover, the deletion of the genes of *pta* and *ackA* in a *gltB* mutant *E. coli* led to 47.18 g/l of L-tryptophan production (and 1.22 g/l of acetate production) in 40 h (Xu et al 2017) (**Table 1**). The overexpression of L-*trp* operator sequences (*trpEDCBA*) and *aroG*^{fbr}, and the inactivation of *trpR*, together with Δ*pykF* and Δ*ptsH* showed relatively slow growth, and thus *galP* and *glk* were overexpressed. Moreover, *pta* gene was disrupted, which results in 39.7 g/l of L-tryptophan production by the fed-batch culture of *E. coli* (Chen et al 2018) (**Table 1**). Moreover, the knockout of *pykA* and *ppc*, and the activation of *pck* and *citT*, *acnBA-icd*, as well as *pyc* (from *C. glutamicum*) in *E. coli* gave 49 g/l

	of L-tryptophan production in 36 h (Du et al 2019) (**Table 1**). Since the feed-forward inhibition of IGPS by ANT prevents the flux toward L-tryptophan biosynthesis, the replacement of the feed-forward inhibition system by feed-forward activation system by the heterologous expression of *trpC* (encoding IGPS) is effective for L-tryptophan synthesis, giving 29 g/l of L-tryptophan production within 42 h with the yield of 0.18 g/g (Chen et al. 2018) (**Table 1**).